الجـــــــــمـــهـــوريـــــــــة الجـــــــــــــــزائـــريـــة
الديمـــــــــــــــقـــراطـيـــة الـشـــــــــــــــعـبـيـــة
REPUBLIQUE ALGERIENNE DEMOCRATIQUE ET POPULAIRE
وزارة التـــــــــــــــعـــليـــم العـــــــــــــــالي و
البـــــــــــــــحث العـــــــــــــلـــمـــــــي
Ministère de l'Enseignement Supérieur et de la Recherche Scientifique
جـــــــــامعة أبي بـكـــــــر بـلـقـــايـد– تـــلمســـــان –
Université Aboubakr Belkaïd– Tlemcen –
Faculté de TECHNOLOGIE

THESE

Présentée pour l'obtention du **grade** de **DOCTORAT 3ème Cycle**

En : Génie Mécanique

Spécialité : Energétique

Par : MISSOUM Khawla

Sujet

Experimental analysis of the improvement of thermal storage by latent heat using metallic additives

Soutenue publiquement, le 23/ 9 / 2023, devant le jury composé de :

SAIM Rachid	Professeur	Univ. Tlemcen	Président
M. KORTI Abdel Illah Nabil	Professeur	Univ. Tlemcen	Directeur de thèse
M.GUELLIL Hocine	MCA	Univ. Tlemcen	Co-Directeur de thèse
BENRAMDANE Med	MCA	Univ. Tlemcen	Examinateur 1
BENZENINE Hamidou	MCA	Univ. Ain Temouchent	Examinateur 2

ACKNOWLEDGMENTS

At the end of this modest project; I would like to thank my GOD for the courage he offered me to reach the end of my studies and realize this work.

First and foremost , I would like to express my gratitude to mu thesis director , Pr KORTI Abdelillah Nabil and Dr GHELLIL Hocine, for their understanding, their availability, and most importantly, their wise counsel, which fueled mu thinking and who have been a great support in the creation of this thesis, they taught me a lot about the challenges to be met in the educational world and shared their knowledge and experiences in this environment, while giving me their confidence and a large independence in the execution of rewarding missions.

Our respect to the members of the jury, Mr. SAIM Rachid, Mr. BENRA MDANNE Mohammed and Mr. BENZENINE Hamidou, who do me the honor to accept and judge this modest work, to bring their reflections and their scientific criticisms

I also like to thank the University of Tlemcen's complete teaching staff.

My family, especially my mother for her constant support and encouragement, I would like to thank my friends, especially Meriem who supported me and still support me. From the bottom of my heart Thank you and May GOD protect you

I want to express my gratitude to everyone who helped make my internship a success and who offered assistance to me while I was writing this thesis

DEDICATIONS

With a big heart full of warmth, I dedicate this memoir to my dearest ones:

To the memory of my father: to the one with a big heart, to the man whose name I proudly carry, to the one I missed since childhood. No dedication can ever describe my love, esteem, commitment, and respect for you. This work is the result of your sacrifices for my education and training. May God, the Almighty, have you in his holy mercy!

To my dear mother, to my angel of life, I dedicate this humble effort to the one without whom I would not have achieved this level, the one who pushed me, encouraged me to enjoy my studies, and who never stops doing so, to my mother.

To you, my brothers and sisters, who have always supported and encouraged me during these years of study.

To all those who are dear to me.

Khawla

Abstract

Latent heat thermal energy storage is an innovative and promising energy management technology. This is one of the new areas of research because it provides a solution to the problems linked between the energies supplied and required. Paraffin is a phase change material commonly used in thermal energy storage applications whose the main drawback is its low thermal conductivity. However, using the metal additives to improve the effective thermal conductivity of phase change material can lead to a decrease of the effective thermal capacity and the stored thermal energy**.**

The first part of the experimental study consists in analyzing the effect of the nature of the metallic additives (Zamak, aluminum, and copper) on the melting of the phase change material. A glass thermal cavity heated by one side is made to can visualize the progress of the melting process. The originality of the study is to try to predict the best duo which respects both the improvement of thermal conductivity and stored energy. The experiments show that the addition of perforated aluminum plates in the paraffin accelerates the melting process by about 19% and increases the stored energy by 5.18%.

The second part of the experimental study analyzes the effect of the volume concentration of aluminum on the melting of Paraffin in a rectangular thermal cavity heated on both sides and perfectly insulated. The positions of the solid-liquid interfaces and the PCM's temperature evolution were noted and used to determine the liquid fractions and heat transfer behavior. The results obtained show that the addition of 1.2, 2.4, and 4.8% aluminum concentration improves the thermal conductivity of the paraffin by 30, 50, and 155%, and decreases the heat convection coefficient by 17.25 and 50%. The increase in aluminum plates reduces the creation of air pores during solidification and the volume contraction of the paraffin during experiments.

Keywords: PCM, thermal storage, latent heat, metal additives, thermal conductivity.

ملخص

تخزين الطاقة الحرارية الكامنة هو تقنية مبتكرة وواعدة لإدارة الطاقة. هذا هو أحد مجالات البحث الجديدة لأنه يوفر حلاً للمشاكل المرتبطة بين الطاقات الموردة والمطلوبة. البارافين هو مادة متغيرة الطور تستخدم بشكل شائع في تطبيقات تخزين الطاقة الحرارية التي يكون عيبها الرئيسي هو الموصلية الحرارية المنخفضة. ومع ذلك ، فإن استخدام الإضافات المعدنية لتحسين التوصيل الحراري الفعال لمادة تغيير الطور يمكن أن يؤدي إلى انخفاض في السعة الحرارية الفعالة والطاقة الحرارية المخزنة.

يتكون الجزء الأول من الدراسة التجريبية من تحليل تأثير طبيعة المضافات المعدنية (الزماك والألمنيوم والنحاس) على ذوبان مادة تغير الطور. يتم صنع تجويف زجاجي حراري يتم تسخينه من جانب واحد لتصور تقدم عملية الانصهار. أصالة الدراسة هي محاولة التنبؤ بأفضل ثنائي يحترم كلا من تحسين التوصيل الحراري والطاقة المخزنة. أظهرت التجارب أن إضافة صفائح الألمنيوم المثقبة في البارافين تسرع عملية الذوبان بحوالي 19٪ وتزيد من الطاقة المخزنة بنسبة 5.18٪.

الجزء الثاني من الدراسة التجريبية يحلل تأثير التركيز الحجمي للألمنيوم على ذوبان البارافين في تجويف حراري مستطيل مسخن من كلا الجانبين ومعزول تماماً. تمت ملاحظة مواضع الواجهات الصلبة والسائلة وتطور درجة حرارة PCM واستخدامها لتحديد الكسور السائلة وسلوك نقل الحرارة. أظهرت النتائج أن إضافة 1.2 ، 2.4 ، و 4.8٪ من الألمنيوم يحسن التوصيل الحراري للبارافين بنسبة 30 ، 50 ، و 155٪ ، ويقلل معامل الحمل الحراري بنسبة 17 , 25 و 50٪. تقلل الزيادة في ألواح الألمنيوم من تكوين مسام الهواء أثناء التصلب وتقلص حجم البارافين أثناء التجارب.

الكلمات المفتاحية:PCM ،التخزين الحراري، الحرارة الكامنة الإضافات المعدنية ،التوصيل الحراري.

Résumé

Le stockage d'énergie thermique par chaleur latente est une technologie de gestion de l'énergie innovante et prometteuse. Il s'agit de l'un des nouveaux domaines de recherche, car il apporte une solution aux problèmes liés à l'écart entre l'énergie fournie et l'énergie requise. La paraffine est un matériau à changement de phase couramment utilisé dans les applications de stockage d'énergie thermique dont le principal inconvénient est sa faible conductivité thermique. Cependant, l'utilisation des additifs métalliques pour améliorer la conductivité thermique effective du matériau à changement de phase peut entraîner une diminution de la capacité thermique effective et de l'énergie thermique stockée.

La première partie de l'étude expérimentale consiste à analyser l'effet de la nature des additifs métalliques (Zamak, aluminium et cuivre) sur la fusion du matériau à changement de phase. Une cavité thermique en verre chauffée d'un seul côté est réalisée pour visualiser la progression du processus de fusion. L'originalité de l'étude est d'essayer de prévoir le meilleur duo qui respecte à la fois l'amélioration de la conductivité thermique et l'énergie stockée. Les expériences montrent que l'ajout de plaques d'aluminium perforées dans la paraffine accélère le processus de fusion d'environ 19% et augmente l'énergie stockée de 5,18%.

La deuxième partie de l'étude expérimentale analyse l'effet de la concentration volumique d'aluminium sur la fusion de la paraffine dans une cavité thermique rectangulaire chauffée des deux côtés et parfaitement isolée. Les positions des interfaces solide-liquide et l'évolution de la température du PCM ont été notées et utilisées pour déterminer les fractions liquides et le comportement du transfert de chaleur. Les résultats obtenus montrent que l'ajout d'une concentration d'aluminium de 1,2, 2,4 et 4,8 % améliore la conductivité thermique de la paraffine de 30, 50 et 155 % et diminue le coefficient de convection thermique de 17,25 et 50 %. L'augmentation des plaques d'aluminium réduit la création de pores d'air pendant la solidification et la contraction du volume de la paraffine pendant les expériences.

Mots clés : MCP, stockage thermique, chaleur latente aditifs métalliques, conductivité thermique

TABLE OF CONTENTS

Chapter 3
Experimental procedure

Chapter 4
Results and Discussion

Chapter 5
Experimental study of the concentration effect of aluminum

LIST OF FIGURES

LIST OF TABLES

NOMENCLATURE

PCM:	Phase change material
TES:	Thermal energy storage
LHTES:	Latent heat thermal energy storage
SHTES:	Sensible heat thermal energy storage
EPCM:	Encapsulated phase change material
HTF:	Heat transfer fluid
HP:	Heat pipe
Cp:	Specific Heat (kJ/kg K)
Lf:	latent heat of fusion of PCM (kJ/kg)
E:	Energy (kJ)
t:	Time (s)
U:	Velocity (m/s)
D:	Diameter (m)
T:	Temperature (K)
T_o:	Ambient Temperature (K)
Re:	Reynolds number
λ:	Heat conductivity W/(m.°C)
h:	Heat transfer coefficient W/(m^2 K)
Nu:	The Nusselt number

General Introduction

General Introduction

A drastic change in the climate due to the emission of greenhouse gasses, growing need for energy, and diminishing reserves of fossil fuel incline mankind towards sustainable and clean energy resources such as solar energy. Even though it is available in abundance, its intermittent nature hinders its widespread implementation as a cost-effective and reliable energy resource. Efficient energy storage is essential to overcome this problem. Out of all available energy storage techniques, thermal energy storage shows the greatest potential as it is a simple, cost-effective, efficient, and reliable method.

Common types of thermal energy storage TES technologies currently available include sensible heat thermal energy storage (SHTES) and latent heat thermal energy storage (LHTES). LHTES is more attractive as it provides a higher energy density and, therefore, requires less storage material compared to SHTES. LHTESalso can provide stored energy at a nearly constant temperature, which corresponds to the phase transition temperature of the phase change material (PCM) and results in maintaining high energetic efficiency.

Nevertheless, the main PCMs' drawbacks are already well-known. First, their thermal conductivity is usually very low (in the order of 0.2 W/mK for paraffin, andup to 1.5 W/mK for inorganic salt hydrates) causing very slow loading (melting) and unloading (solidification) processes. Several studies have already been conducted to investigate how to enhance PCMs' thermal conductivity. Another PCMs limitation is linked to the high-volume change during the phase change process. In fact, in the case of asymmetric heating the melting process starts from the heated surface, and the liquid-solid interface moves forward through the solid region. Solidification is a process associated with a decrease in volume that can imply the generation of a void volume in the center of the module and limit the reliability in cyclic working conditions.

This work presents an experimental study of the melting of paraffin (considered as a PCM) in an attempt to improve its thermal performance by adding different metallic additives. The thesis has five chapters organized as follows:

Chapter 1 is devoted to a bibliographical study of the research work on the dynamic behavior of the melting process of PCM and the improvement of its thermal conductivity.

Chapter 2 presents the technologies used in TES and the different PCM used. It also presents methods for enhancing heat transfer in PCMs.

Chapter 3 presents the different stages of the construction of the two test benches as well as the experimental procedure for the different manipulations. It also presents the developed interface measurement using Labview software.

Chapter 4 presents the experimental results carried out in order to have the best additive that respects both the improvement of thermal conductivity and the stored energy.

Chapter 5 summarizes the results and their interpretation in order to analyze the effect of aluminum concentration on the dynamic and thermal behavior during melting of the paraffin.

Finally, the study is concluded with a general conclusion summarizing the main findings of the research.

Bibliographical Research

1.1 Introduction

Heat transfer processes involving solid–liquid phase change have been of growing interest to researchers in recent years. This is prompted by various applications that are associated with phase change materials (PCM). The major advantages of these materials are their large heat storage capacity, variety of phase change temperatures, and their nearly isothermal behavior during charging and discharging processes [1,2]. These materials can be incorporated with other thermal systems such as solar thermal systems [3,4], waste heat recovery [5,6],a thermal regulator of buildings [7,8], electronic devices [9–10], spacecraft [11] and smart textiles [12] to increase their performances and reliabilities**.**

1.2 Melting process

To date, numerous phase change materials (PCM) have been developed for application in latent heat storage systems. There are many issues in the process from the development of PCM to using them in storage systems, which should be resolved. The problem of heat transfer in PCMs during the phase change process is the most important one. Latent heat storage containers usually have simple geometrical forms such as a sphere, cylinder, cylindrical annulus, rectangular enclosure, etc. A large number of papers were published on melting and solidification processes in PCMs [13].

The study [14] is focused on the melting of lauric acid in a rectangular thermal storage unit heated from one side. Image processing of photographs together with recorded temperatures is used to calculate the melt fractions, temporal heat storage, and heat transfer characteristics, including the average Nusselt number on the hot wall as well as the local heat transfer rates on the melt front. Moreover, solid -liquid interface morphology and temperature field are employed to infer dominant heat transfer mechanisms and time dependent flow structures during different stages of the melting process. Results indicate that during the initial stage of melting, heat conduction is the dominant mode of heat transfer, followed by a transition from conduction to convection regime and convection dominated heat transfer at later times. Approaching the end of the melting process, the bulk temperature of the liquid

PCM increases and stratified temperature field appears at upper part of the enclosure which reveals depression of the convection currents.

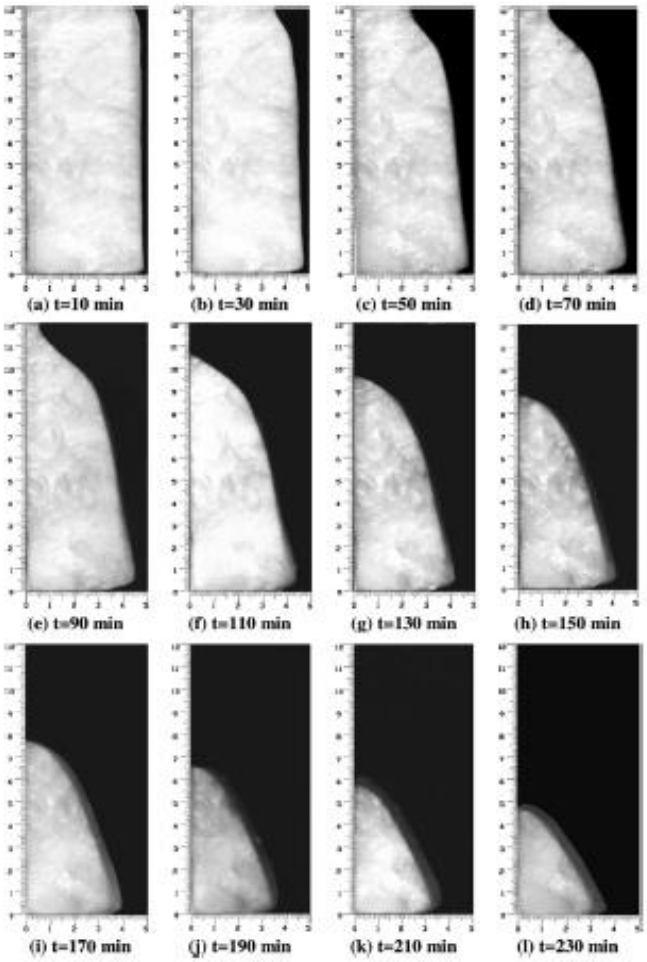

Fig.1.1.Instantaneous photographs of the lauric acid melting in the rectangular enclosure with hot wall temperature of 60 ^{0}C.

Marduga et al [15] carry out a comparative analysis of experimental results and numerical simulations on the melting of the Phase Change Material tetracosane contained within a cube and heated from below. Simulations employ a Stefan number Ste=0.65, Prandtl number Pr=54, and Rayleigh number covers a range up to 108. The simulations show distinct regimes of the melting process: (i) conductive regime, (ii) stable growth regime, (iii) coarsening regime, (iv) turbulent regime. We show how the solid/liquid interface easily observed in the experiment is enough to identify these regimes and so the internal state of the velocity and temperature fields.

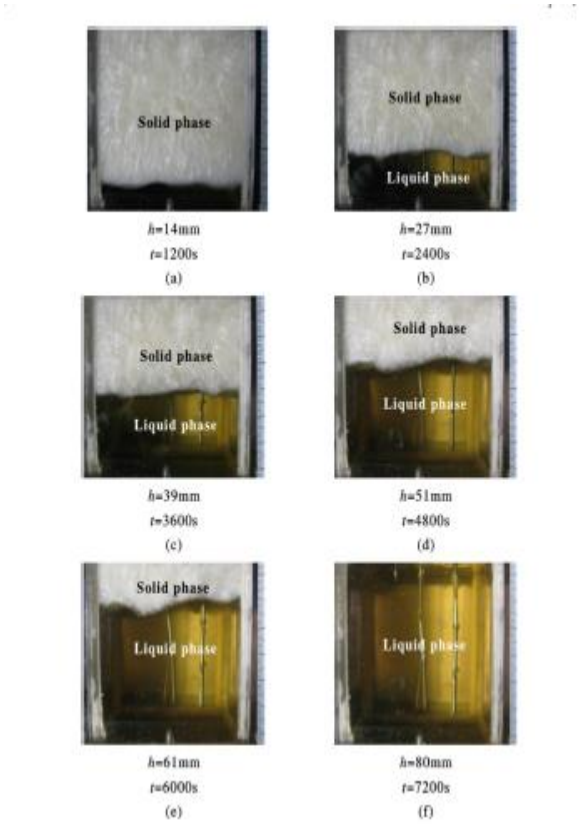

Fig.1.2. (color online) Snapshots at different Times of tetracosane melting when the bottom wall is held at a constant temperature Tw=80 ^{0}C.

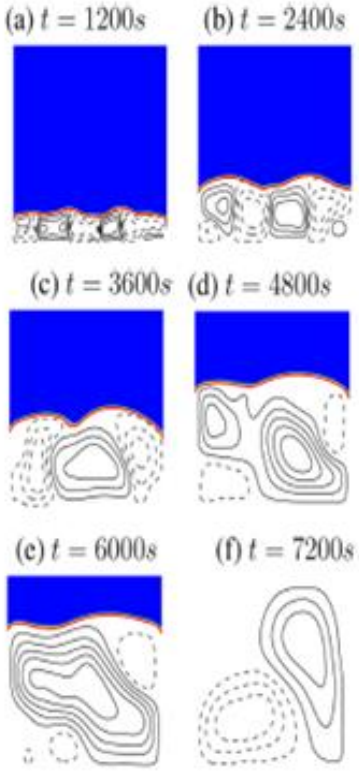

Fig.1. 3. (color online) Snapshots of the streamlines at representative times of the turbulent regime.

In this work [16], numerical experiments were performed to compare the heat transfer and thermodynamic performance of melting process inside the square-shaped thermal energy storage system with three different heating configurations: an isothermal heating from left side-wall or bottom-wall or top-wall and with three adiabatic walls. The hot wall is maintained at a temperature higher than the melting temperature of the phase change material (PCM), while all other walls are perfectly insulated. The transient numerical simulations were performed for melting Gallium (a low Prandtl number Pr=0.0216, low Stefan number, Ste=0.014, PCM with high latent heat to density ratio) at moderate Rayleigh number (Ra = 10^5). The bottom-heating configuration yielded the maximum Nusselt number but has a slightly higher total change in entropy generation compared to other heating, configurations.

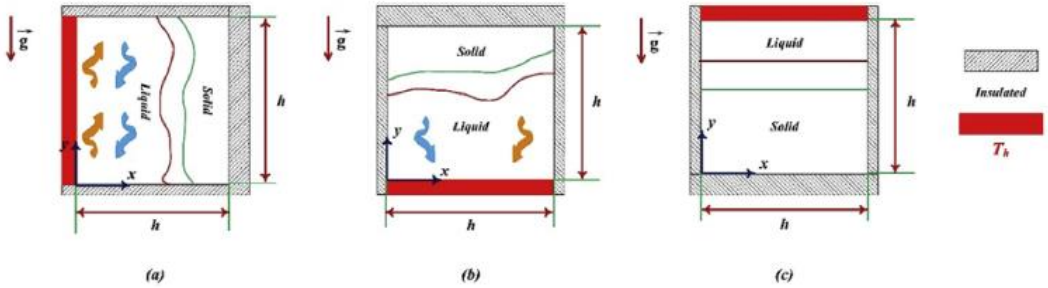

Fig.1.4.Schematic diagram of a energy storage device for melting the phase change material inside a square cavity.

The transient melting process of a phase change material (PCM) is strongly affected by its inclination angle caused by the behavior of buoyancy-driven natural convection. An experimental study [17] is carried out to investigate the effect of this inclination on the thermal behavior during PCM melting contained in a square cavity. The range of inclination angle from 0° (vertical), 45° (inclined), and 90° (bottom) is considered. Paraffin with a melting range of 49-54°C is used as PCM. The volumetric shrinkage of PCM during solidification preceding the melting experiments leads to the development of a large void in the free surface PCM-air (Fig.1.5). The effects of inclination and shrinkage phenomenon are analyzed by visualizing the solid-liquid interface and measuring temperatures by thermocouples and infrared camera.

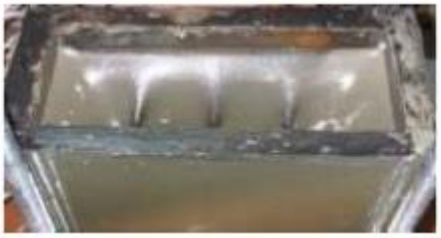

Fig.1.5. Picture of the concave form at the free surface of paraffin.

Results show that the inclination angle has a great influence on the natural convection behavior, and affects the melting front progression and the heat transfer rate. The total melting time for the bottom and inclined cavities cases were, on

average, 56% and 48% less than the vertical one, respectively. The volumetric shrinkage disrupts significantly the melting process in the vertical and inclined cases.

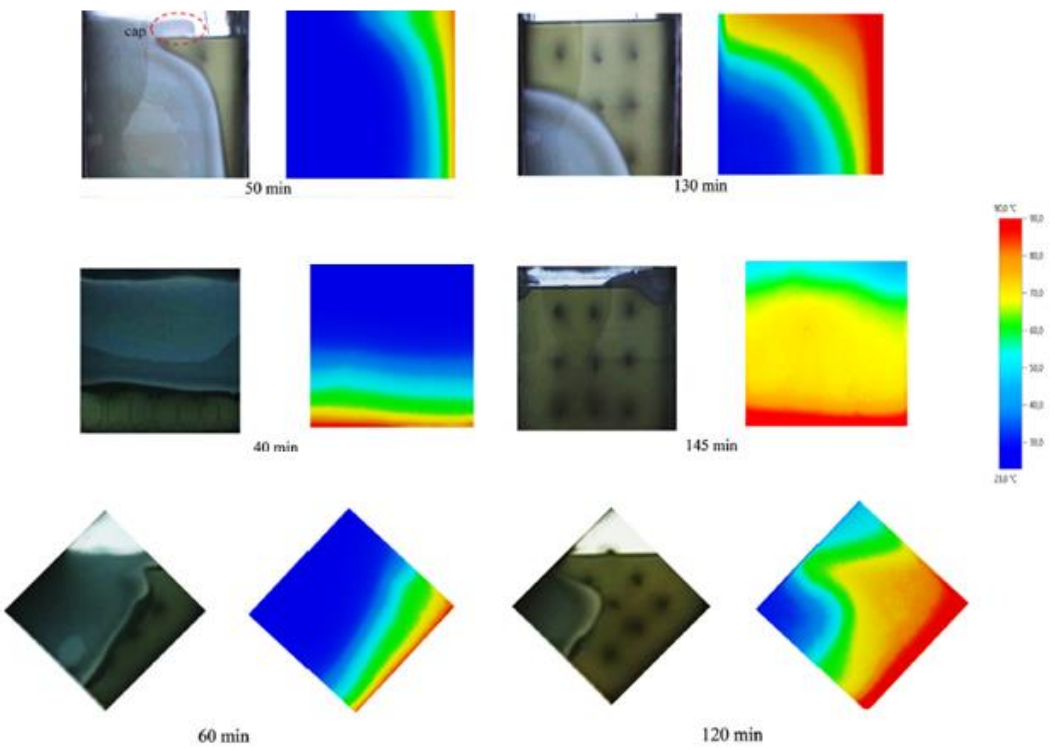

Fig.1.6. Time evolution of the melting process of the paraffin (left) and IR image (right)

Bechiri et al [18] present a numerical investigation to study the melting of Phase Change Material (PCM) partially filled in a vertical cylindrical tube. The top space of the tube was filled with air to take into account the volumetric expansion of PCM. The obtained results have been analyzed and compared with the literature, and a good agreement was showen. Then, a parametric study was carried out to establish correlations for the liquid fraction and time of complete melting as a function of all dimensionless parameters that govern this problem, such as Fourier number, Grashof number, Stefan number, wall to PCM thermal diffusivity ratio, tube aspect ratio, shell-to-tube diameter ratio and dimensionless initial temperature. The results show that all parameters of the problem can really affect the phase change phenomena and consequently, affect the melting time.

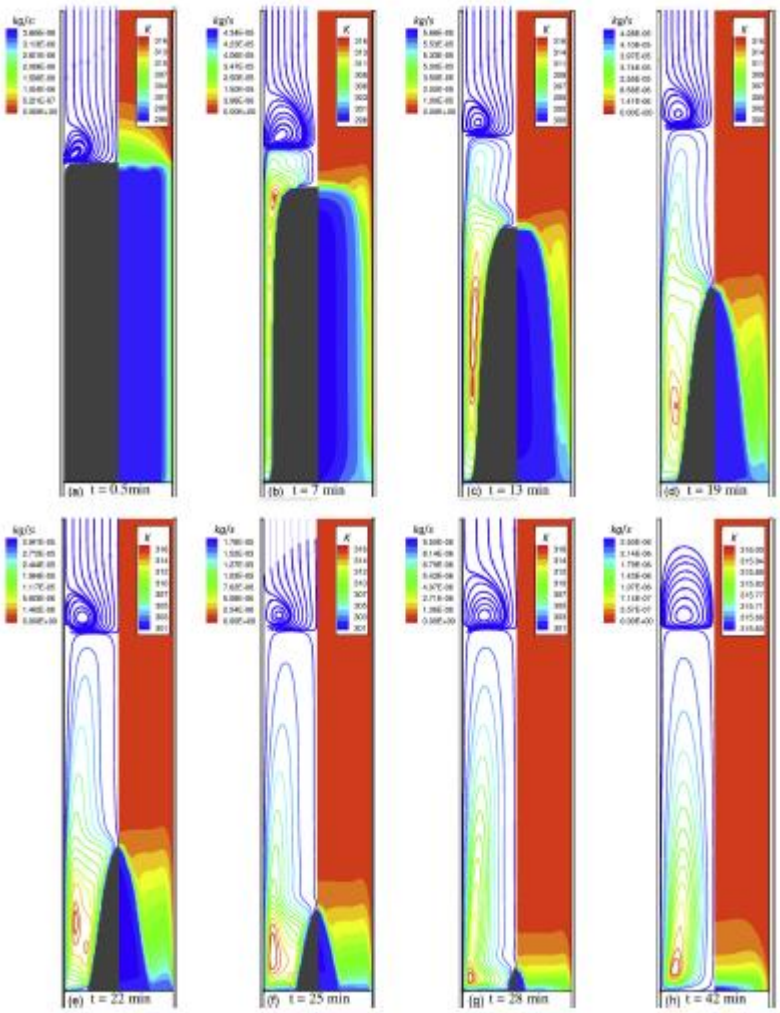

Fig.1.7. Simulated melting process for case 3. For each subfigure, (right) temperature contours, (left) PCM solid fraction in gray and streamline contours in PCM liquid

Well-controlled and well-characterized experimental measurements are obtained during the melting of a moderate-Prandtl-number material (n-eicosane) in a cylindrical enclosure heated from the side [19]. The study aims to provide benchmark experimental measurements for the validation of numerical codes. The melt front was captured photographically and its location was ascertained using digital image processing techniques. An illustrative numerical comparison exercise was also undertaken using a multi-block finite volume method and the enthalpy method for a range of Stefan numbers. Very good agreement was obtained between the predictions and the experiment for Stefan numbers of up to 0.1807. The experimental results for a Stefan number of 0.0836 are recommended as being the most suitable for numerical

benchmarking, since the boundary conditions are best controlled in this set of experiments

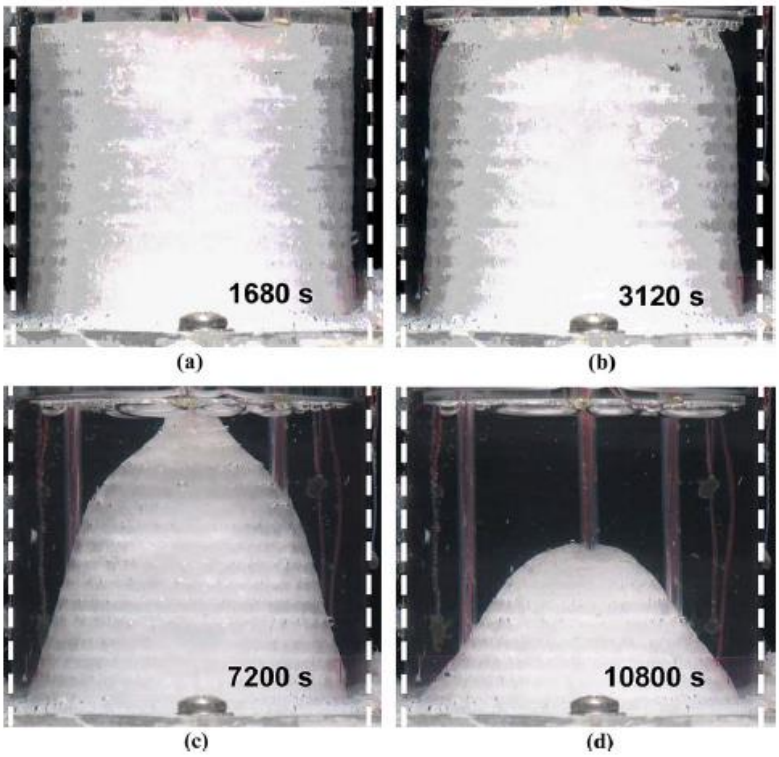

Fig.1.8. Photographs taken during the melting of wax within the cylindrical enclosure for a wall temperature of 45 ^{0}C at four different times

.

A computational study of the effects of buoyancy-driven convection on constrained melting of phase change materials within spherical containers is presented [20]. Early during the melting process, the conduction mode of heat transfer is dominant, giving rise to concentric temperature contours. As the buoyancy-driven convection is strengthened due to the growth of the melt zone, melting in the top region of the sphere is much faster than in the bottom region due to the enhancement of the conduction mode of heat transfer. When buoyancy effects are very marked, as many as three time-dependent recirculating vortices are observed. In comparison to diffusion controlled melting, buoyancy-driven convection accelerates the melting process markedly.

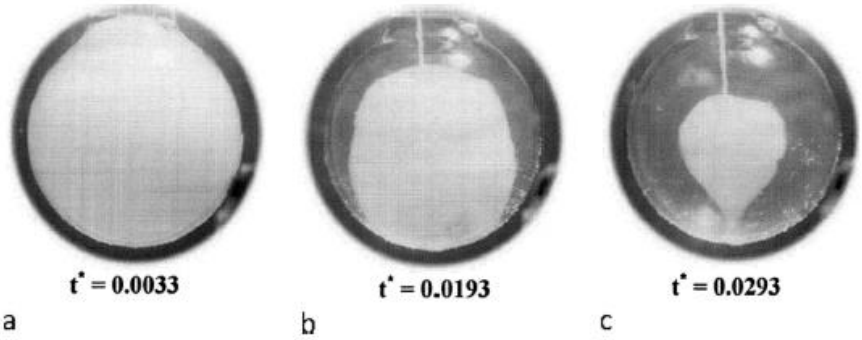

Fig.1.9. Instantaneous photographs of melting of wax inside a spherical bulb

An experimental and computational investigation directed at understanding the role of buoyancy-driven convection during constrained melting of phase change materials (PCM) inside a spherical capsule is reported [21]. Paraffin wax n-octadecane was constrained during melting inside a transparent glass sphere through the use of thermocouples installed inside the sphere. The melting phase front and melting fraction of the PCM are analyzed and compared with the numerical solution obtained from the CFD code Fluent. Following a short period of symmetric melting due to the prominence of diffusion, expedited phase change in the top region of the sphere and a wavy surface at the bottom of the PCM are observed. The computational predictions point to the strong thermal stratification in the upper half of the sphere that results from the rising of the molten liquid along the inner surface of the sphere thus displacing the colder fluid. The waviness and excessive melting of the bottom of the PCM are shown to be underestimated by the experimental observation. This discrepancy is linked to the use of a support structure to hold the sphere. Measured temperature data and computational results near the bottom indicate the establishment of an unstable fluid layer that promotes chaotic fluctuations and is responsible the waviness of the bottom of the PCM.

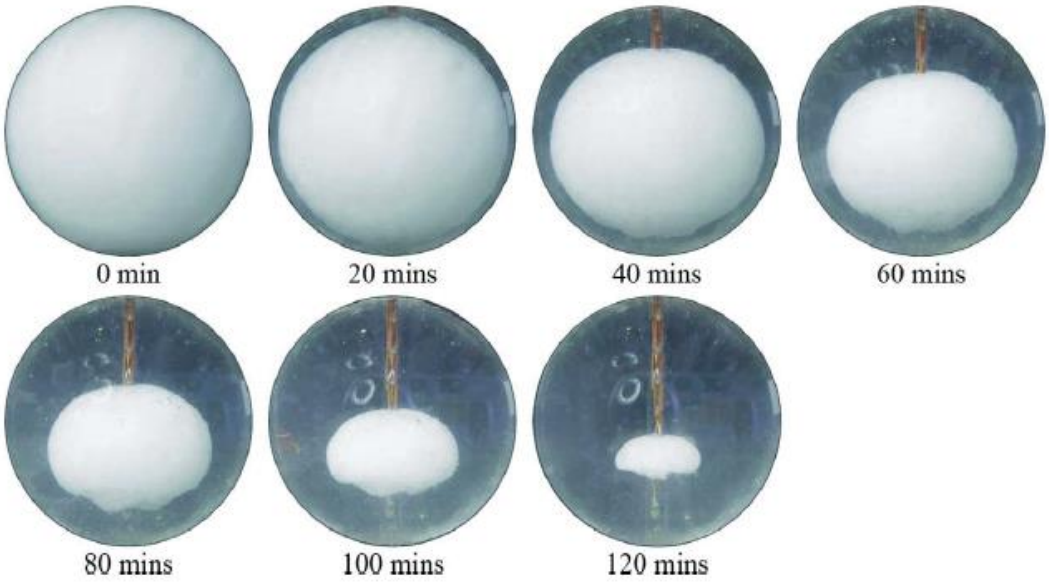

Fig.1.10. Instantaneous photographs of the melting of PCM inside the spherical capsule after 0, 20, 40, 60, 80, 100, and 120 min.

1.3 Improvement of heat transfer in PCM

A significant downside of PCMs is their low thermal conductivity, which decreases the heat transfer rate and restricts the deployment of PCMs in large-scale LHTES units [22] .To enhance the thermal performance of the LHTES, many techniques have been established to improve the thermal conductivity of PCMs such as using fins [23,24], porous structures with high thermal conductivity [25,26], heat pipes [27] and nanoparticles [28].

1.3.1 Use of fins

Due to the simplicity, low cost ,and ease of fabrication, a majority of the heat enhancement techniques have been based on fins. Fins are typically used to increase the effective heat transfer area between HTF and PCM and therefore enhance the thermal performance the TES system [43].

kamkari et al [29] present an experimental investigation of phase change material (PCM) melting in a transparent rectangular enclosure with and without

horizontal partial fins. The enclosure was heated isothermally from one side while the other walls were thermally insulated. Experiments were performed with wall temperatures of 55, 60, and 70 ^{0}C ($3{,}6 \times 10^8 \leq Ra \leq 8{,}3 \times 10^8$) for finned and unfinned enclosures. Experimental results indicated that increasing the number of fins decreased the melting time and increased the total heat transfer rate while the surface-averaged Nusselt number reduced. Melting enhancement ratio and overall fin effectiveness increased with increasing the number of fins and decreased with raising the wall temperature. Melting enhancement ratios decreased with time after reaching some maximum values indicating that partial fins are more beneficial during the initial time of the melting.

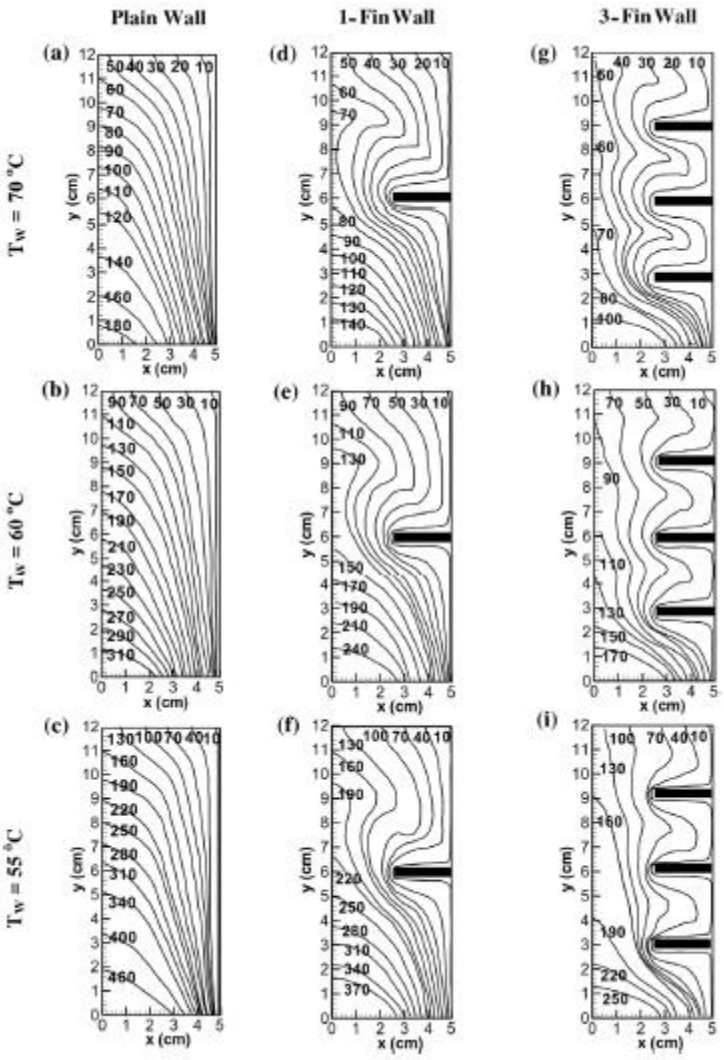

Fig.1.11. Solid–liquid interface progress during the melting of PCM in the finned and unfinned enclosures at different wall temperatures.

A comprehensive study [30] was conducted to analyze the effect of fin material on PCM melting in a rectangular enclosure. Four commonly employed indicators, surface averaged Nusselt number, melting time, total stored energy and mean power, and two proposed, stored energy per mass and cost per energy stored, were used to evaluate the influence of fin material roundly.

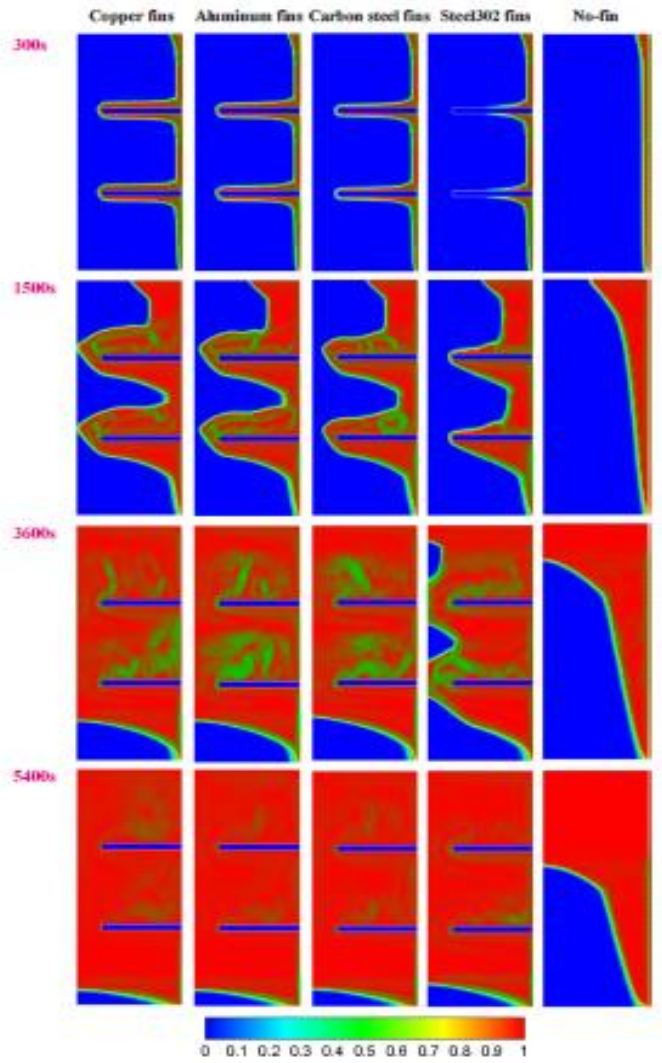

Fig.1.12. Instantaneous liquid fraction contours and velocity vectors for different schemes at the flow time of 300 s, 1500 s, 3600 s and 5400 s.

Results show that compared with the no-fin scheme, the PCM melts faster and the melting time is reduced by 41.6%, 41.0%, 40.1% ,and 37.2% with inserting copper, aluminum, carbon steel ,and steel302 fins. A significant reduction in stored energy per mass is presented by adding fins and the decline range is the highest for the copper fin scheme and the lowest for the aluminum fin scheme, which is 27% and

9.4% respectively. Among the four fin schemes, the cost per energy stored is the largest for the copper, 5.6% higher than the no-fin case. The selection of fin material is affected by adopted indicators. If four commonly used indicators are considered only, the copper and carbon steel fin schemes are highly recommended, while the aluminum fin scheme is highly recommended if six indicators are considered simultaneously. A criterion, selecting fin material with higher thermal conductivity, high specific heat capacity, low density, and low cost as fins, is proposed.

Elevated operating temperatures reduce the efficiency of photovoltaic devices. The use of a phase change material to moderate building-integrated photovoltaic temperature rise has been investigated by experiments and numerical simulations. Experimental data are used to validate the previously developed two-dimensional finite volume heat transfer model conjugated hydrodynamically to solve the Navier–Stokes and energy equations [31]. Temperatures, velocity fields ,and vortex formation within the system were predicted for a variety of configurations using the experimentally validated numerical model. Temperature distributions predicted for different insolation and ambient temperatures at the photovoltaic surface show that the moderation of temperature achieved can lead to significant improvements in the operational efficiency of photovoltaic facades

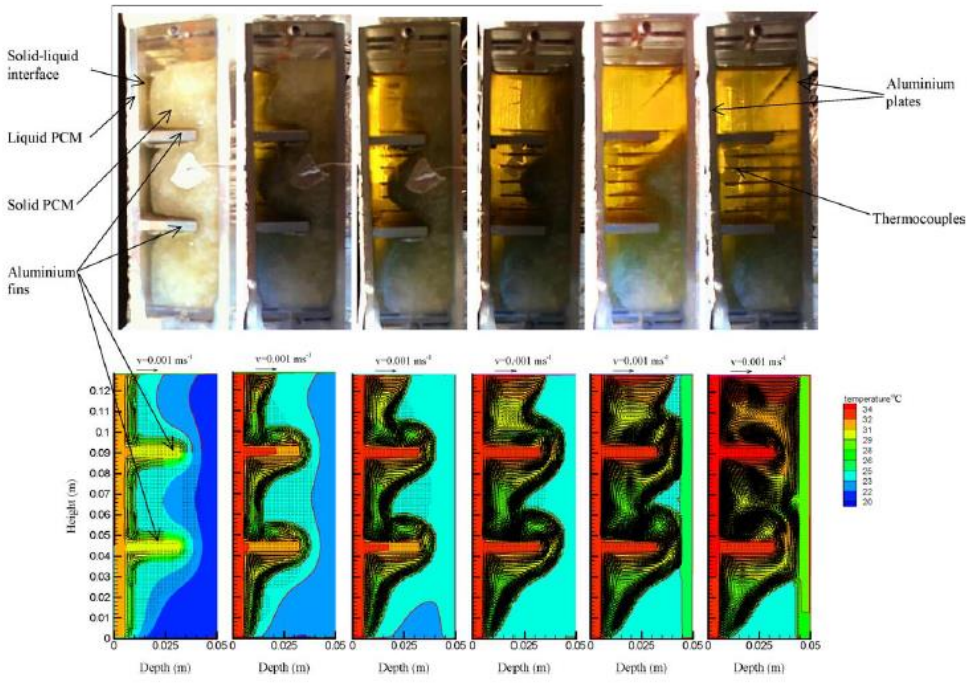

Fig.1.13. Photovoltaic image and predicted isotherms and velocities for a PV/PCM system with fins during the PCM melt process

An experimental study is carried out to analyze the performance of a novel latent heat thermal energy storage (LHTES) unit on charging and discharging processes [32]. A finned tube air heat exchanger is filled with phase change material PCM and enclosed in an insulated storage unit. The experiments showed that the fins can accelerates the time of the start and the end of fusion by about 55 and 72%, respectively. The charging phase can be prolonged to 94%by increasing the power supply by 32%, which also allowed them to store and recover more than 5 times of thermal energy.

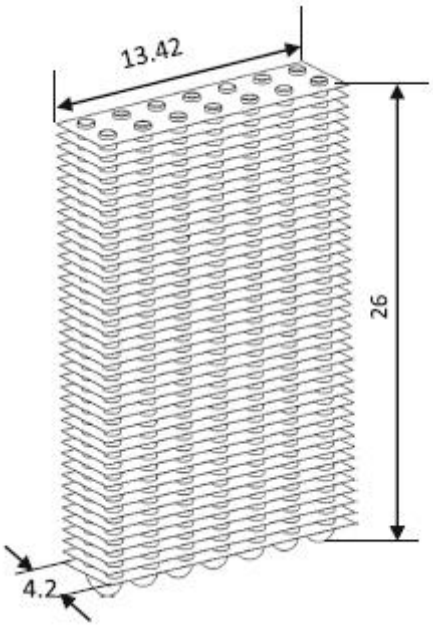

Fig.1.14. Finned U-tubes exchanger (cm) filled with PCMand including Ktype Thermocouples

In this study, enhancement in the melting rate of PCM by the addition of fins in rectangular enclosures was experimentally investigated under different inclination angles by kamkari et al [33]. The melting process of lauric acid in side-heated enclosures with different numbers of fins was evaluated for inclination angles of 90^0 (vertical), 45^0 and 0^0 (horizontal). To visualize the melting process, the enclosure was fabricated from transparent acrylic material except for one side made of an aluminum plate to heat the enclosure isothermally. It was found that for both finned and

unfinned enclosures the melting rate increases by reducing the inclination angle. Heat transfer enhancements obtained by the 0-fin horizontal and 3-fin vertical enclosures compared to the 0-fin vertical enclosure were 115% and 56%, respectively. Among the different cases studied, the 3-fin horizontal enclosure showed the maximum heat transfer rate and consequently the minimum melting time.

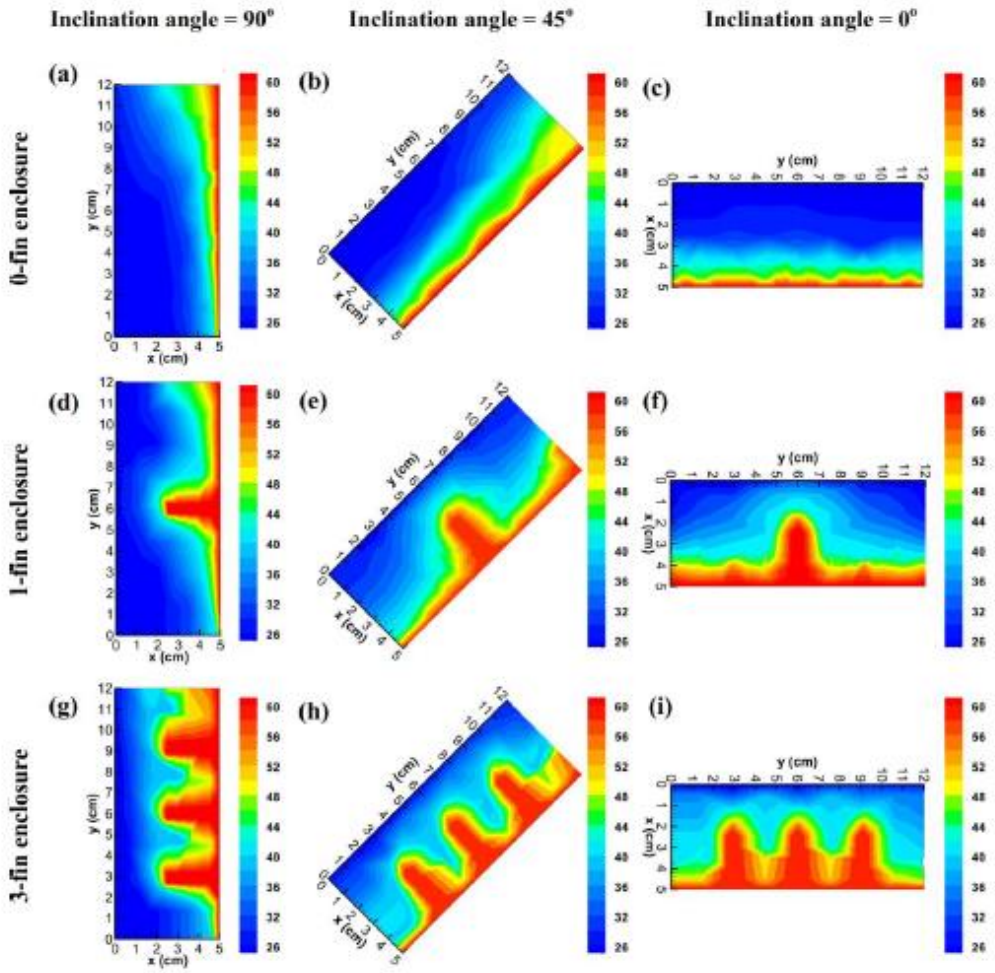

Fig.1.15. Temperature distributions in the finned and unfinned enclosures under different inclination

The aim of this study [34] is to present a correlation to estimate the optimum number of fins and optimum PCM volume fraction in a PCM-based heat sink. Around 900 various geometries of the heat sink in the height range of 10-30 mm, and fin thickness range of 0.2-0.5mm were studied for two different input heat fluxes of 5000 and 10000 W/ m^2 to find the optimal number of fins. The Results reveal that the

optimal number of fins decreases by increasing the fin thickness. The increase in heat sink height results in higher optimal fin spacing, which consequently decreases the optimal number of fins. For a heat sink with constant width, a larger number of fins is required to prevent interfering with thermal performance, as the heat flux increases.

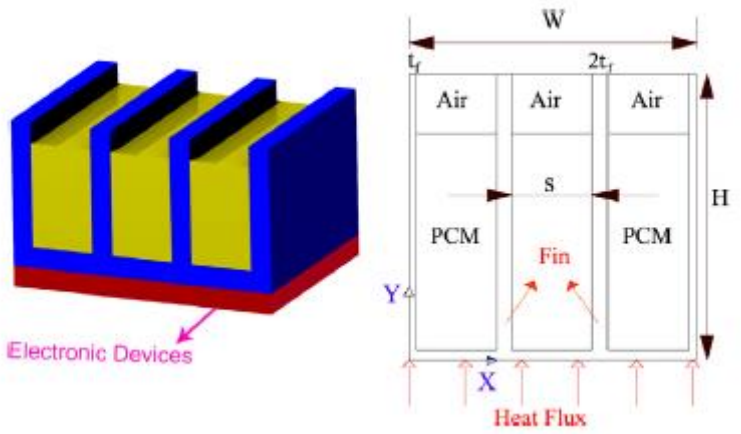

Fig.1.16.A sample of PCM-based heat with two fins and three enclosures.

This paper [35] experimentally studies and compares the addition of fins and the addition of metal wool in latent heat thermal energy storage (TES) systems as heat transfer enhancement techniques. Despite the well-known suitability of fins as an enhancement technique, their implementation cost in the TES system is one of its main drawbacks. Four different latent heat TES systems based on the shell-and-tube heat exchanger concept were designed using n-octadecane as phase change material (PCM). One of them was used as a reference, while in the remaining configurations, the heat transfer surface was increased using of seventeen rectangular fins and by means of metallic wool arbitrarily distributed within the PCM and compacted in a finned shape. The addition of metal wool showed an enhancement, during the charge, higher than 10% when it was arbitrarily distributed while compacting the metal wool in a finned shape showed practically no improvement.

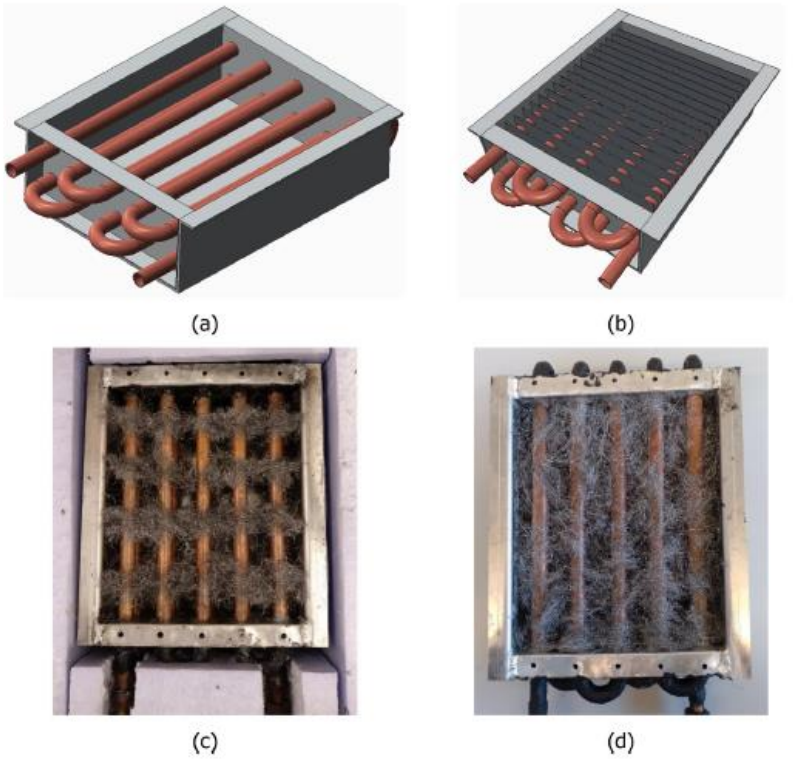

Fig.1.17. Schematic overview and actual pictures of the different latent heat exchangers tested in the present study: (a) HEX_NF: Reference; (b) HEX_17F: With seventeen fins; (c) HEX_MW1: With metallic wool distributed in a finned shape around the HTF tubes bundle; (d) HEX_MW2: With metallic wool arbitrarily distributed around the HTF tubes bundle.

Chi-ming et al [36] combined this study building construction practice, microencapsulated phase change materials (mPCM), and aluminum honeycomb structures to construct an mPCM honeycomb wallboard prototype. The heat transfer characteristics and thermal storage behaviors of this prototype and other modules (mPCM only, mPCM+EG, and mPCM+iron-wire) were investigated experimentally. The results indicated that the aluminum honeycomb used for structural support and enhancing the thermal conductivity in the prototype rapidly transferred the heat flux into the mPCM. Consequently, the latent heat can be used to increase the time lag of the peak load, effectively shifting the peak hours of electricity use in the summer and achieving a lower module surface temperature than other modules. Thus, the mPCM+honeycomb exhibited better control over the surface temperature, which makes it suitable for use in places where the exterior surface temperature must be controlled.

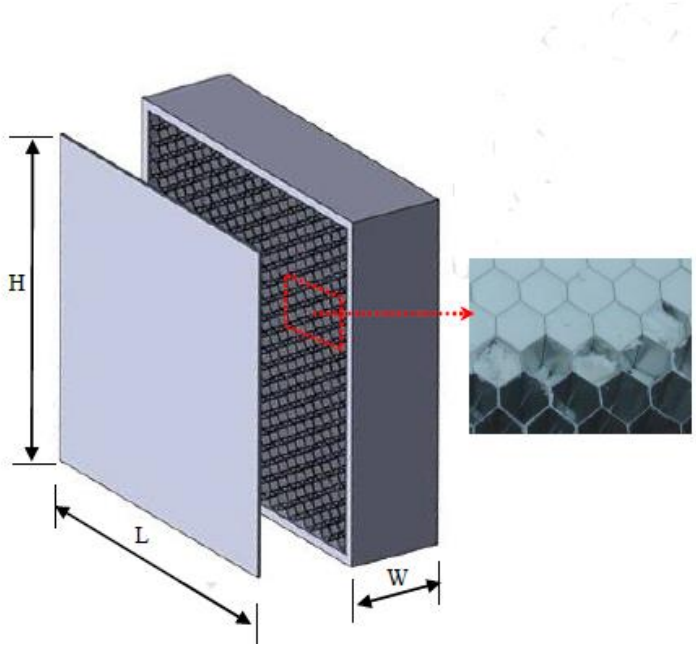

Fig.1.18. Investigated target (mPCM honeycomb wallboard)

The present research [37] is motivated by the need to intensify the buoyancy-driven convection flow in the phase change material to enhance the thermal performance of the system. In this paper, the effect of applying perforated fins on the thermal performance enhancement of a vertical shell and tube latent heat energy storage heat exchanger is experimentally investigated and the results are compared with those of the unfinned and solid finned heat exchangers as the base cases. Lauric acid as the phase change material is placed in the shell side and the water is passed through the inner tube. The fins and tubes were made of copper. The experimental results showed that the time-averaged Nusselt number of the perforated finned heat exchanger is about 30% higher than that of the solid finned heat exchanger due to the minor hindering effect of the perforated fins on the development of the convection flows. Moreover, the total melting time of the perforated finned heat exchanger is about 7% lower than that of the solid finned heat exchanger.

Fig.1.19. Photograph of the unfinned, solid finned and perforated finned HXs

Tay et al [38] experimentally validated a computational fluid dynamics (CFD) model for tubes coiled in a phase change thermal energy storage system has been conducted. Using the validated CFD model, three CFD models have been developed. The first model was developed having pins embedded on a tube with heat transfer fluid (HTF) flowing in it, with PCM surrounding the tube. Different configurations of pins on the tube have been analyzed. The second model developed is similar to the first model; however, fins were embedded instead of pins. Different configurations of fins on the tube were also investigated. The last model developed was a plain copper tube surrounded by PCM with HTF flowing in it. This model was used as a benchmark for comparison of the first two models. The models were analyzed for the freezing process. From this study, it was concluded that fins on the tube are better than pins on the tube.

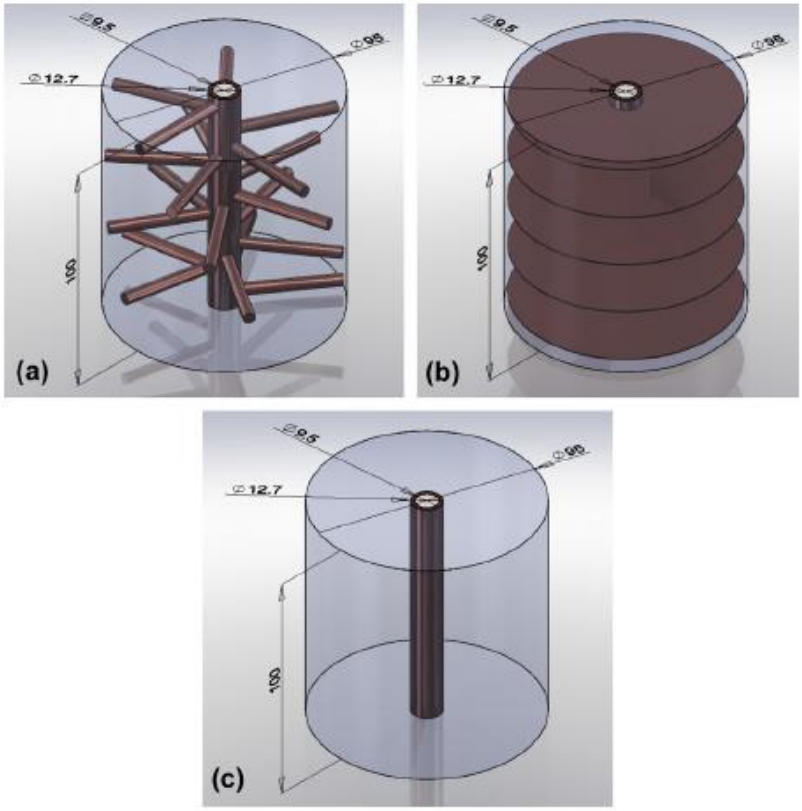

Fig.1.20. Typical schematic of (a) pinned tube, (b) finned tube and (c) plain tube.

In this work [39], a detailed numerical study is carried out to analyze the impact of fin geometry (including fin length, fin-ratio ,and the angle between neighbor fins) and outer tube conductivity the PCM melting process; the influence of the natural convection in the horizontal sleeve-tube unit within the longitudinal fins is further examined. Results show that a small fin ratio can reduce melting time, but not remarkably; the angle between neighbor fins has little impact on the melting process, however, there is an optimization of the angle between neighbor fins to reduce melting time in the full-scale unit. The outer tube conductivity has a great impact on the melting process whether considering the natural convection or not.

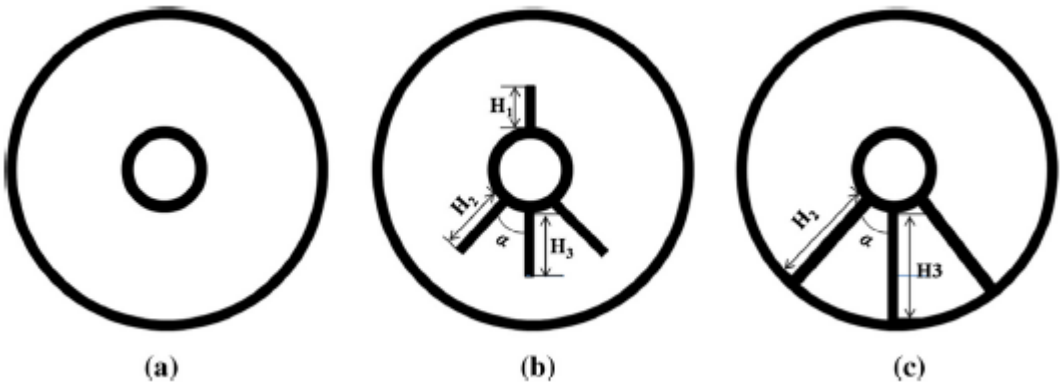

Fig.1.21. Schematic of the sleeve-tube LTES units (a) no fin; (b) four half-scale fins; (c) three full-scale fins.

Aziz et al [40] studied the effect of heat transfer enhancement in thermal energy storage (TES) systems comprising an encapsulated PCM in a sphere. To enhance the performance, the design modification method by the employment of pins and copper plating was adopted and carried out by computational fluid dynamics (CFD) and experimental studies. The phase change times (PCTs) of the systems were analyzed as a performance measure. Consistent with the experimental results, simulation analysis in ANSYS CFX showed that utilizing pins for heat transfer enhancement reduced the PCT of the PCM by 27% while design modification with copper coating and embedded pins reduced the PCT by 37% relative to a plain sphere. These improved results facilitate the use of a conductor and copper plates as an alternative technique for the performance improvement of a PCM encapsulated in a sphere.

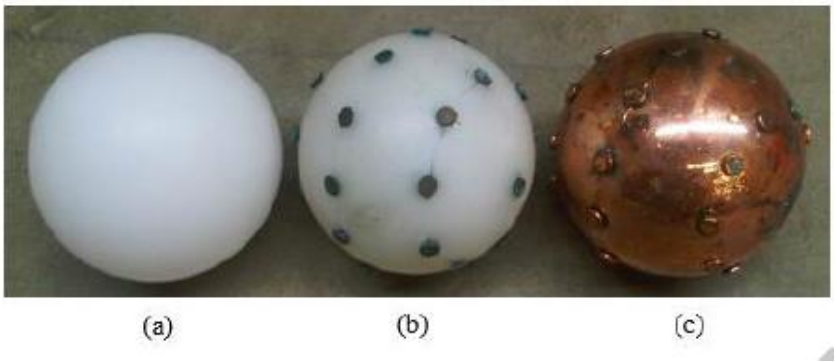

Fig.1.22. Design of modifications made on a plain plastic sphere: (a) **a plain plastic sphere,** (b) **a plain sphere encapsulated with 32 copper pins, and** (c) **a copper-plated sphere with 32 internally built copper pins**

In the present study [41], experiments were conducted to explore and report the effect of fin orientation (orthogonal and circumferential) on the heat transfer enhancement of a PCM filled in a spherical capsule. The temperature profile of paraffin PCM filled in an orthogonal and circumferential internally finned spherical capsule of the charging and discharging process was compared respectively with no fin configuration. The inference from the results is that for the same surface area, an orthogonally oriented fin resulted an appreciable reduction in total time taken for the complete charging/discharging process than the circumferential fin and no fin configuration. The reduction in charging duration of 22 % and 42 % was observed in orthogonal fin orientation compared to circumferential fin and no fin configurations, respectively. Similarly, a 15 % and 38 % reduction in discharging duration was observed in orthogonal fin compared to circumferential fin and no fin configurations, respectively

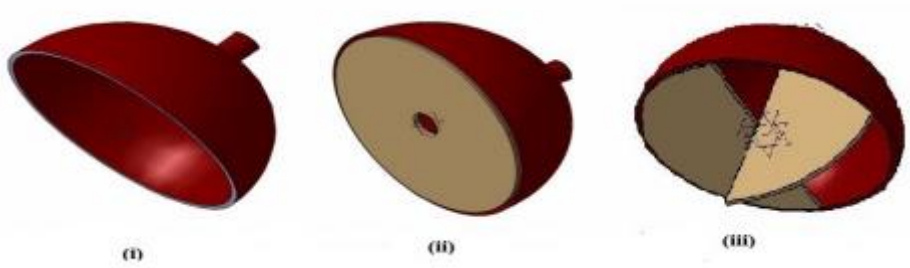

Fig.1.23. Cross section of Spherical container with different fin configurations i) without fin, ii) Circumferentially finned spherical container, iii) Orthogonally finned spherical container

Compared to other enhancement techniques, the amount of experimental studies carried out for fins is significant. Table 1.1 summarizes some of the experimental studies carried out for LHTES systems [43].

Table.1.1. Studies of heat transfer enhancement with fins

Fin geomety	System geometry	Fin material	Nots	Ref
Rectangular	Cylindrical	Aluminum	Solidification time was inversely proportional to the number of fins.	[42]
Rectangular	Rectangular	Steel	Close to 40% decrease in solidification time compared to the base case.	[44]
Rectangular	Rectangular	Aluminum alloy	Increasing the fin height and number of fins increased the thermal performance of the system.	[45]
Rectangular	Shell and tube	Copper	Fin length gives higher PCM charging rate.	[46]
Rectangular	Shell and tube	Brass	12.5%(inlet at 80oC) and 24.52%(inlet at 85oC) decrease in melting time compared to the base case.	[47]
Rectangular	Rectangular shell and tube	Aluminum	Increase in flow rate reduced both melting and solidification time whereas this drop is more significant for the melting than solidification.	[48]
Rectangular	Triplex concentric tubes(TTHX)	Copper	Melting time was decreased by 34.7% for the highest number of fin configuration compared to the base case.	[49]
Rectangular	TTHX	Copper	Solidification time was decreased by 35% highest number of fin configuration compared to the base case.	[50]
Rectangular	TTHX	Copper	The internal-external fin arrangement decreased the melting time by 43.3% compared to the base case.	[51]
Circular	Cylindrical tube	Stainless steel	Heat transfer coefficient was doubled with the use of thick-finned arrangement.	[52]

Table.1.1.(continued)

Circular	Shell and tube	Bronze	The amount of stored energy increases with the increase in fin radius and decrease in fin space.	[53]
Circular/longitudinal	Cylindrical tube	Copper	Enhancement of the heat transfer rate was high in longitudinal fin arrangement compared to the circular fin arrangement.	[54]
Spiral	Cylindrical tube	Copper	Thermal conductivity improvement was three times high compared to the base case.	[55]

All the fin arrangements described in the literature have used metallic PCM containers. Therefore, the tested operating temperatures were below 600^{o}C.

1.3.2 Enhancement with porous materials

Several studies have been done on thermal conductivity improvements by impregnation of PCMs into porous conductive materials [56–58]. Having a porous material with high thermal conductivity makes the overall thermal conductivity of the PCM-porous material combination higher than the pure PCM [57]. Aluminum foam and expanded graphite (EG) are widely used as porous materials to increase the thermal conductivity of PCMs. The improvement is mainly due to their high thermal conductivities and relatively low or medium densities [59].

Righetti et al [60] experimentally investigate the effects of six open-cell aluminum foams and a 3-D periodic aluminum structure during the phase change process of paraffin wax with melting temperatures of 40 °C in a hybrid water thermal storage unit. when the aluminum foams were used, the loading and unloading times were reduced up to twelve times. The tests also permitted to study of the effect of the porosity of the foams; in particular, the loading and unloading times decrease as the porosity decreases. Besides, the 3-D periodic structure obtained by wrapping a sheet

of aluminum net permitted to halving the loading and unloading times as compared to the case of an empty tube. All the cellular structured materials, either stochastic or periodic, also eliminated the issue related to the void volume generation during the solidification process, which usually occurs in the empty tube because of the specific volume change in the liquid-solid phase change.

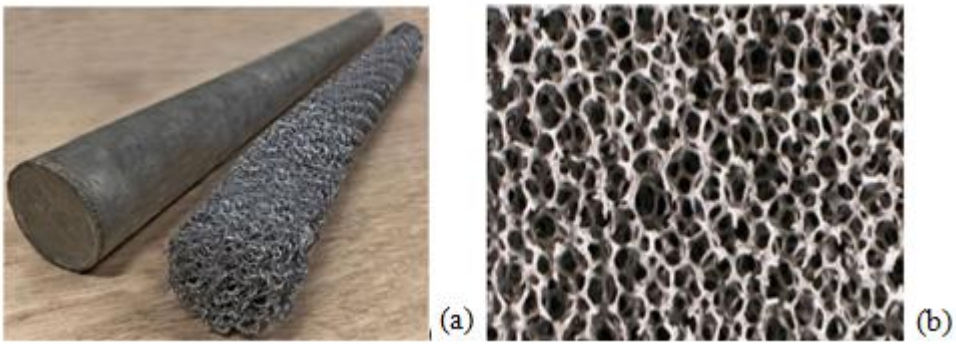

Fig.1.24. Picture of the wrapped tube with porosity of 92% (a).10 PPI aluminum foam (b).

Varun et al [61] highlight an optimal concentration and position of metal foam-PCM composite (MFPC) to elevate thermal performance without altering an overall melting time. Thus, a novel configuration MFPC is proposed according to the optimum thermal conductivity enhancer (TCE) density, a criterion defined based on the temporal variation of local temperature gradient during the melting process. The fundamental principle of the criterion is positioning the metal foam only at the maximum thermal potential region for the effective utilization efficiency of the metal foam. The numerical results showed that the proposed configuration with the provision of MFPC at a high thermal potential region alleviates local conductive transport with enhancement in the overall melting rate. It is seen that the withdrawal of metal mass at low thermal potential region encompasses the beneficial influence of natural convective transport, which is observed to be impeded in the previous configuration.

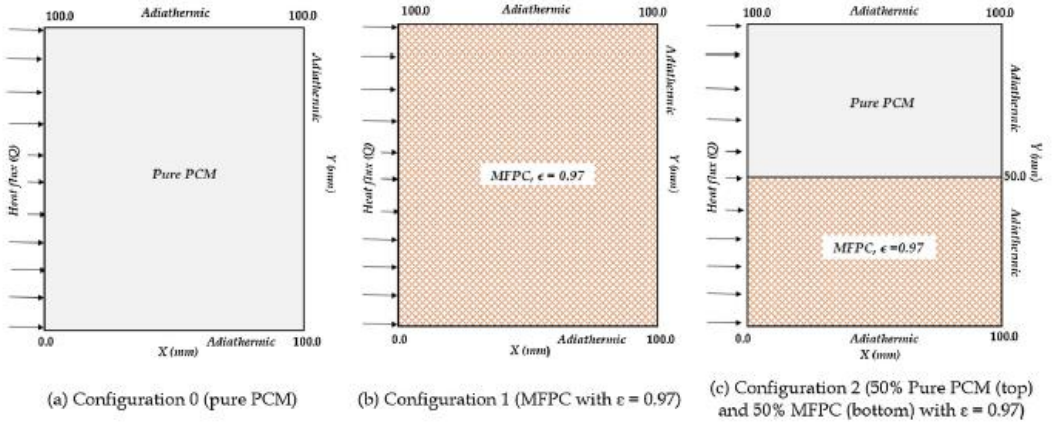

(a) Configuration 0 (pure PCM) (b) Configuration 1 (MFPC with ε = 0.97) (c) Configuration 2 (50% Pure PCM (top) and 50% MFPC (bottom) with ε = 0.97)

Fig.1.25. Schematic of Configuration 2 under the optimum TCE density criterion and reference Configurations 0 and 1.

The present study [62] deals with the melting and solidification of PCM inside a cylindrical container with different shapes of shells and also different arrangements of inner tubes. Nine different cases with an identical amount of PCM are considered for the investigation. Results show that conduction is the dominant mechanism at an earlier time. Later, natural convection has a significant effect on the melting process where PCM at the upper half of the container is melted while a large amount of it is still solid at the lower half. Following this, copper foam is inserted inside PCM to enhance the phase change rate which is solved by the non-equilibrium thermal condition between metal foam and PCM. Inserting metal foam increases the melting and solidification rates up to 92% and 94%, respectively. However, it suppresses the natural convection, especially in melting process.

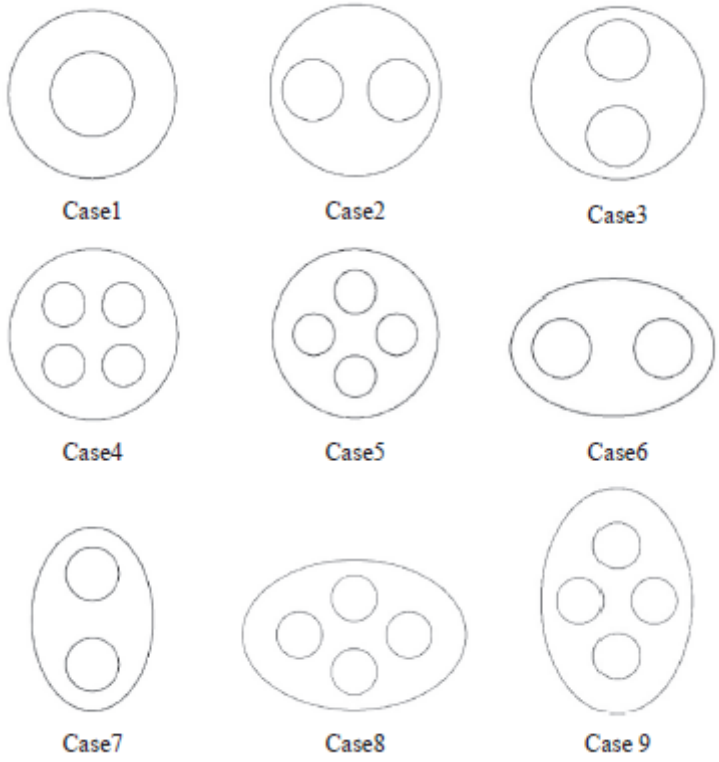

Fig.1.26. Schematic of the investigated cases.

The objective of this numerical study [63] is to develop a latent heat storage (LHS) air heater in both charging and discharging processes to find the geometrical and operating conditions for dwelling space heating. The storage heater aims to provide a uniform output temperature according to the required heating load of a typical room in the required heating hours. The phase change material (PCM) is embedded in a copper porous structure to enhance the rate of heat transfer and overcome the low thermal conductivity of PCMs. The results show the significant advantages of composite metal foam/PCM-air heat exchanger in comparison with the PCM-only unit on both the discharging time (56.5% reduction) and the uniformity of output temperature. The system with a height of 30 cm, PCM ,and air channel thickness of 15 cm and 2 cm, respectively, and a depth of 1 m, is capable to provide the desired output temperature of 47 °C for almost 17.4 h with air mass flow rate of 0.01 kg/s. The charging analyses show that the dimensions of the required rectangular heating element with constant temperature of 100 °C is 15×60 cm located at both sides of the unit.

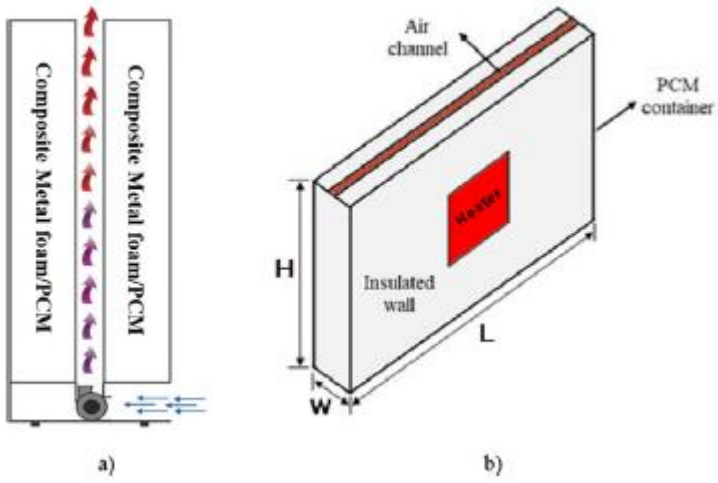

Fig.1.27. The schematic of a composite PCM-air heater in the a) discharging and b) charging process.

A quite a few experimental studies were done on PCM-porous material composite systems, some of which are shown in Table 1.2. [43].

Table.1.2 Studies of heat transfer enhancement by porous materials

Porous material	PCM material	Notes	Ref
Graphite matrix	Paraffin	Thermal conductivity of the composite matrix was 20 times greater than that of the pure PCM.	[64]
Aluminium foam	Paraffin	The inclusion of aluminum foam decreased the discharging duration by 42.42% and charging duration by 15.37%.	[65]
Graphite foams (GFs)	Paraffin	Thickness of ligaments and pore size of the foam are significant parameters in improving the thermal diffusivity and the storage capacity of the system.	[66]

Table.1.2 (continued)

Compressed expanded natural graphite (CENG)	Paraffin	Thermal conductivity improvement of the paraffin/CENG composite was more than 28 times of the pure paraffin.	[67]
Copper porous foam (CPF)	Eicosane (C20H42)	Thermal conductivity was increased from 0.423 W/mK to 3.06 W/mK.	[68]
Copper, steel alloy and EG	NaNO3	Compared to the pure PCM, heat transfer rate was doubled during the solid phase but remained almost same in the liquid phase due to the weakening of natural convection	[69]
Copper foam, copper-steel alloy and EG	NaNO3	heat transfer was improved by foams of copper and copper-steel alloy as well as EG.	[70]
EG	LiNO3–KCl, LiNO3–NaNO3, LiNO3–NaCl	Substantial improvements of thermal conductivity were achieved for the eutectic mixtures.	[71]
Copper foam, Nickel foam	NaNO3-KNO3	Inclusion of metal foam reduced the natural convection of the PCM composite mixture compared to the pure PCM system.	[72]
Expanded graphite (EG)	Paraffin	Thermal conductivity was increased with the increase of mass fraction of EG(2-10%).	[73]

Most of the studies have been done on low-temperature applications. But the noticeable thing is the improvement in discharging time due to the solid phase thermal conductivity improvement. Natural convection was usually prominent during melting in the case of pure molten salt but it was weakened by the use of metal foams or

porous materials. Therefore, the charging time improvement was negated due to the increase in the discharge time in many cases.

1.3.3 Dispersion of high conductivity Nanoparticles

Thermal characteristics such as latent potential during phase shift, supercooling and thermal conductivity of the phase changing materials (PCM) are the crucial parameters, which decide their thermal storage capability. In this current investigation [74], such thermal characteristics of a PCM were studied under the influence of copper oxide (CuO) and aluminum oxide (Al2O3) nanoparticles at a low mass concentration. The nanoparticle doped PCMs were prepared by the way of two-step procedure and named as nPCM 1 and nPCM 2. Then, the required tests had steered with the support of necessary instruments. The results revealed that the supercooling of the PCM was curtailed by 40% and 31.42%, respectively by CuO and Al2O3 nanoparticles. Whereas, PCM's thermal conductivity was enriched by 60.56% and 39.44%, while using CuO and Al2O3 nanoparticles, respectively. Contrariwise, the inherent latent potential concerning to the tested PCM was suppressed meagerly during thermal cycling by the addition of nanoparticles. As a whole, CuO nanoparticles showcased a better improvement in necessary thermal parameters of the PCM in relative to the Al2O3 nanoparticles

In this paper [75], an experimental analysis of organic PCM is conducted. It includes an experimental study of paraffin type organic phase change material while suggesting a way to improve the low thermal conductivity, a feature that is the main disadvantage of especially organic phase change materials. In particular, temperature profiles of PCM for different hot source temperatures are examined, while determining the heat stored in the material and the speed at which the melting front moves under the assumption of uniform movement of the melt interface and solid material. Subsequently, and in order to increase the conductivity of the PCM and thus the rate of evolution, copper and aluminum oxide nanoparticles powder are added and the hybrid PCM is compared in terms of temperature profiles and storage capacity with the pure PCM. The presence of 0.165% Cu nanoparticles reduces the thermal charge duration by 25.3% while the presence of Cu-Al2O3 hybrid nanoparticles at a concentration of $0.165\% - 0.816\%$ reduces the duration by 10.8%.

Fig.1.28. Photograph of Al2O3 nanoparticle powder prior to addition

Fig.1.29. Photograph of Cu nanoparticle powder prior to addition to PCM

In this paper [76]. Paraffin mixed with nanoparticles Al2O3, CuO, and multi walled carbon nanotubes (MWCNTs) were prepared for cooling multiple heat sources. For thermal management of heat sources, performances of the composite phase change materials (PCMs) were investigated at different heating power. Enhanced performance in terms of heat sources temperature, temperature difference between two heat sources, and thermal resistance was experimentally tested and analyzed at various mass fractions of nanoparticle and various power levels. It is found that by using 1.0 w_t% Al2O3 composite PCMs the minimal thermal resistance is achieved at the range from 0.63 C/W to 0.71 C/W for all power levels, and the heat storage and heat conduction of the presented composite PCMs are enhanced as well as the melting ratio.

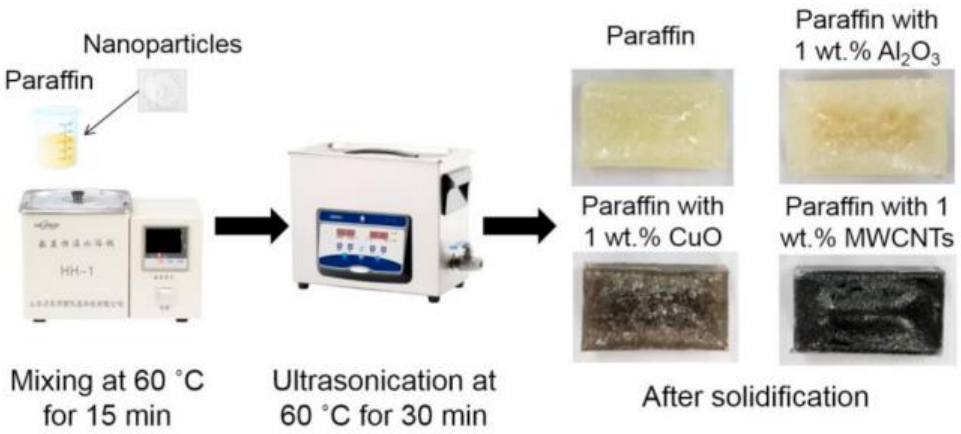

Fig.1.30. Preparation process of the composite PCMs.

A new Evacuated Tube Solar Collector (ETSC) incorporating a Nano-PCM with fins is presented and studied by Elarem et al [77]. The numerical mathematical 2D model of phase change heat transfer is highlighted. The effect of adding nanoparticles of copper (Cu) to paraffin wax on system performance was investigated. The heat transfer during the energy storage process is simulated using the AnsysFluent. The results showed that adding fins has a great effect on the phase change heat transfer of the paraffin in the ETSC. It was noted that the PCM melts faster as the thickness of the fins gets thinner. Also, the addition of 1% of Cu to the PCM was found to be the optimum mass concentration at which the HTF outlet temperature increased by 2 K. Moreover, it was found that the ultimate flow rate that caused the entire mass of the PCM to melt is 0.003 kg/s.

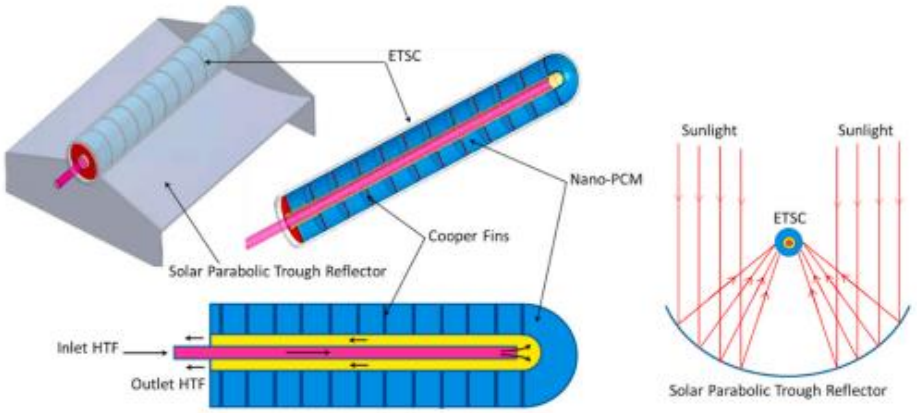

Fig.1.31. The physical model of the ETSC with Solar Parabolic Trough Reflector system, and the longitudinal section of the ETSC.

In this study [78], the charging process of vertical shell-tube latent heat storage (LHS) system with two heat transfer fluid (HTF) injection orientations was investigated. A two-dimensional numerical model based on the finite volume method (FVM) was developed and verified with the experimental data. The PCM melting with pure conduction mode is regarded as a reference for analyzing the heat transfer characteristics. Results show that heat transfer is stronger for top injected HTF during the convection dominant stage, and the bottom injected HTF offers better heat transfer during the last conduction stage. The effects of PCM thickness to height ratio (R) and nanoparticles concentration (ϕ) were investigated. It is found that the melting time for

the bottom injected HTF is shorter compared to the top injected HTF when R less than 0.050, and longer when R > 0.050. The nanoparticles provides better enhancement on PCM melting with bottom injection HTF. It is also found the enhancement potential of nanoparticles is weakened with the increase of R. Furthermore, R = 0.05 is recommended for maximizing thermal performance.

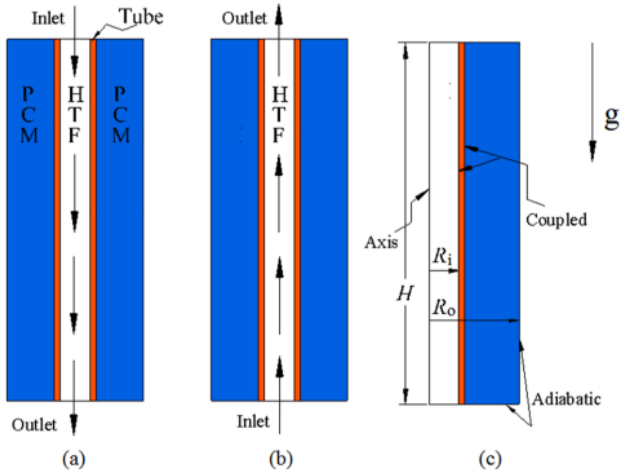

Fig.1.32. Schematic diagram of vertical shell-tube LHS unit with HTF from (a) top, (b) bottom injections, and (c) computational domain.

Table 1.3 summarizes some of the experimental studies on thermal conductivity improvement of PCMs containing nanoparticles. [43].

Table.1.3. Studies of nanoparticles use in PCM systems

Nanoparticle	PCM type	Notes	Ref
Al2O3 nanoparticles	*n-octadecane*	The natural convection heat transfer in the melted region degraded with the increase of nanoparticles.	[79]
TiO2 nanoparticles	*n*-octadecane	The maximum improvement happened at 3 wt% of nanoparticles in the mixture. Increasing over 4 wt% reduced the thermal conductivity in the liquid phase.	[80]
Carbon nanotubes(CNTs) & nanofibers(CNFs)	Paraffin and soy wax	The enhancement of thermal conductivity is high in CNF mixtures in contrast to CNT mixtures.	[81]

Table.1.3. (continued)

CNT	Palmitic(PA)–stearic acid(SA)	The thermal conductivity was increased by close to 20%, 26%, 26% and 30% for the CNT mass fractions of 5 wt%, 6 wt%, 7 wt% and 8 wt% respectively.	[82]
Single and multi-walled carbon nanotubes	Paraffin	A highest enhancement of close to 13% was achieved for the PCM containing single-walled carbon nanotubes.	[83]
Multi-walled carbon nanotubes(MWCNT)	Palmitic acid	Thermal conductivity improvement was 36% in the solid state and 56% in the liquid states for the mixture of 5 wt% MWCNT and PCM.	[84]
MWCNT	Paraffin	Thermal conductivity improvement was 35% in the solid state and 45% in the liquid states for the mixture of 2 wt% MWCNT and PCM.	[85]
MWCNT/graphite	Paraffin	MWCNTs were more effective compared to graphite as a thermal conductivity enhancer.	[86]
MWCNT/CNF/graphene nanoplatelets(GNPs)	Paraffin	PCM with GNPs showed the highest thermal conductivity enhancement of 164% at 5 wt%.	[87]
GNPs	Lauric acid	The thermal conductivity improvement by GNP(1 vol%) was close to 230% compared to the base case.	[88]
Cu nanowires	Tetradecanol	The overall thermal conductivity increased with the increase of Cu nanowires	[89]
CuO nanoparticles	KNO3/NaNO3/ KNO3-NaNO3 eutectic	Substantial improvements in thermal conductivity were achieved for both the eutectic salt and pure nitrate salts with the addition of nanoparticles.	[90]

Thermal Energy Storage with PCM

2.1 Introduction

A drastic change in the climate due to the emission of greenhouse gasses, growing need for energy, and diminishing reserves of fossil fuel incline mankind towards sustainable and clean energy resources such as solar energy. Even though it is available in abundance, its intermittent nature hinders its widespread implementation as a cost-effective and reliable energy resource. Efficient energy storage is essential to overcome this problem. Out of all available energy storage techniques, thermal energy storage shows the greatest potential as it is a simple, cost-effective, efficient, and reliable method [91].

2.2 Thermal Energy Storage

Thermal energy storage (TES) is a technology that can enable greater and more efficient use of these fluctuating energy sources by matching the energy supply with the demand, as it consists of stocking thermal energy by heating a material (the "storage medium") capable to release the thermal energy stored at a later time . In this way, this technology can help balance energy consumption and reduce peak demand, CO2 emissions, and costs, while increasing the overall efficiency of energy systems [92][93].

2.2.1 Categories of Thermal Energy Storage

TES can be classified into three different categories. These are mentioned in Figure.2.1 and discussed in the following sections [94].

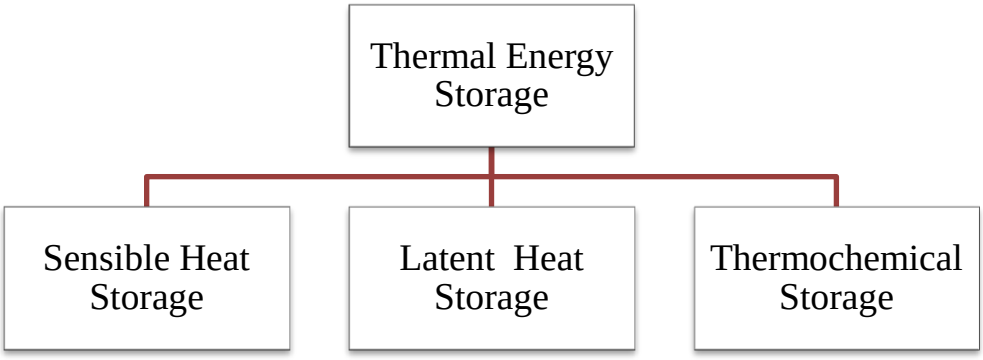

Fig.2.1. Category of thermal energy storage

2.2.1.1 Sensible Heat Storage

The energy storage capacity of sensible heat storage (SHS) depends on the temperature difference between the inlet ,and outlet, the specific heat capacity of the storage material and the total mass of the storage media. [95].This type of storage is extensively investigated and used commercially in power plants [96, 97]. It is expressed by the formula

$$Q = \int_{T_i}^{T_f} mC_p \, dT = mC_p(T_f - T_i) \qquad (2.1)$$

Q = amount of heat (kJ)

m = mass of storage material (kg)

Cp = specific heat capacity (kJ/ kg ^{0}C)

T_i = initial temperatures of SHS (^{0}C)

T_f= final temperatures of SHS (^{0}C)

2.2.1.2 Latent Heat Storage

Latent heat storage occurs when a material changes its phase from one physical state to another. When heating/cooling, a material that undergoes this phenomenon and releases/absorbs heat in a narrow temperature range is called phase change material (PCM). Four types of phase transition exist [98]: solid-solid (crystalline heat), solid-liquid (fusion heat), liquid-gas (vaporization heat), and solid-gas (sublimation heat). Among them, PCM based on solid-liquid transition is widely used in TES for its simplicity and wide temperature availability [99][100][101][102]. As explained in Figure 2.2, the material changes its phase from solid to liquid when temperature increases, and more amount of heat is exchanged during the latent storage in comparison to the sensible storage for the same temperature change.

The stored energy of PCM in different heating stages is calculated as:

$$Q = \int_{T_1}^{T_2} mC_{p.s} \, dT \qquad (T_2 < T_m) \qquad (2.2)$$

$$Q = \int_{T_1}^{T_m} m.C_{p.s}.dT + m.\Delta H_m \qquad (T_2 = T_m) \qquad (2.3)$$

$$Q = \int_{T_1}^{T_m} m.C_{p.s}.dT + m.\Delta H_m + \int_{T_m}^{T_2} m.C_{p.l}.dT \qquad (T_m < T_2) \qquad (2.4)$$

Where:

T_m = the phase change temperature.

ΔH_m = the phase change enthalpy.

$C_{p.c}$ = the heat capacity of solid phase PCM.

$C_{p.l}$ = the heat capacity of liquid phase PCM.

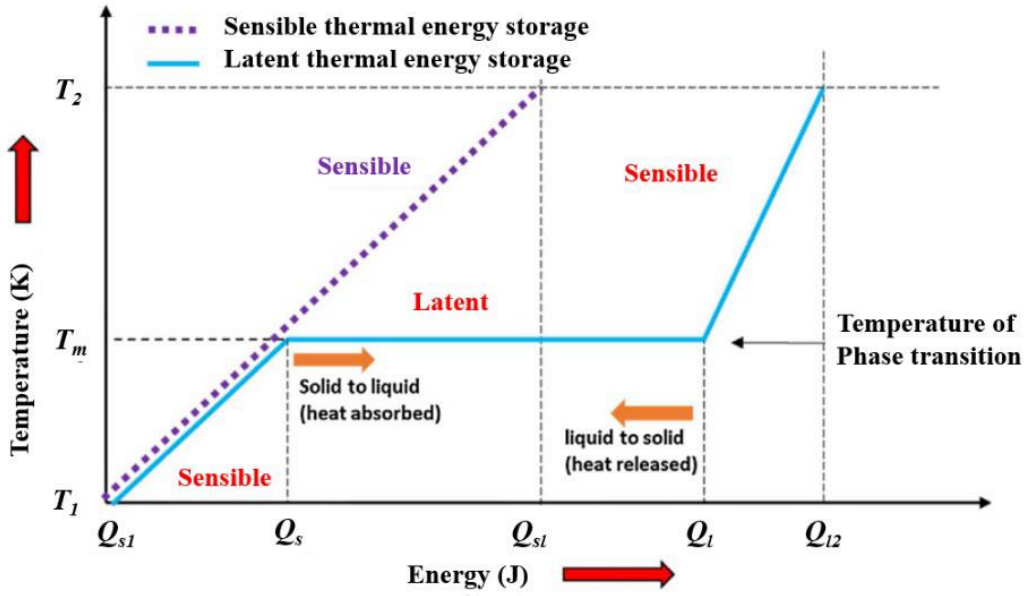

Fig.2.2. Phase change temperature profiles of solid-liquid transition [103][104].

The phase change temperature of PCM commonly maintains a relatively stable value, allowing a constant temperature heat exchange for process control. But in some real cases, the phase change does not happen in a such stable platform and there is a small temperature range in phase transition appears [103]. When calculating the apparent heat capacity, the latent heat depends on transient temperature due to this temperature range [105][106][107][108].“Subcooling” (or supercooling) is another phenomenon that when PCM begins to solidify and release heat, the initial freezing temperature is below the melting temperature, caused by the nucleation rate [109][110].

2.2.1.3 Thermochemical Storage

Chemical heat storage relies on reversible chemical reactions, during which the energy is absorbed or released by breaking or reforming chemical bonds [111]. It is an emerging field presenting the advantages of high energy density, with compact and long-term storage potential. On the other hand, it is more expensive and technically complex to implement compared with sensible and latent heat storage technology.

Chemical heat storage can be divided into thermochemical and sorption processes: the first one is based on the energy released and absorbed during the breaking and the formation of molecular bonds for completely reversible chemical reactions, while sorption systems involve adsorption and absorption processes.

During thermochemical processes, thermal energy can be absorbed when the endothermic dissociation of a material (C) takes place, constituting the charging procedure. This process leads to the formation of two separate components (A and B), which have different properties and can be stored at ambient temperature for long periods with few or no thermal losses.

Finally, the discharging process occurs when the reversed procedure is performed and components A and B are mixed through an exothermic reaction that leads to the reformation of the initial material C. The described procedures can be represented by the following equation:

$$C + heat \rightleftharpoons A + B \qquad (2.5)$$

Where C is the thermochemical material and A and B are the reactants.

Conserning sorption processes, adsorption takes place when a molecular or atomic layer is shaped, following the accumulation of an adsorptive on the surface of an adsorbent, while absorption consists in the formation of a solution which is occurring when a substance is distributed into a liquid or solid [112].

2.2.2 Comparison of different types of TES

The different thermal storage types 8sensible, latent, thermochemical) are suitable for different applications. The main factors affecting the suitability are the storage time (daily, long term, seasonal), the economic viability and the operating conditions. Table 2.1 shows the Comparison of different types of TES

In order, to select a TES system for a determined application several criteria have to be taken into account, such as technical, economic ,and environmental criteria [113], [114]. The technical criteria include storage capacity, lifespan, size, resources used, the efficiency, safety, etc. The economic requirements are mainly the system cost and the commercial availability. And finally, the environmental criteria require that the used materials are non-toxic or hazardous and must not cause adverse effects on the environment during the production, the distribution, the installation or operation [115].

Table.2.1. Comparison of different types of TES based on various performance parameters [120]

Performance parameter	Type of Thermal Energy Storage		
	Sensible TES	**Latent TES**	**Chemical TES (Sorption and thermochemical)**
Temperature range	Up to : 110 ^{0}C (water tanks) 50^{0}C (aquifers and ground storage) 400 ^{0}C (concrete)	20-40 ^{0}C (paraffin) 30-80 ^{0}C (salt hydrates)	20-200 ^{0}C
Storage density	Low (with high temperature interval):0.2 GJ/m^3(for typical water tanks)	Moderate (with low temperature interval): 0.3-0.5 GJ/m^3	Normally high : 0.5-3 GJ/m^3
Lifetime	Long	Often limited due to storage material cycling	Depends on reactant degradation and side reactions
Technology status	Available commercially	Available commercially for some temperatures and materials	Generally not Available , but undergoing

Table.2.1 (continued)

Advantages	Low cost Reliable Simple application With available materials	Medium storage density Small volumes Short distance Transport possibility	High storage density Low heat losses (storage at ambient temperatures) Long storage period Long distance transport possibility Highly compact Energy storage
Disadvantages	Significant heat loss over time (depending on level of insulation) Large volume needed	Low heat conductivity Corrosivity of materials Significant heat losses (depending on level of insulation)	High capital costs Technically complex

Currently, regarding the state of development, storage capability, commercial availability and durability, the developmental degree of the three TES types is visually depicted in Figure 2.3 [116].

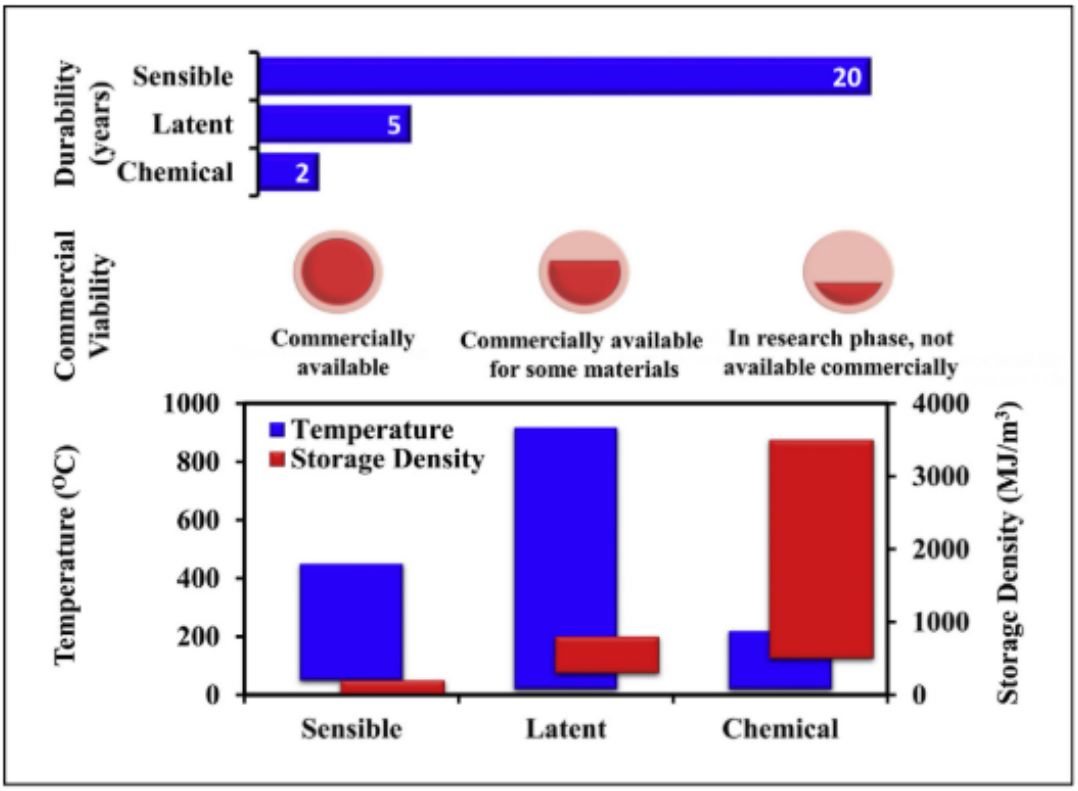

Fig.2.3. Storage capabilities, commercial viabilities and durability aspects of PCM for thermal energy storage [116]

The sensible TES has been traditionally used even the storage density is not optimal due to the simplicity of its use and plenty availability in nature, it poses the longer durability and is fully commercially available.

Latent heat TES can be used at very different temperatures, depending on the selected PCM, and it provides the largest temperature operational range of the three types. It has a good storage density compared to sensible TES. Even though it has been studied during the last decades, the developmental degree do not yet fulfill the market needs. One of the main reasons for this situation is the lack of PCM materials to satisfy all the requisites needed, and other important one are the high prices that the storage device can reach for commercialization [117].

The thermochemical TES pose the higher storage densities, however pose very short durability and is not commercially available because it is still a developing technology, but very promising for the future [118]–[119].

2.3 Phase change material

When a material undergoes a change of phase, an endothermic or exothermic process occurs, leading the material to store or release a considerably high amount of energy in the form of heat, which generally occurs at a single temperature or within a fixed range of temperature. This type of heat is known as latent heat; the heat storage capacity per unit mass during a phase change is inherent to each material [121].

The concept of phase change materials circumscribes those materials that undergo a solid liquid transformation at a temperature within the operating range of a selected thermal application [122]. Their attractiveness lies in the fact that they can store a significant amount of energy in small volumes while remaining at an almost constant temperature. This attractiveness represents the major advantage of these materials as storage mediums if compared with thermal storage by sensible heat, where we need a broad temperature difference or large volumes to achieve considerable heat storage.

The PCM can be found in a wide range of temperatures and chemical compositions, whereby they can be used for numerous applications, such as [123]: building air conditioning, electronics cooling, waste heat recovery, textiles, preservation of food, solar energy storage, fabrics, and other

2.3.1 Classification of PCM types

Over the last 40 years, different classes of materials, including hydrates salts, paraffin waxes, fatty acids, eutectic of organics and inorganic compounds, and polymers have been considered as potential PCM. Abhat [124] in 1983 classified PCM into two categories: organic and inorganic materials. Later in 2009, Sharma et al. [125], extended this classification into three categories: organic, inorganic and eutectic, with subcategories in each of them, as shown in figure 2.4 [125], [126]. In this section we present a brief description of those categories:

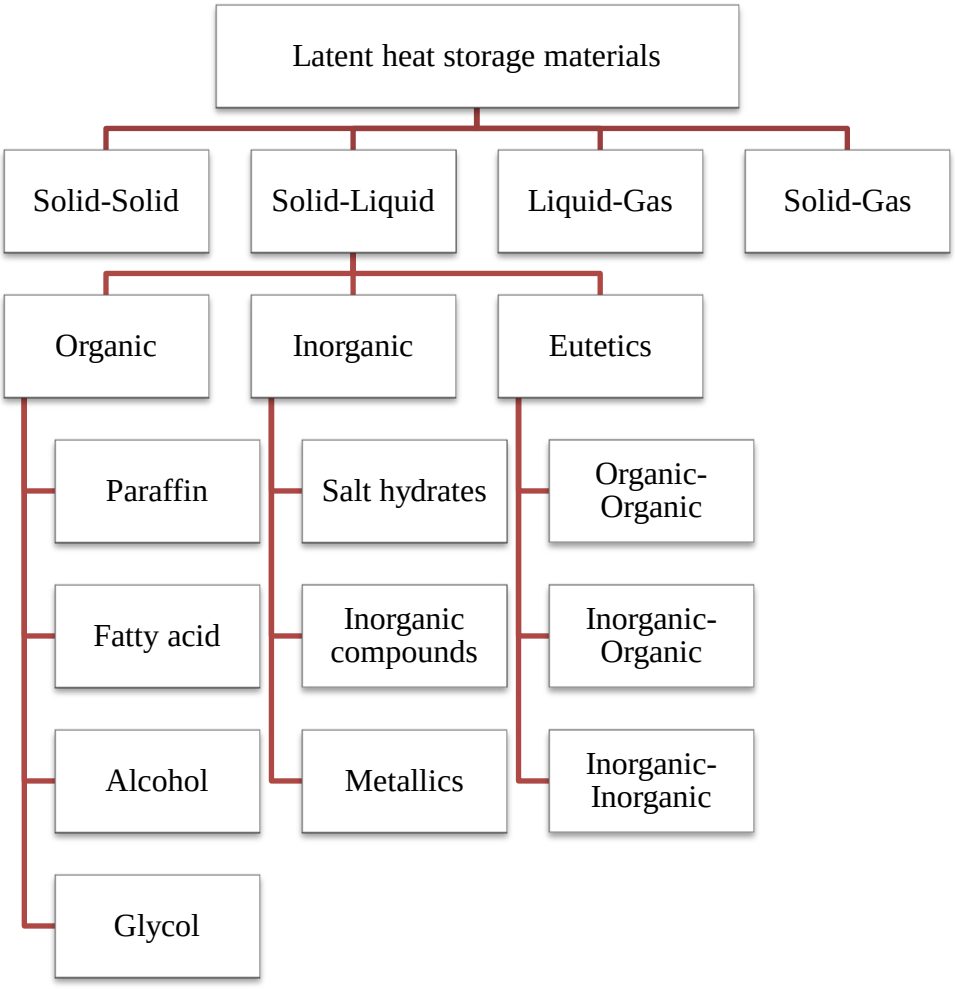

Fig.2.4. Classification of latent heat storage materials

2.3.1.1 Organic materials

Organic PCM are further described as paraffin and non-paraffins. They present congruent melting, which means that melting and solidification repeatedly occur without phase segregation and degradation of their latent heat of fusion; also they present little or no supercooling effects, and they are usually noncorrosive materials. These organic PCMs are sub-divided into the following categories [121]:

- ***Paraffin***. They consist of a mixture of *n*-chain alkanes CH3 — (CH2)— CH3. Paraffin is available in a large temperature range as shown in figure 2.5 , which makes them attractive for several thermal applications. They also present a reasonable cost, predictable behavior, and reliability, they are non-corrosive, and chemically inert below 500 °C. The commercial use of paraffin comes from the distillation of crude oil. Although their use as thermal storage material is attractive, they present some drawbacks such as low thermal conductivity, and in some cases, they are not compatible with plastic containers [121].

- ***Non-paraffin.*** In this group are included materials such as esters, fatty acids, alcohols, and glycols. They are the most numerous of the phase change materials with highly varied properties, representing the largest category of candidate materials for phase change storage [125]. Among their properties, we have a high heat of fusion, low thermal conductivity, varying levels of toxicity, inflammability and instability at high temperatures. From this group, the fatty acids are attractive for thermal energy storage due to their higher heat of fusion, compared to paraffin. These PCMs also show reproducible behaviors during melting and solidification, with no supercooling. However, their cost is about 2-2,5 times the cost of paraffin [121].

2.3.1.2 Inorganic materials

They are further classified as salt hydrate and metallics.

- ***Salt hydrates.*** These materials are alloys of inorganic salts and water forming a typical crystalline solid of the formula AB-nH_2O. Since most of the hydrated salts present poor nucleating properties, they show supercooling in the liquid before

solidification. Their most attractive properties are their high latent heat of fusion per unit volume, relatively high thermal conductivity and small volume changes on melting. Some of them present congruent behaviors, while others are incongruent. The major issue with them is that most of the salt hydrates that are suitable as storage materials melt incongruent [121].

- ***Metallics.*** In This category are included low melting metals and metals eutectic. Their major advantage is their high thermal conductivity. although, they present major issues as storage materials such as their generally high weight, low heat of fusion per volume until ,and low specific heat [121].

2.3.1.3 Eutectic materials

Eutectic materials are made from a minimum melting composition of two or more components, each of which melts and freezes congruently. During the crystallization phase, a mixture of the components is formed, hence acting as a single component. Their major attractiveness is their ability to obtain more desired properties such as a specific melting point or a higher heat storage capacity per unit volume [127]. The thermophysical properties of eutectic are still a field for further investigations for thermal energy storage as many combinations have yet to be tested and proved.

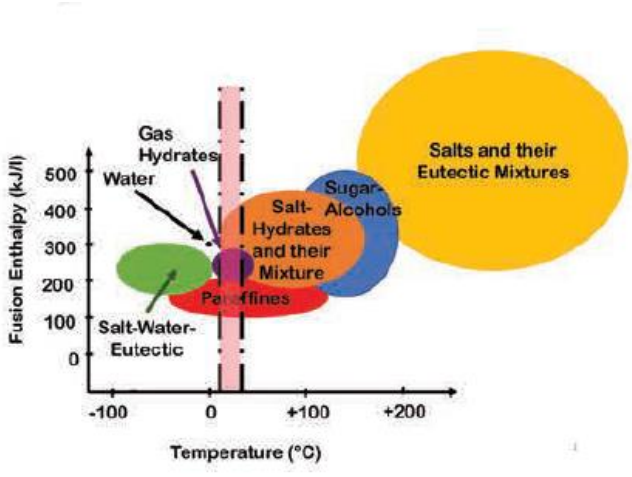

Fig.2.5. Different types of PCM according to their melting temperature and enthalpy

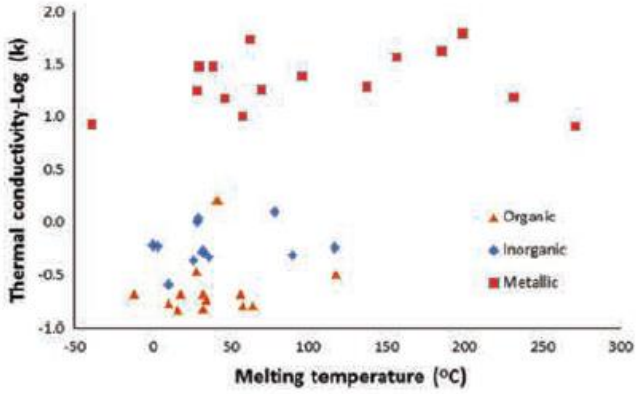

Fig.2.6. Thermal conductivity distribution for different types of PCM

The final selection of the PCM material would depend on several factors, including cost, thermal, mechanic, kinetic, physical and chemical properties, which are related to the final application in which the material is going to be used. To highlight the advantages, and disadvantages of these materials, Kalnæs and Jelle [127] gathered the principal features of each type of material. These features are summarized in Table 2.2.

Table.2.2. Overview of the advantages and disadvantages of each PCM group of materials (developed by Kalnæs and jelle

Organic	Inorganic	Eutectic
Advantages		
▪ No supercooling ▪ No phase segregation ▪ Large temperature range ▪ Compatible with conventional construction materials ▪ Chemically stable ▪ Recyclable ▪ High heat of fusion	▪ High volumetric latent heat storage capacity ▪ Higher thermal conductivity than organic PCM ▪ Low cost ▪ Non-flammable ▪ Sharpe phase change	▪ Sharp melting points ▪ Properties can match specific requirements

Table.2.2 (continued)

Disadvantages		
▪ Flammable ▪ Low thermal conductivity ▪ Low volumetric latent heat storage capacity	▪ Corrosive to metals ▪ Phase segregation ▪ Supercooling ▪ High volume change	▪ Limited data and information ▪ High cost

Comparing the PCM types, commercial paraffin is the expensive and has a considerable thermal storage density (200 kJ/kg or 150 MJ/m3). Furthermore, it has a low or negligible supercooling effect, and is chemically, physically, and thermally stable. PCM with these characteristics are available within a range of temperatures and can be incorporated into building solutions [128]. The main problem is the low thermal conductivity (the mean value for paraffin is 0.2 W/mK even though some commercial organic PCM solutions present thermal conductivity values up to 0.8 W/mK).

Hydrated salts have the highest thermal storage capacity comparatively to paraffin- based solutions, however ,they are chemically unstable and when they are heated to high temperatures, they degrade losing a percentage of their water content for every heating cycle [129].

2.3.2 Phase Change Material Selection

Similar to the materials used in sensible heat TES, PCMs must comply with specific criteria for appropriate utilization in TES. For example, there are some standard requirements between the two sensible and latent heat materials, such as significant thermal heat capacity, conductivity, stability under cycling, and cost efficient [130].

Furthermore, PCMs have to satisfy special rules related to their natures, for example, the amount of latent heat of fusion, melting point, the density difference between liquid and solid phases, and compatibility with the encapsulation materials. Various researchers suggested categorizing the mostly required properties for PCM in

TES into five aspects: thermal, physical, kinetic, chemical, and economic aspects. Table 2.3 lists the most commonly prescribed PCM features for use in TES [131].

Table.2.3.Prescribed features to use PCM in TES

Criteria	Descriptions
Thermal	• Phase change temperature within the operating temperature of the application • High enthalpy of fusion • Significant volumetric heat capacity • Suitable thermal conductivity for both phases
Physical	• Significant surface for heat exchange • Minimum density difference between liquid-solid phases • Low vapor pressure
Kinetic	• Lowest possible subcooling • Suitable crystallization rate
Chemical	• Stable with minimal material decomposition and properties deviation during the projected lifetime under thermal cycling • Nontoxic • Comply with the fire safety rules • Compatible with its encapsulation materials (minimal corrosion) during the project lifetime
Economical	• Sufficient supply is available with economical prices

The phase transition temperature of the PCM must match the operating temperature for the desired application. High enthalpy of fusion and the high density would provide a high energy per volume of PCM material. This minimizes the size of the storage containers and the amount of PCM used. A higher specific heat would increase the sensible energy portion of the storage, and a high thermal conductivity would reduce the charging and discharging times [132].

The small volume expansion during phase transition is necessary for designing simpler and more cost-effective containment or encapsulation methods. Low vapor pressures reduce the contamination and ease the encapsulation process. To prevent irreversible segregation, the PCMs must melt congruently.

Supercooling interferes with the extraction of energy and is very common in salt hydrates. It is essential to minimize the supercooling effect as much as possible in thermal cyclic operations to get the best out of the discharge cycle [133]. The selected PCM should display good chemical stability and corrosion resistance. PCMs can also degrade as a result of crystallization due to water loss, decomposition ,or chemical reactions with the containers. Toxicity and flammability must be considered for safety measures, and finally, the commercial availability and cost should be evaluated since the final TES system must be cost-effective and comparable with existing storage systems [51].

2.3.3 PCM disadvantages

PCMs have excellent advantages. However, they come with functional challenges such as low thermal conductivity and subcooling, as well as corrosion, high cost of materials, the extra cost of the envelope, non-isotropic melting, degradation of thermo-physical properties under long cycling, and volume changing due to density differences between phases [135]. The two mostly addressed disadvantages are low thermal conductivity and subcooling.

2.3.3.1 Low thermal conductivity

The performance of TES using PCM is influenced by the thermal conductivity of the material [136]. The charging process is expected to prolong when low thermal conductivity is presented in the PCM due to the slow movement of the melting front within the PCM. Furthermore, the energy-retrieving process during discharge is less

efficient due to thermal diffusion losses within the material itself in addition to the slow movement of the melting front in the PCM, which is both caused by the low PCM's thermal conductivity.

The Low thermal conductivity characterizes most PCMs, except for metallic based materials. The lowest thermal conductivity is found in organic based PCMs, followed by inorganic-based PCMs [136].

Figure 2.4 plots the thermal conductivities of potential PCMs for high temperature applications as a function of melting temperature for eutectics, hydroxides, nitrates, bromides, carbonates, chlorides, and fluorides. It shows that most of these molten salts have conductivity below 2 W/m.K. Moreover, Na2CO3 attracts attention in the multi-tower solar array because it has a high melting temperature [138].

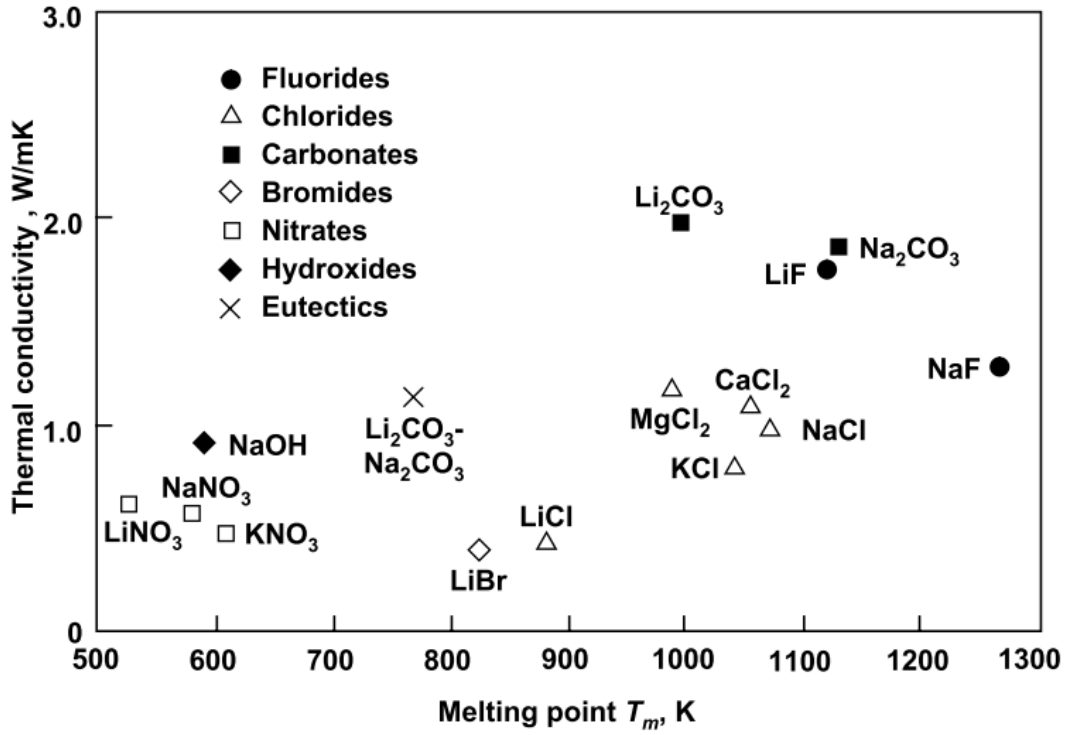

Fig.2.7. Thermal conductivity for high-temperature PCMs [138]

2.3.3.2 Subcooling

Most PCMs demonstrate hysteresis behavior during the phase change process [139]. This phenomenon is often called sub-cooling (or undercooling) in the Liquid-Solid phase change. Subcooling causes the inverse phase change to occur at a different temperature than the original temperature that caused it. The same

phenomenon is called superheating in Gas-Liquid phase change [140]. The subcooling in PCM is analyzed by using a Differential-Scanning-Calorimetry (DSC) device [141]. Subcooling is illustrated in Figure 2.8 in two materials paraffin and hexadecane-water emulsion. The figure plots the heat flow during the heating and cooling process against measured temperatures for both materials. The paraffin shows a lower degree of subcooling. It starts melting at nearly 18ºC, and it starts its solidification at about 15ºC. While the water emulsion demonstrates a more significant subcooling, it starts the melting process at 18ºC and freezes at near zero. The shape of that curve is different for the same material, which reflects a different response to melting compared to solidification.

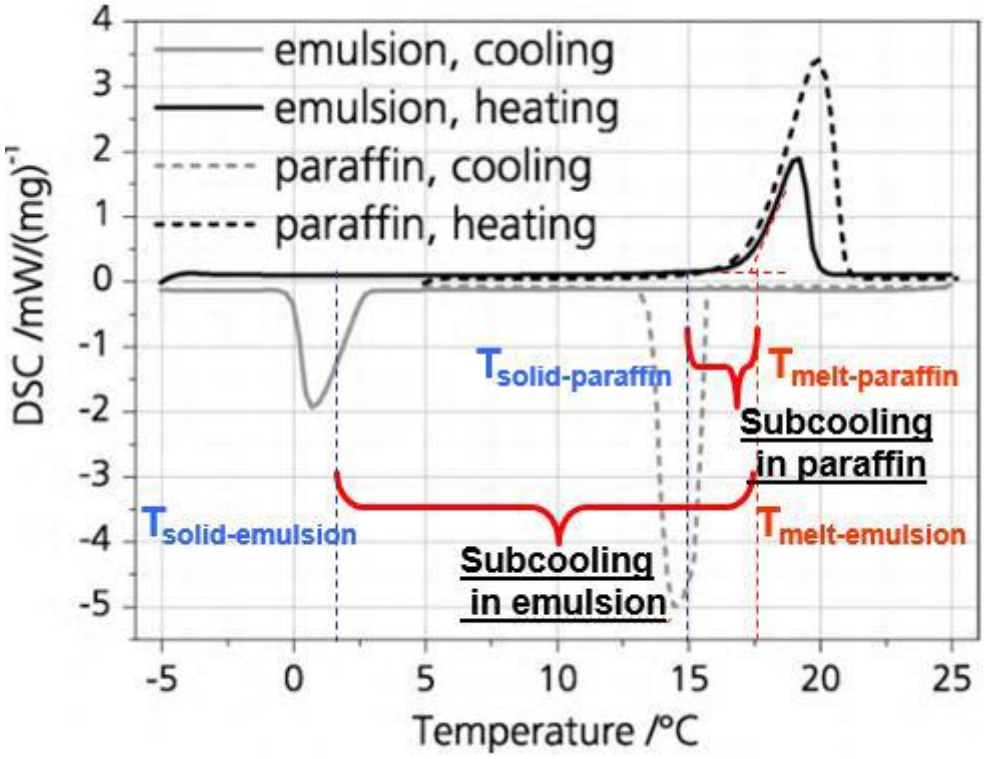

Fig.2.8. DCS Heat flow for two PCMs paraffin and water emulsion

Even though the temperature ascends to the melting temperature again, this influence is not required in TES because it degrades the quality of stored energy [142]. Water, which is one of the most used PCMs, could solidify at a temperature range between -4~-7ºC under atmospheric pressure but melts at 0ºC [143].

The subcooling in PCM is mainly influenced by material properties, amount of material, rate of heating and cooling, and the roughness of the PCM container. Faucheux et al. [144] evaluated the influence of the capsule surface roughness on the water-ethanol PCM solidification process. They found that increasing the roughness of the PCM envelope reduces the subcooling. Furthermore, A. Safari et al. [143] reported that the higher the cooling rate, the higher the subcooling.

2.3.4 Method of PCM Containment

To ensure a long-lasting and efficient LHTES system, the method of PCM containment is critical. PCMs are typically placed in cylindrical [145,146,147] or rectangular-shaped containers [145,148] . The most analyzed LHTES arrangement is the shell and tube configuration[149–150].

The method of PCM containment has a direct impact on the heat transfer rate of the overall system, thus affecting the charge and discharge times and the thermal performance of the LHTES system. Appropriate PCM container geometry coupled with the right heat enhancement technique can provide better overall performance for the LHTES system.

2.3.4.1 Heat Enhancement Techniques for LHTES

As stated earlier, most PCMs, except metals or metal alloys, have low thermal conductivity and as a result, would lead to slow charging and discharging rates.The thermal conductivity of non-metal PCMs usually falls below 0.6 W/m.K range [151,152]. Initial melting of a PCM in the charging cycle enables a natural convection driven process, thus making it comparatively faster than the discharging process [153]. The impact of having low thermal conductivity is prominent during the solidification process as it forms a solid layer at the inner surface of the capsule, thus making it a conduction driven process. Agyenim et al.[154] listed several techniques to improve the heat transfer rate for LHTES systems. Figure 2.6 shows the drawings and pictures of some of the heat transfer enhancement techniques that were reviewed in this study.

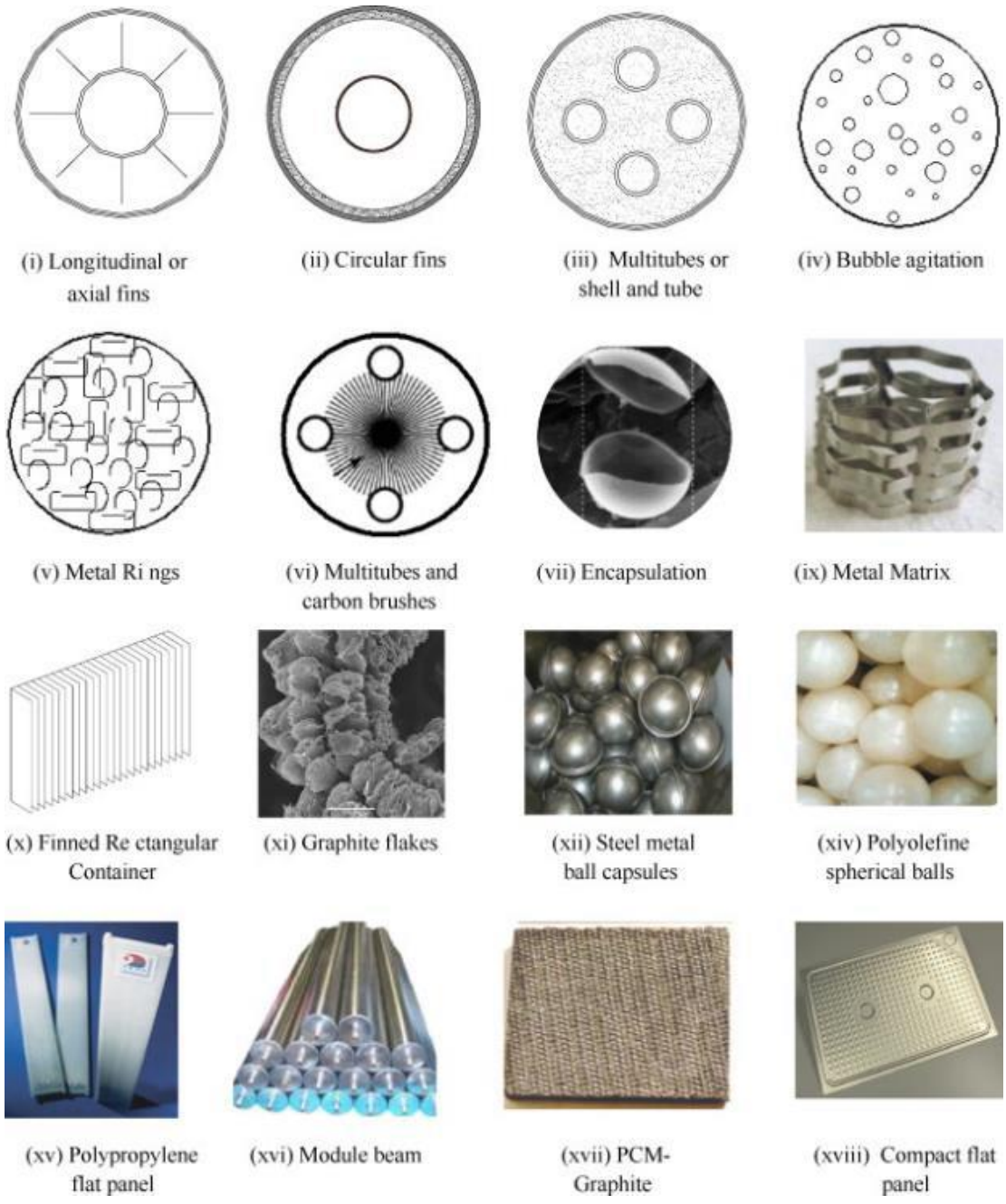

Fig.2.9 .Various heat transfer enhancement techniques [155].

Ibrahim et al. [156] separated the enhancement techniques into three categories and reviewed the recent developments in each category.

Table.2.4. Thermal enhancements for LHTES [156]

Heat transfer enhancement	Thermal conductivity enhancement	Combined techniques for heat transfer enhancement
• **Embedded fins** • **Heat pipes** • **Multiple PCMs** • **Encapsulation**	• Dispersion of high conductivity nanoparticles • Porous materials • Low-density , high conductive materials	• Finned heat pipes • Combined heat pipe-metal foil • Fins with multiple PCMs

Out of all the techniques, the most popular enhancement technique is the use of extended surfaces such as fins.

2.3.4.1.1 Use of Fins

Due to the simplicity, low cost ,and ease of fabrication, a majority of the heat enhancement techniques have been based on fins. Fins are typically used to increase the effective heat transfer area between HTF and PCM and therefore enhance the thermal performance of the TES system.

Thermal conductivity, corrosion potential with HTF/PCM, cost ,and density are usually the crucial parameters when it comes to the selection of fin materials [157]. Materials like aluminum, copper, and graphite foil are selected primarily for their high thermal conductivity (over 100 W/m.K), and materials like carbon steel are selected due to their low cost. Stainless steel is also used as a fin material because of its corrosion resistance [157].

Several studies have been done on fins of different configurations in LHTES systems. There are two standard configurations of fins in LHTES systems [157]:

1. Systems that involve heat storage and retrieval through a HTF
2. Systems that serve as a heat sink/reservoir through hot/cold boundary wall

In heat sink type-LHTES (no HTF), the fins are located inside the PCM. Even with the HTF, the fins are usually embedded in the material with the lower relative thermal conductivity, which in most cases is the PCM side [158].

Melting and solidification process dynamics influence the configuration and orientation of the fin [159]. Lacroix and Benmadda [160] conducted research on the horizontal fin configuration in a rectangular boxes and concluded that instead of having a larger number of short fins, it is more effective to have fewer long fins in the system. Optimization of the number of fins depends on the wall temperature. Shatikian et al. [161] found that the performance of the enhancement depends upon the optimization of both the number of fins and thickness. Steinmann [161] tested aluminum fins in NaNO3 PCM for 400 hours and found that aluminum fins are compatible with NaNO3. Other materials like graphite foil, steel , and copper can also be employed as the fin material.

2.3.4.1.2 Use of Heat Pipes

A heat pipe (HP) can deal with high heat transfers as its operation involves phase change (evaporation and condensation). Some researchers analyzed the improvement in the charging and discharging processes of PCM with the use of HP [163–164]. Gravity assisted and wick assisted are some of the common types of heat pipes. Operating temperature range, geometric size, and configuration of the TES system are some of the key parameters for the selection of HPs for TES systems. One typical configuration of storage systems that can adopt HPs for heat transfer enhancement is the shell and tube type TES.

A large number of numerical studies were carried out on analyzing the effect of HP configuration, orientation, and number of HPs on the thermal performance of LHTES systems, but the experimental studies were limited [163–165,167,164]. Robak et al. [166] experimentally compared the effect of HP and fins in a LHTES system and found that the overall melting rates for the heat pipe systems were, on average, 70% greater than the non-HP setup and 50% greater than the system with fins. Tiari et al. [168] used a primary central heat pipe with an array of secondary heat pipes for a PCM containing a vertical cylindrical type container. Both melting and solidifying behaviors were analyzed with the use of photographic images as well as internal temperature measurements. Increasing the incoming hot HTF flow rate from 1.89 L/min to 7.57 L/min led to a 30% improvement in the charging process. Increasing the temperature of the incoming HTF from 63 °C to 73 °C during charging resulted in

55% reduction in the system's charging time. Both of the experimental works mentioned above are for low temperature applications. No experimental studies have been reported in the literature for high temperature applications using this technique.

2.3.4.1.3 Multiple PCM Systems

Multi-PCM-based LHTES refers to using several PCMs with various melting points in the storage system. Employing multiple PCMs with decreasing melting points ensures a higher temperature difference between the HTF and the PCM in the flow direction, which will lead to higher heat transfer performance of the system [169]. Wang et al. [170] were the first group to introduce a novel technique to enhance the heat transfer rate. Michels and Pitz-Paal [171] conducted an experimental exploration of multiple PCMs in shell and tube configuration. Synthetic oil was used as the HTF and allowed to go through the tube and three PCMs were placed in the shell side. It was found from the experiment that single PCM storage with a higher melting point has a lower storage/retrieval capacity compared with multi-PCM storage with three PCMs. Charging and discharging experiments were demonstrated with three different melting point PCMs by Farid and Kanzawa [172]. They observed an improvement of ten percent in the heat transfer rate. Cylindrical enclosures were used to load three different PCMs and the air was used as HTF. In the case of the multi-PCM system, all the PCM started melting at the same time whereas for single capsules, it started at different times. Multi PCM system is one of the more efficient ways to improve the performance of the system by enhancing the heat transfer rate. However, the selection of the right combination of PCMs is still a challenge [173].

2.3.4.1.4 Dispersion of High Conductivity Nanoparticles

Dispersing particles in the PCM is one of the most efficient and simplest ways to enhance the conductivity of the PCM [173]. Hoover [174] is the pioneer of researching particle impregnation techniques to improve thermal conductivity. Khodadadi et al. [175] conducted an extensive review on the enhancement of the heat transfer rate by dispersing particles in the PCM. Lots of materials have been employed as the particles such as metals (Ag, Cu, and Al), metal oxides (Al2O3, MgO, CuO ,and TiO2), carbon nanotubes, graphite, silver nanowires, and carbon

based nanoparticles (graphene flakes) [175]. Mettawee and Assassa [176] conducted an experimental investigation to improve the thermal conductivity of PCM by dispersion of micro aluminum particles. It was found that there was a sixty percent reduction in the charging time as compared to pure PCM by adding the particle Zeng et al. [176] investigated the effect of silver

nanoparticles in 1-tetra decanol and found that silver nanoparticles did not show any strong reaction with 1-tetradecanol. Overall, the thermal conductivity of the PCM increased with the increase of silver nanoparticles. Xie et al.[178], Hong et al.[179] , Weinstein et al. [180] , Zeng et al. [181], and Kim and Drzal [182] employed alumina (Al2O3), MgO, graphite nanofibers, multi-walled carbon nanotubes, and exfoliated graphite nanoplatelets, respectively and all observed the enhancement of the heat transfer rate. Recently, researchers have shown great interest in graphene to improve the thermal conductivity of PCM [183-184].

Khodadadi and Hosseinizadeh [185] reported that the overall latent heat of the PCM composite decreased with the increasing wt% of the particles, though the thermal conductivity of the composite increased. Hence, optimization of the mass fraction of the particle and latent heat of the PCM is quite important.

2.3.4.1.5 Enhancement with Porous Materials

Porous matrices made of steel, stainless steel, aluminum, copper, and graphite can be impregnated in the PCM based LHTES to enhance the heat transfer rate. Mesalhy et al. [186] numerically investigated a horizontal cylindrical annulus structure and concluded that the performance of the enhancement technique depends upon the pore size and the thermal conductivity of the material in the matrix. Recently, Fiedler et al. [187] compared aluminum and copper based porous matrices and found that the copper matrix had approximately 80% more effective thermal conductivity than the aluminum matrix. Even though the melting and solidification time of the storage material reduces by employing the metal structures significantly, compatibility of the PCM and the porous structure has always been an issue.

2.3.4.1.6 Dispersion of Low-density Materials

Metal particles are usually denser than the PCM and as a result distributing them in the PCM is hard. The enhancement expected from these metal particles would be hindered by having these particles settled at the bottom of the PCM container. One alternative technique is to use low-density high conductivity particles. Carbon fiber is one such substitute for high-density metal particles. Carbon fiber has a relatively low density, and its thermal performance is in the same range as copper and aluminum [188].

Fukai et al. [189] experimentally tested the improvement of thermal conductivity in a carbon fiber-paraffin system. Carbon fibers were tested for two orientations; random and brush type. The brush type gave the best performance and it was found that the effect of fiber length on the thermal performance was minimal. Hamada et al. [190] tested the effects of carbon-fiber chips and carbon brushes in low-temperature n-octadecane PCM systems and found that heat transfer improvement for the carbon brusher was higher than the fiber chips arrangement.

2.3.4.1.7 Combined Techniques for Heat Transfer Improvement

The approach of combining two or more heat transfer techniques to achieve more enhancement in the overall thermal performance has become more popular in the recent past. Table 2.5 shows some of the experimental studies of combined heat transfer technique used in LHTES systems [51].

Table.2.5. Studies of combined heat techniques in LHTES systems

Combined methods	System geometry	Notes	**Ref**
Fins & heat pipe(HP)	Rectangular heat pipe heat exchanger	The rate of energy retrieval from the PCM was increased by 86% and the effectiveness of HP was increased by 24%.	[192]
Fins & HP	Rectangular heat pipe heat exchanger	The amount of energy stored was increased by 140% in the 12-HP configuration compared to the base case.	[193]
HP & metal foil	Cylindrical enclosure	Melting and solidification rates were doubled in contrast to the HP only system.	[194]

Table.2.5 (continued)

Copper form & fins	Rectangular container	The thermal conductivity improvement was 3.7 times that of the system without fins.	[195]
HP & metal foam, HP & metal foil	Cylindrical enclosure	High melting and solidification rates were achieved with both HP with foil arrangement and HP with foam arrangement.	[196]
Macro-encapsulation & foam, Macro-encapsulation & sponge	Cylindrical capsules	The effective conductivity improvement with foam was 15% and with sponge was 32%.	[197]

This area of research is still developing, and so far a majority of the studies have been focused on finned-HP type enhancements. The combination of encapsulation with IR absorbing particles [191] was investigated and later adopted in this study to further improve the heat transfer of encapsulation.

2.3.4.2 Encapsulation

Encapsulation can overcome the low thermal conductivity of a PCM by reducing the path length and increasing the surface area for heat transfer. Encapsulation is typically done by covering the PCM with a suitable coating or shell material [195]. The use of proper encapsulation has the following advantages [199,200]:

- Enhancement of heat transfer rate by increasing the effective surface area
- Isolation of the PCM from HTF and the container vessel.
- Potential for greater exergetic efficiency with the use of a cascaded PCM arrangement
- Enhancement in thermal and mechanical stability of the system
- Reduction in tankage cost

Encapsulated phase change materials (EPCM) are small capsules with the PCM in its core [201]. Different shapes and sizes of EPCM have been adopted for different applications. Based on size, encapsulated PCMs can be classified into the following:

- Nano-encapsulation (0-1000 nm)
- Micro-encapsulation (1-1000 μm)
- Macro-encapsulation (above 1 mm)

Considerable work has been carried out on micro encapsulation of the low melting point (50-120 ^{o}C) inorganic salt hydrates and organic materials such as waxes, terpenes, low molecular weight polymers, etc [202-203]. Compared to macroencapsulation, the microencapsulation of PCMs provides faster charging and discharging rates because of the shorter distance for heat transfer. However, the lower PCM-to-coating mass ratio (~1:1) greatly reduces the energy storage density of the storage media and increases the storage capital cost [204]. Recently, Zhang et al. [205] encapsulated NaNO3/KNO3 PCM in AISI 321 tubular capsules. Zheng et al. [206] fabricated spherical capsules with copper as the PCM and chromium-nickel as the shell material. The fabricated capsules have been shown to withstand 1000 thermal cycles. Vincent and Silva [207] tested paraffin wax in rectangular steel shells in horizontally hollow brick for 8 days. Zhao [208] and Zheng et al. [209] have reported an encapsulation technique that uses stainless steel/carbon steel as the shell material. The process follows a post-formed approach where cylindrical steel capsules are fabricated first and then filled with PCM followed by welding a cap at the top. The major challenge in this approach is countering the corrosion of the metal cans from the molten salt at high temperatures. Mathur et al. [210] have demonstrated a ceramic-based macro encapsulation technique for sodium nitrate pellets (5-15 mm in diameter). The technique involves the decomposition of a sacrificial polymer layer to provide a void between the coating and core PCM, which is needed for accommodating the expansion of the PCM during the phase transition period.

2.3.5 Physical phenomena during phase change

Whether we are studying melting or solidification, phase change results in a complex problem mainly because it involves the presence of more than one phase, creating a boundary between them, that varies in time and space. If our goal is to ease the designing and use of PCM systems, we should provide users with tools that, despite the complexities of the process, can acceptably predict the behavior and performance without going into tedious methods. To achieve this, we need a deep understanding of the phenomena so that these phenomena can be simplified without affecting their effect on phase change [121].

According to Regin [211], the heat transfer analysis of the phase change problem is much more complicated than single phase problems due to :

- The non-linearity of the problem resulting from the motion of the solid-liquid interface during phase change.
- Inadequate knowledge of the heat transfer process at the solid-liquid interface, because of the buoyancy-driven natural convection in the liquid PCM.
- Uncertainty of the interface thermal resistance between the container and the solid PCM.
- Volume change with the change of phase (upon shrinkage).
- The presence of voids in the solid PCM.

Several physical phenomena are inherent to PCM during melting and solidification. Their effects in phase change and therefore, in the modeling of these processes vary according to the specific conditions of the problem, such as the shape of containers, storage material, geometry arrangement, thermal applications among others, which leads to retain or discard such phenomena under certain circumstances. In here we briefly mention the most important phenomena to be retained.

1. ***Moving solid-liquid interface.***

The position of the solid-liquid interface not only distinguishes one phase from the other, but it also reflects the quantity of the PCM that has already melted or solidified at a certain instant. This measure is of great importance because it can reveal the amount of heat that has been stored or discharged from the PCM. This is probably the most important feature to determine during phase change [212], leading to the need for a prediction of this parameter as accurate as possible.

2. ***Density change in phase change.***

During the phase change, we can identify two types of density changes in the material [213]: (*i*) due to change of temperature in a phase, since density depends on the temperature, and (*ii*) due to the difference between the solid and liquid density at the melting temperature. Solid density is usually higher for most PCM, whereas the water is a notable exception [212]. When melting occurs, the PCM occupies more volume, increasing the pressure on the container; whereas for solidification, when shrinkage occurs, the PCM occupy less volume, under-pressurizing the container. This last entails void formation (bubbles or gaps from the vapor of the material and other gases) within the PCM. These voids are more likely to be formed between the PCM and the container since the weakest forces of adhesion are between them.

3. Buoyancy effects in the melt region.

The temperature difference not only leads to a change in the density of the PCM, but it also induces flows in the liquid PCM due to the presence of gravity, promoting the natural convection. These flow interactions with the remaining solid, create 2-D melting patterns. These patterns are linked to the amount of PCM remaining on the process by a certain instant; therefore, it should be addressed when studying phase change. The role of natural convection in solidification is much less important and in many cases may be discarded [212].

4. Phase change over a wide temperature range.

Pure substances offer a sharply, well defined phase change temperature, which is desirable for most of the thermal applications since the temperature of operation can be well predicted. However, these materials present a high cost, making them impractical solutions as a storage material. Nevertheless, there are commercial PCM that present attractive phase change temperature ranges. In either way, this parameter must be taken into account during the design and modeling of PCM systems.

5. Enthalpy hysteresis.

Some PCM can present subcooling or superheating effects during phase change, where phase change does not occur at the expected temperature. For instance, for building applications, this is a phenomenon which should be avoided in the PCM. Melting and solidification for several shapes of containers and PCM have been widely studied. The first to acknowledge the moving boundary problem of phase change was Jožef Stefan, and since then, this problem has been called the "*Stefan Problem*."

Usually, if we want to understand a physical problem, we resort to experimental and analytical approaches to accomplish this task. The problem with the analytical solutions for the Stefan problem is that they are mostly available for one-dimensional cases, and for simple boundary conditions. They have been addressed in the literature, especially in heat transfer textbooks as the theoretical solution of phase change problems [214], [213], [136].

Experimental Procedure

3.1 Introduction

Phase change processes are progressively used in nature and in various fields of science and engineering. As a result, there is a very extensive literature on the variety of these problems. The objective of this chapter is to develop an experimental study in which two test benches are carried out. The experimental procedure and the various measuring instruments used are presented in this chapter. All the experiments are carried out at the energy and applied thermal laboratory (ETAP) at the University of Tlemcen.

3.2 Improvement of paraffin melting process using different metal additives

3.2.1 Presentation of the experimental setup

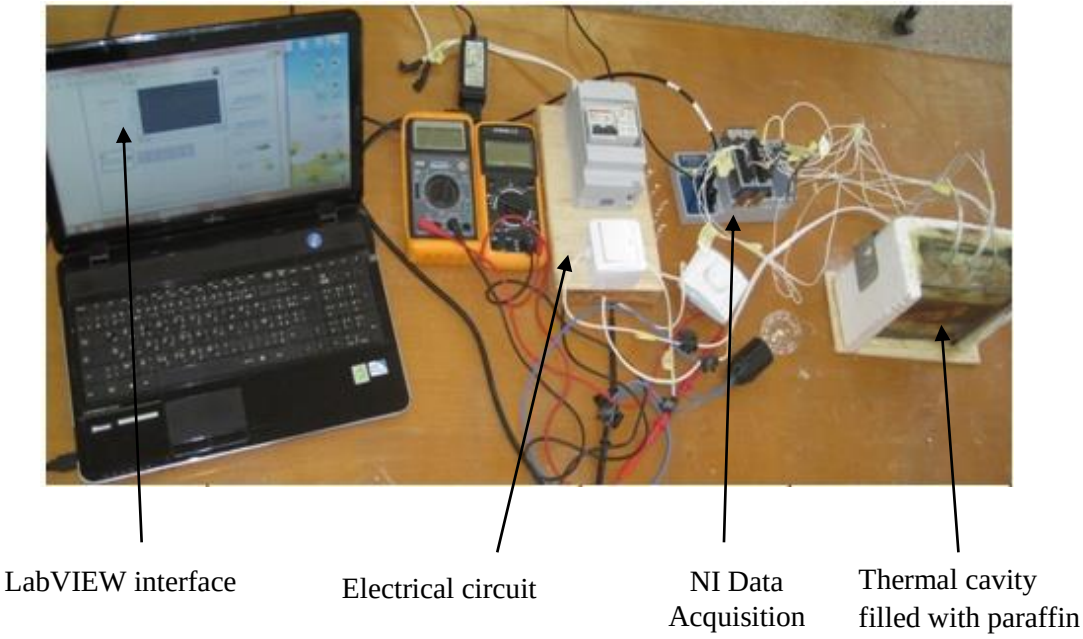

Fig. 3.1. Different materials and accessories for the installation

The experimental setup (Fig. 3.1) is realized to analyze the thermal behavior of paraffin melting. This work consists in studying the dynamic behavior of the melting front and the temperature evolution of the paraffin (PCM). The PCM is filled in a square thermal cavity of dimension $15 \times 15.8 \times 5$ cm^3. The cavity is made of glass to facilitate visualization of the movement of the melting front using an infrared thermal camera. The thermo-physical properties of the paraffin used are shown in Table 3.1.

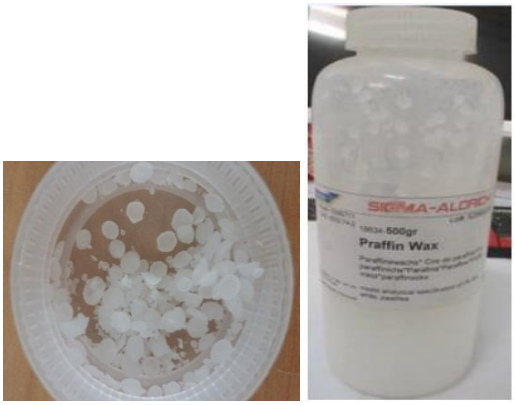

Fig. 3.2. Paraffin wax used

Table.3.1. Thermo-physical properties of the material used

Denomination	Solid density 25°C (kg/l)	Liquid density 80°C (kg/l)	Melting point (°C)	Meltingen thalpy (kJ/kg)	Heat conductivity W/(m.°C)	Specific heat Capacity(kJ/kg.K)
$C_{24}H_{50}$ Tetracosane	0.86	0.79	49-52	162.42	0.2	2
Zamak	6.8	---	380-386	104.6	119	0.419
Aluminum	2.7	---	658	415	237	0.896
Copper	8.954	---	1083	205	386	0.380

3.2.2 Filling the cavity with paraffin

Before starting the experiment, it is necessary to fill the liquid paraffin (molten) in the cavity. Then, the experiments can start after the complete solidification and cooling of the paraffin at ambient temperature (initial). At this time, it observed the formation of an air pore on the upper (free) surface of the paraffin (paraffin–air interface), Fig.3.3. This developed air pore is the result of the convection heat flow (vortex) that develops in the liquid phase during the melting and solidification process of paraffin. Thus, during the start of the experiments, it is reported that the upper surface of the paraffin does not have a flat platform. The initial paraffin-air interface has a curvature result of cyclic melting paraffin.

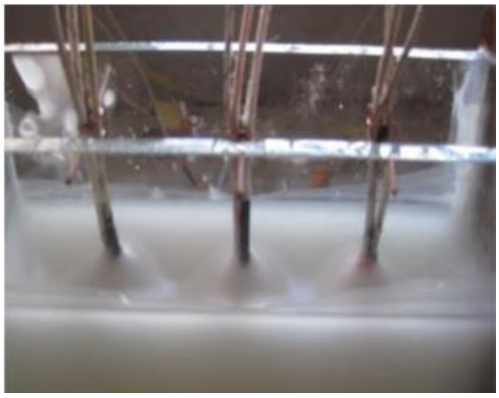

Fig. 3.3. Air pore existing in the initial free surface of paraffin.

The paraffin volume occupies 83% of the total volume of the thermal cavity. The air space is necessary to prevent glass fracture due to the expansion of the paraffin during melting. The thermal cavity is thermally insulated in three faces using glass wool and polystyrene surrounded by wood.

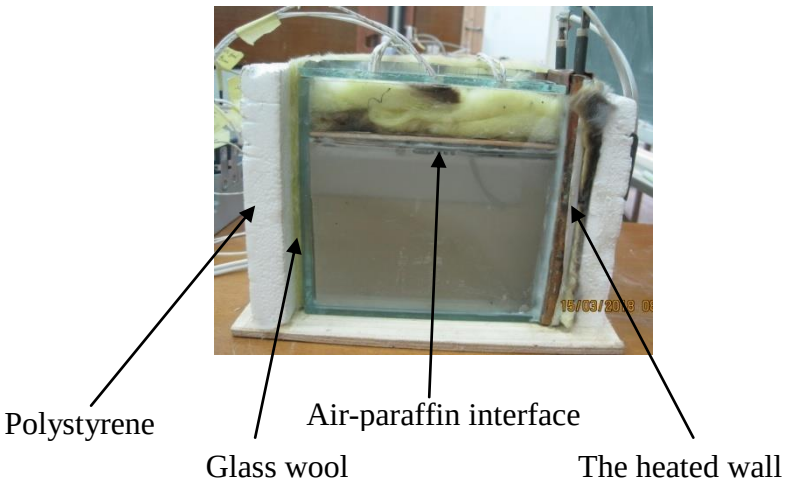

Fig.3.4. Thermal cavity insulation

3.2.3 Temperature measurement

The right face of the cavity is heated using an electrical variable heater manufactured on laboratory. Eight K-type thermocouples (Testo AG 606 1ST) are placed in the thermal cavity to measure the temperature evolution of the PCM. They are located as shown in Fig. 3.5. The temperature recording is assured using NI data

acquisition type cDAQ-9174 (Fig. 3.6) and a graphical interface software developed using Labview.

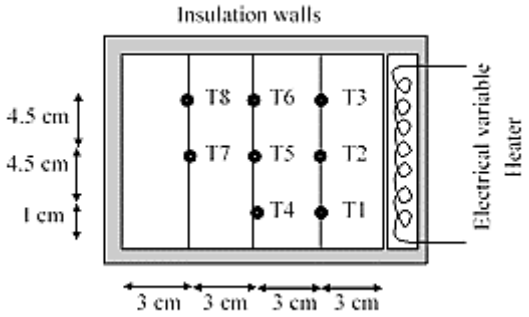

Fig. 3.5. Arrangements of the K-type thermocouples in thermal cavity.

Fig. 3.6. Connection of thermocouples to the NI acquisition chain

3.2.4 Experimental procedure

The first part of the experiments consists of studying the dynamic and thermal behavior of paraffin during the melting. The electrical heater develops a thermal power of 1.8 W necessary to melt the paraffin. To improve the thermal conductivity of the paraffin and to accelerate the melting process, it is proposed to add metallic additives (Zamak grid, aluminum and copper perforated plates)(Fig. 3.7).

To ensure a constant PCM-additive mass ratio throughout the different experiments, the volume of the additives is measured using a graduated beaker in order to respect the same volume of paraffin in the thermal cavity (Fig. 3.8).

Fig. 3.7. Immersion of plates (aluminum and copper)

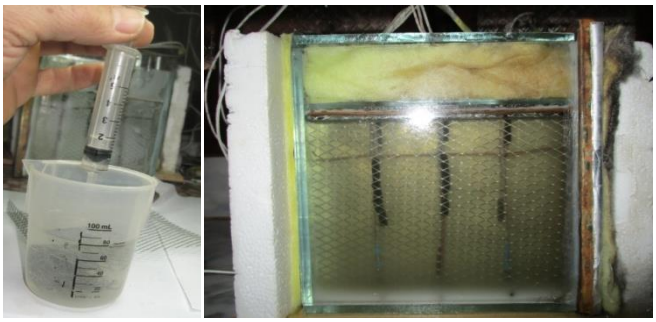

Fig. 3.8. Measuring the volume of the grid and its location in the thermal cavity

3.3 Effect of additive concentration

3.3.1 Presentation of the experimental setup

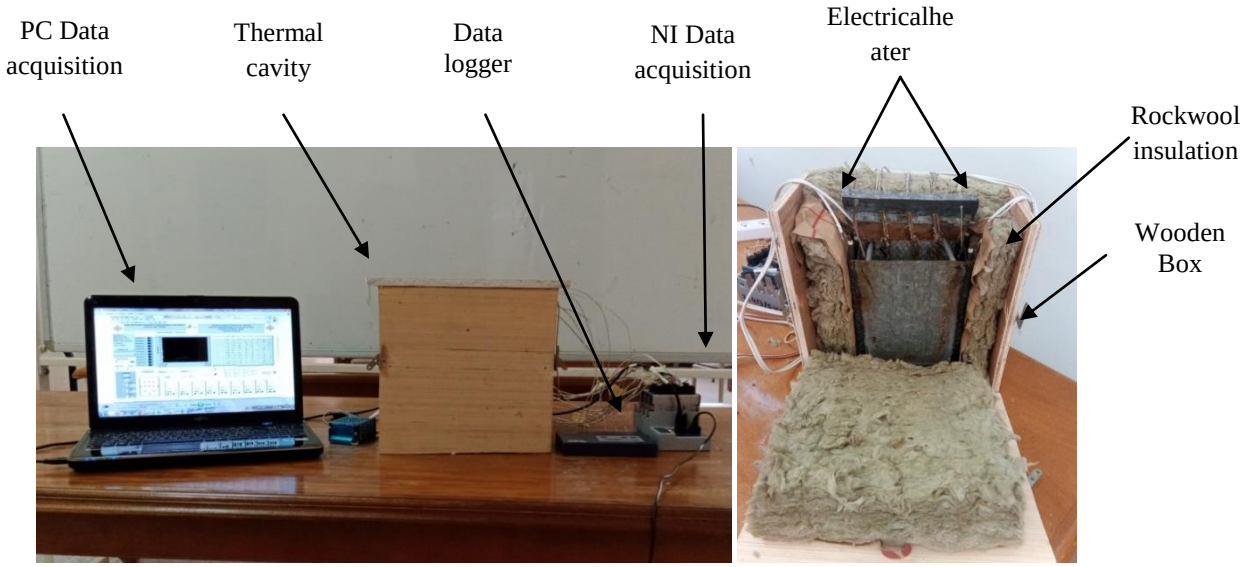

Fig. 3.9. Picture of the laboratory setup

A second experimental set-up carried out to study the thermal behavior of paraffin melting with a single additive for different volume concentrations. The selected additive is chosen from the results of the first part.

An experimental apparatus has been designed and built to accurately measure the instantaneous temperature distribution within the PCM in a rectangular thermal cavity. A 1 mm thick steel plate was used to make the thermal cavity with an inside dimension of 60 mm in width, 190 mm in height, and 155 mm in length. The right and left walls of the cavity are heated by an electrical heater to provide a constant heat flux (15 W). The side faces are insulated by a 70 mm thickness of rock wool (λ = 0.04 W/m K, C_p =1030 J/(kg.K)). To increase thermal insulation, the thermal cavity with its insulation are placed in a wooden box (λ = 0.17 W/m°C) having 10 mm thick (Fig.3.9).

3.3.2 Filling the cavity with paraffin

The PCM paraffin (C24H50 Tetracosane) is melted on an electrical resistor and then poured into the test cavity. To ensure that the resulting solid paraffin is in substantially the same physical conditions before each experiment, the cavity is maintained at room temperature for 24 hours. The volume of the PCM occupies approximately 70% of the total volume of the thermal cavity. After each solidification, a concave shape forms at the open top surface of the PCM. This event is mainly caused by the volumetric shrinkage of material during solidification. This will directly influence the evolution of the melting front at the upper part of the PCM, (Fig.3.10).

Fig.3.10. Air pore existing in the initial free surface of paraffin

3.3.3 Temperature measurement

A 1mm thick Zamak grid used as a support to place 9 K-type thermocouples inside the PCM zone, and record the temperature evolution of the PCM every 2s. Two (02) K-type thermocouples are placed on the hot walls surfaces to monitor the temperature during the experiments and another K-type thermocouple for the ambient temperature. All the thermocouples are connected to a PC via a data logger (NI c-DAQ 9174) using a thermal module (NI 9211) to record temperatures during the melting process.

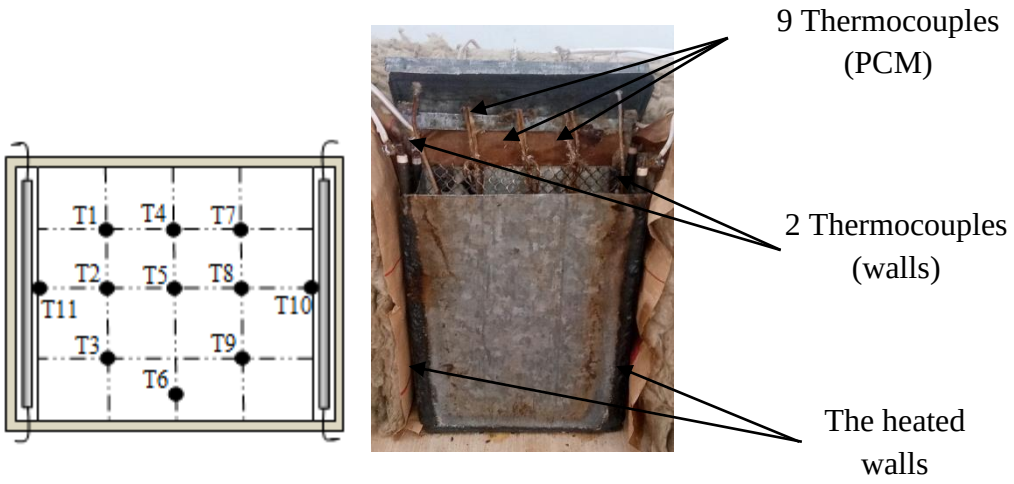

Fig. 3.11.Arrangements of the K-type thermocouples on thermal cavity.

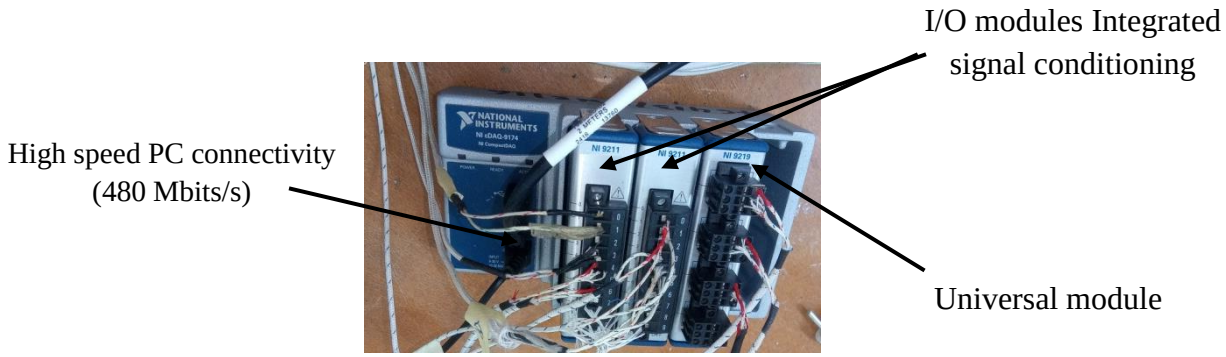

Fig. 3.12. NI acquisition module with temperature sensors

The experimental enclosure was designed to minimize heat loss; some heat is transferred to the ambiance by natural convection and radiation. However, the radiation heat transfer can be neglected due to the low surface temperature of the insulation. To estimate the heat lost due to natural convection from the insulation surface we need six thermocouples were placed before and after the rock wool and wood, temperatures were recorded by a data logger at a time interval of 5 min.

The total heat loss from the enclosure can be calculated using the following:

$$Q_{loss} = \sum_{t_i}^{t} \left[M_{ins} C_{ins} \left(T_{ins}^{t+\Delta t} - T_{ins}^{t} \right) + \left(-K_{ins} S_{ins} \frac{\Delta T_{ins}}{\Delta x} \right) \Delta t \right]$$

$$-K_{ins} S_{ins} \frac{\Delta T_{ins}}{\Delta x} = h\, S_{ins} \left(T_{ins} - T_{\infty} \right) \qquad (3.1)$$

Where Q_{loss} (kJ) is the summing up of thermal energy stored by insulation (Rockwool) and evacuated in the ambiance through the insulation. M_{ins}, C_{ins}, and K_{ins} are the mass, heat capacity, and thermal conductivity of Rockwool. $T_{ins}^{t+\Delta t}$ is the actual average temperature of insulation and T_{ins}^{t} is the previous average temperature . Δx is the thickness of the insulation.

3.3.4 Experimental procedure

To ensure better precision of the results, three series of experiments are repeated for each experiment. The PCM's temperature history is then compared to ultimately choose an average arithmetic value. All experiments start with a solid-state PCM of a uniform temperature of 20°C and end when the lower temperature (T_6) exceeds the melting temperature. At this time, the PCM will be approximately completely melted. To accelerate paraffin melting, aluminum plates 160 mm in length, 130 mm in width and 0.127 mm in thickness are placed with the same space in the thermal cavity. Each perforated plate has a mass of 5g (0.6% MT) and 56 perforations of 9 mm diameter each (Fig. 3.13). The experiments are tested using 2, 4 and 8 plates (Fig. 3.14).

Table.3.2. the concentration of aluminium

	Paraffin	2 plates	4 plates	8 plates
Mass (kg)	0.823	0.01	0.02	0.04
%		1.2%	2.4%	4.8%

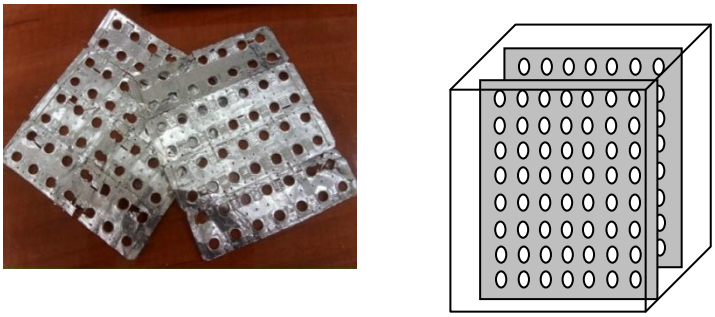

Fig. 3.13. Perforated aluminium plates

2 aluminium plates

4 aluminium plates

8 aluminium plates

Fig. 3.14. thermal cavity integrating different aluminum plates

3.4 Interface (Labview)

The Labview graphical interface is developed to can follow and record the thermal behavior during experiment. It consists of three (03) different windows:

- The first window contains graphs, tables, switches, time counters, LEDs , and message boxes to visualize the graphical and numerical evolution of temperatures.
- The second window contains graphs, LEDs, table, and numerical displays to follow the evolution of the solid-liquid interface and to determine the liquid fraction.
- A third window has been created to follow the evolution of the stored energy (sensible and latent) and to determine the heat transfer characteristics (***h***,**Nu**)

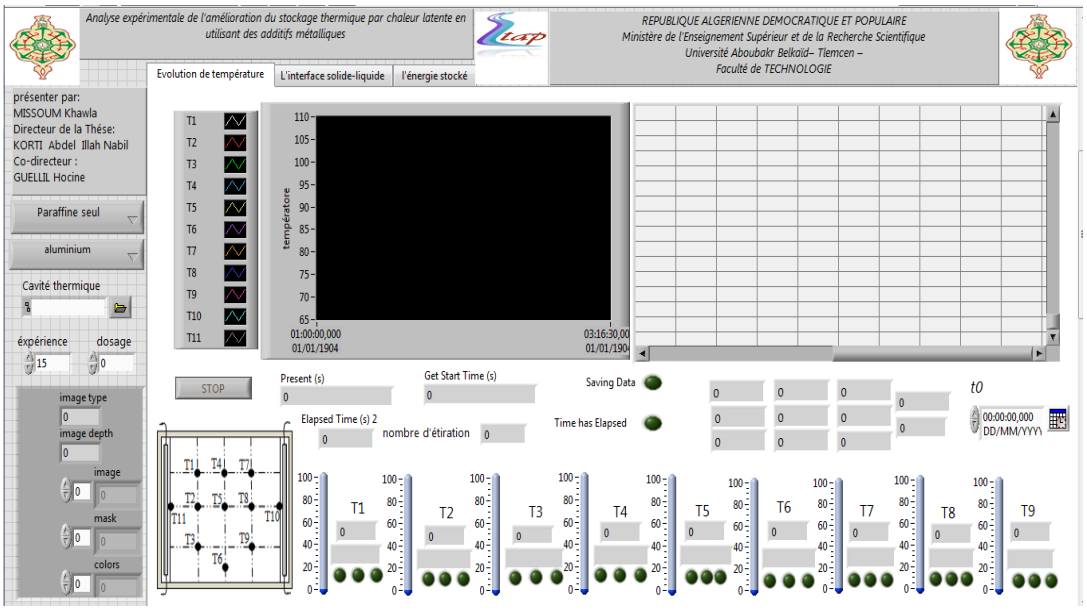

Fig.3.15. Presentation of the interface (window 1)

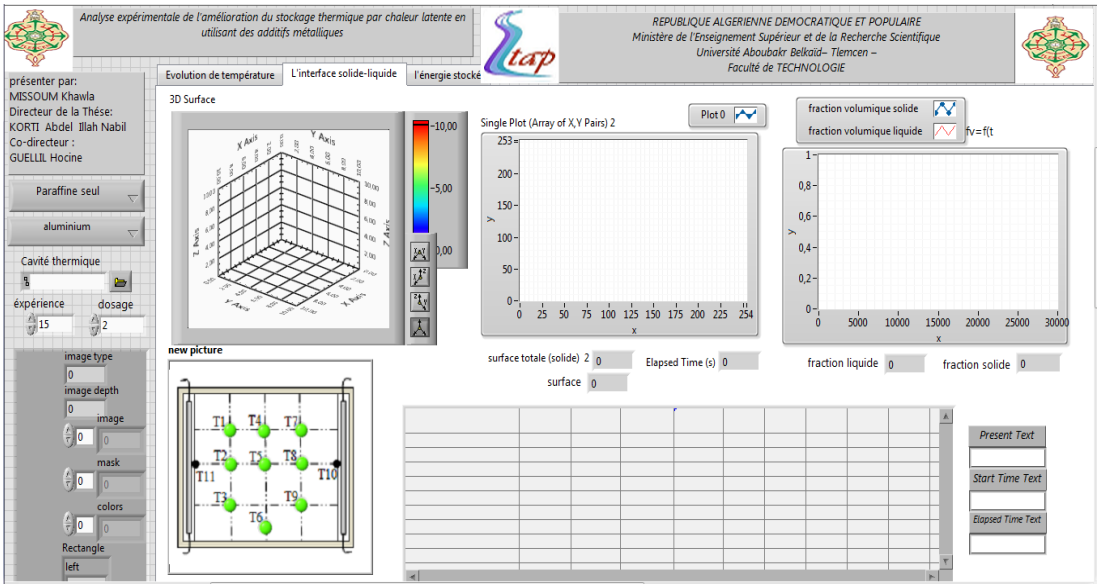

Fig.3.16. Presentation of the interface (window 2)

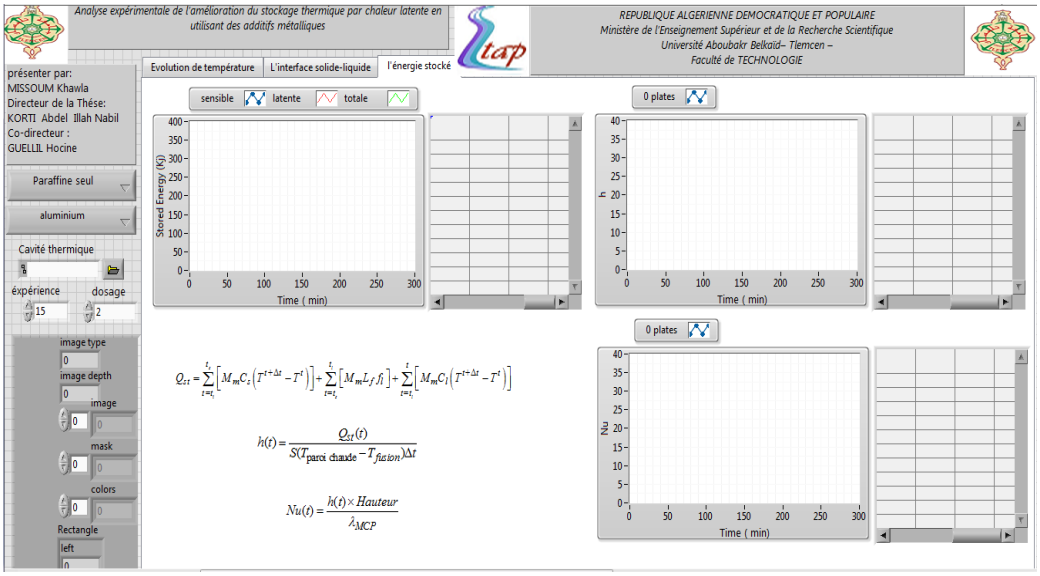

Fig.3.17. Presentation of the interface (window 3)

3.5 Sensor calibration, accuracy and sensitivity

Simple methods exist to reduce measurement errors. It is necessary to choose sensors with same quality and from the same manufacturer (Fig. 3.18). Then, calibrate these sensors with another reliable sensor of good quality used as a calibration reference (Fig. 3.19, sensor type testo AQ 606). The sensors are calibrated by placing them in hot water. The evolution of the temperatures allows us to compare the reliability, the accuracy and the response time of each sensor.

Fig. 3.18. Type K sensors with flat heads used in experiments

Fig. 3.19. Reference sensor Calibration

3.6 Uncertainty analysis

The uncertainty of experimental results is often affected by the inevitable errors in experimental measurement and depends on the uncertainty of measuring instruments. The maximum uncertainty in temperature measurement is equal to ±0.5 ^{0}C. The PCM mass measurement error is ±0.8 g and the maximum uncertainty of measuring the PCM mass is 0.11%. The length measurement error is ±0.5mm and the consequent maximum uncertainty of measuring the length is 0.4%.

The liquid fraction is estimated via photography. The maximum uncertainty of measuring the total area with an image processing system with a resolution of 540 × 864 pixels is [16].

$$\frac{\Delta V_0}{V_0} = \frac{1}{540} + \frac{1}{864(H_m/W_m)} = 0.3\% \qquad (3.2)$$

Where H_m and W_m are height and width of PCM (m).

Since the minimum solid phase fraction measured was 3%, the maximum deviation in determining the area of the solid phase is

$$\frac{\Delta V_S}{V_S} = \frac{1}{540} + \frac{1}{864(H_m/W_m)(V_S/V_0)} = 4.16\% \qquad (3.3)$$

Thus, the maximum uncertainty in determining the melt fraction from the photos is:

$$\frac{\Delta V_l}{V_l} = \frac{\Delta V_s}{V_s} + \frac{\Delta V_0}{V_0} = 4.46\% \quad (3.4)$$

Where V_s, V_l and V_0 are volume of solid, liquid, and total of PCM (m^3).

Assuming that the final results are derived from independent variables $y_1, y_2; \ldots; y_n$, the uncertainty of result W is obtained by appropriately combining the uncertainty of the independent variables $W(y_i)$ as fellow [17]:

$$K = f(y_1, y_2, \ldots, y_n)$$
$$W(K) = \sqrt{\sum_{i=1}^{n} \left(\frac{\partial f}{\partial y} W(y_i)\right)^2} \quad (3.5)$$

By applying this method, the average uncertainty of energy stored is 4.58%.

Results and Discussion

4.1 Introduction

This chapter presents an experimental study to analyze the thermal behavior of paraffin melting in a thermal cavity incorporating different metals (zamak, aluminum and copper) in different configurations. The originality of the study is to try to determine the best additive that allows both the improvement of the thermal conductivity and the stored energy.

4.2 Pure Paraffin

4.2.1 Evolution of the melting front

The first experiment consists in analysing the melting behaviour of paraffin alone in a glass cavity heated by one side in the right wall. Before the melting process starts, we notice that the upper free surface of the paraffin shows a certain hollow curvature. This is due to the contraction and recoil of the paraffin during the solidification process. This contraction phenomenon causes the creation of air pockets on the upper free surface and inside the paraffin. Fig. 4.1 shows photos of the melting process of pure paraffin. Fig. 4.2 shows the time evolution of the position and shape of the solid–liquid interface. GetData Graph Digitizer is used to extract and plot the numerical shape of the fusion front similar to the one captured during the experiments. It is observed that melting starts near the heated (right) face of the cavity. After 30 min, the melting front moves towards the left face with a curved form, the percentage of molten paraffin reaches approximately 22%. A cap shape is observed in the upper part of the melting front. The initial curvature existing in the upper (free) surface of the paraffin (air pore) is the essential cause of this cap shape. Afterwards, the melting front develops with a curved inclined shape until the end of the fusion at 180 min. The curved shape is due to the natural convection phenomenon developed in the liquid phase during the melting. This mechanism causes circulation in the molten paraffin; this is due to the buoyancy forces induced by the density gradients due to temperature differences. In addition, it observed that the liquid paraffin rises upwards and the solid paraffin exists always at the bottom of the cavity.

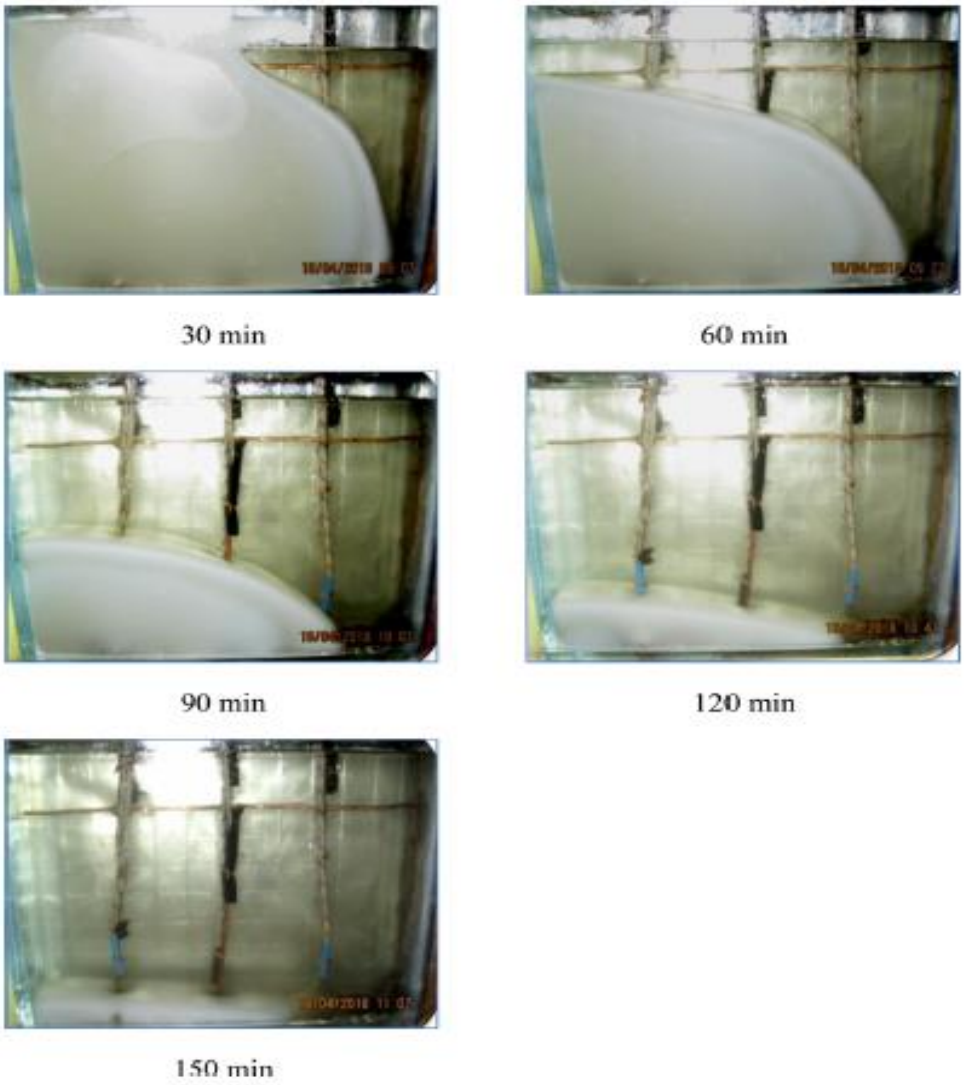

Fig. 4.1. Photos of time evolution of the position and shape of the solid-liquid interface.

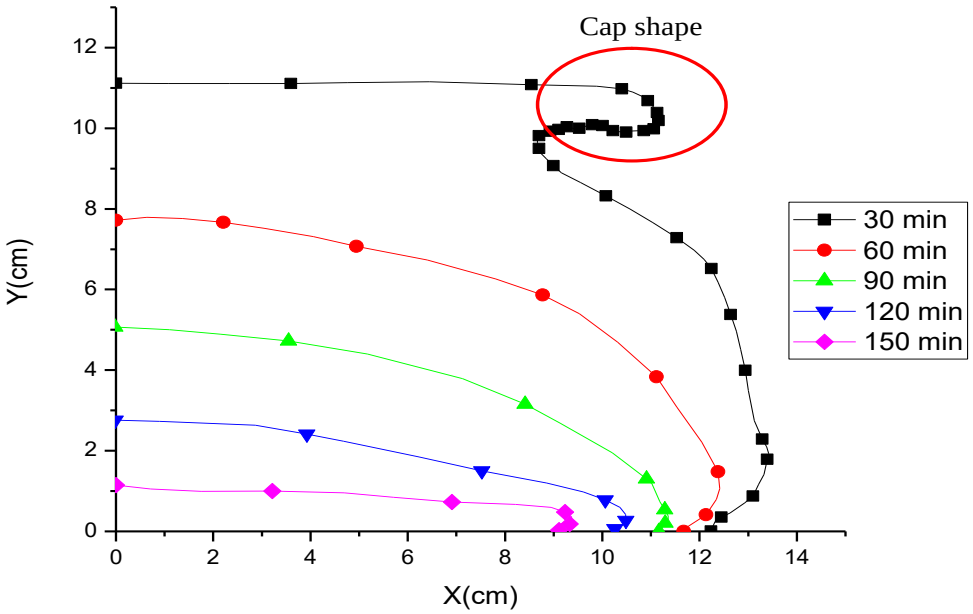

Fig. 4.2. Time evolution of the position and shape of the solid–liquid interface.

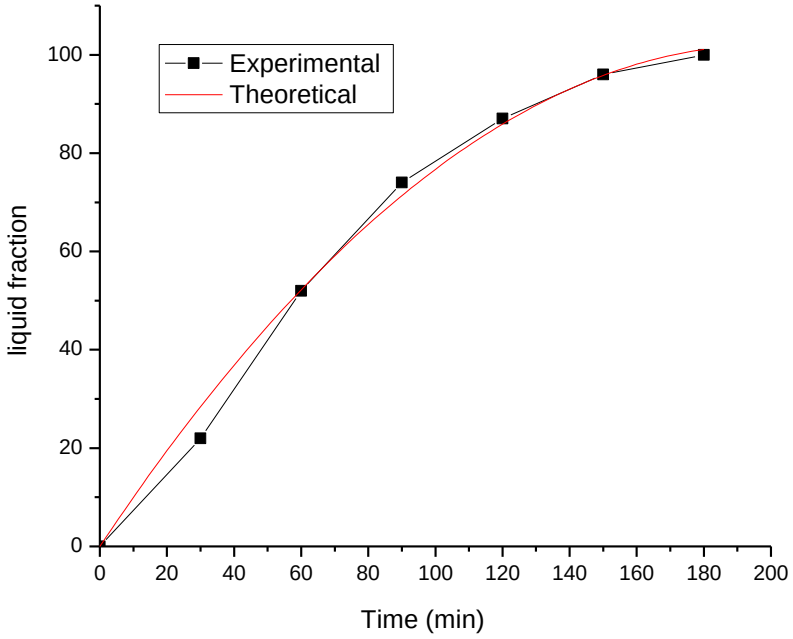

Fig. 4.3. Time evolution of the liquid volume fraction.

Fig. 4.3 shows the time evolution of the liquid fraction f_l during paraffin melting. It represents the ratio of the volume of liquid paraffin to the total volume of paraffin. It approximated using Autocad to calculate the liquid area at each moment of the experiment. The results show that the liquid fraction reaches approximately 52,

74, 87 and 96% after 60, 90, 120, and 150 min, respectively. Thus, it is observed that the melting rate of the paraffin accelerates after around 30 min due to the development of natural convection which gradually dominates the melting of the paraffin. After about 90 min, the melting rate decreases and thermal equilibrium is gradually established.

The time evolution of the liquid fraction can be mathematically approximated by a following second-degree polynomial equation:

$$f_l(t) = -0.0028t^2 + 1.082t - 2.857 \quad (4.1)$$

4.2.2 Evolution of the temperature of the paraffin

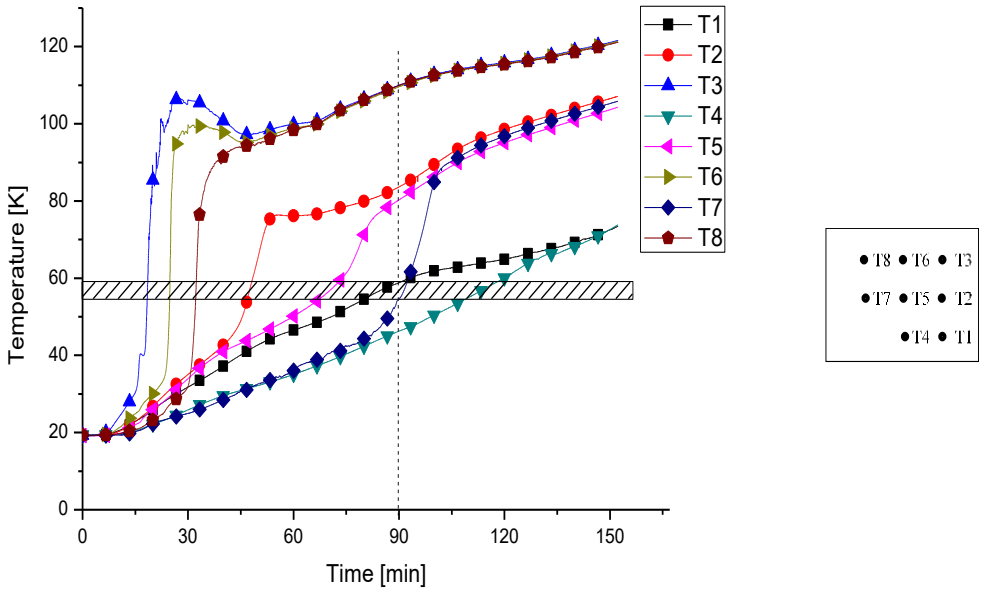

Fig. 4.4. Time evolution of temperature during paraffin melting.

Fig. 4.4 shows the time evolution of the paraffin temperature during melting. After 90 min, Fig. 4.1 shows that the melting front reaches the positions of T1 and T7. At this time, the temperatures of T1 and T7 reach 54°C and 59°C, respectively. It can be considered that the melting temperature range is around 54–59°C. At 30min, natural convection developed in the molten paraffin causes a quick increase of the

temperatures at the upper side of paraffin, and (T3, T6) reaches about (106°C and 98.5°C). The bottom sides (T1, T2) are in a solid state and reach about (31.75°C and 35°C). Thus, convection heat flow in the liquid phase increases the heating of paraffin compared to the conduction in the solid phase. Afterward, temperatures T3 and T6 decrease when T8 begins to melt by absorbing the necessary latent heat from T3 and T6 regions. At 40 min, (T1, T2 and T8) reach the values of (37.19°C, 42.57°C and 91.35°C), respectively. Due to the conduction mode, the positions of T1 and T2 have not yet reached the melting point. The melting progressively develops with a curved and inclined melting front and the last recorded melting point is T4 after about 120 min. The complete melting is achieved after about 180 min.

4.3 Paraffin with a Zamak grid

To accelerate the melting of paraffin, we propose to integrate different materials in the thermal cavity. The first material added is two parallel grids made of Zamak (Fig. 4.5). The choice of Zamak is due to its metallic composition and its good price. Zamak is a family of alloys with a base metal of zinc and alloying elements of aluminum, magnesium, and copper. It has a good thermal conductivity of around 108 W/mK. The addition of a material in the paraffin modifies its effective conductivity and so the melting velocity. The effective conductivity obtained depends on the thermal conductivity and the volume and mass ratio of the material added to the paraffin. In order to compare with the previous results, the volume of paraffin with Zamak is equal to the volume in paraffin alone (pure) of the first case.

Fig. 4.5. Form of the Zamak grid used in the cavity.

4.3.1 Evolution of the melting front

Fig. 4.6 shows the comparison between the time evolution of the paraffin melting front with and without a Zamak grid. The results show clearly that the addition of a Zamak grid causes a delay of the paraffin melting. Indeed, the Zamak grid absorbs a part of the heat provided by the heat source and delays the melting process of paraffin. In addition, it is observed that the slope of the melting front of pure paraffin is greater than that of the Zamak grid. This shows that the convection heat flow is more intense in the case of pure paraffin. Indeed, the addition of solid materials to paraffin improves heat conduction and reduces heat convection. The addition of materials with good thermal conductivity to the paraffin can slow down the melting process by changing the effective heat capacity of the mixture and so the thermal diffusivity.

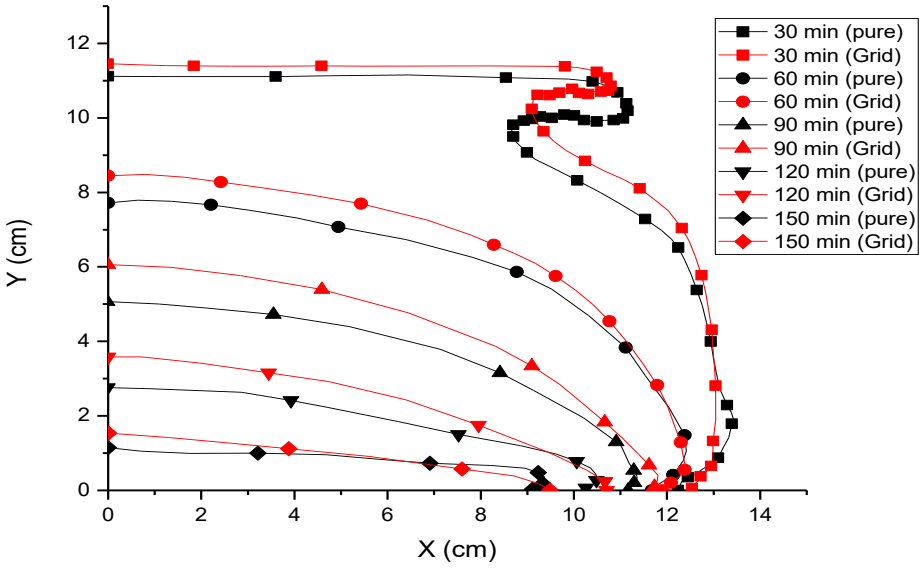

Fig. 4.6. Evolution of the paraffin melting front with and without Zamak grid.

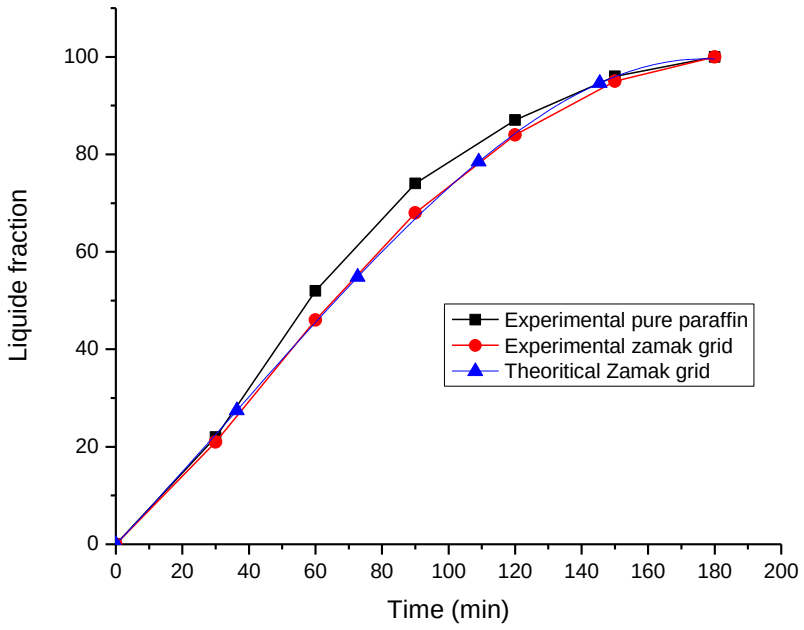

Fig. 4.7. Evolution of the liquid volume fraction with and without the Zamak grid.

Fig. 4.7 shows the comparison between the evolution of the liquid fraction of paraffin with and without a Zamak grid. It is noted that the melting of pure (alone) paraffin is initially faster than with the Zamak grid until about 90 min, by about 8%. After that, the melting velocity of the paraffin with the Zamak grid increases, and the complete melting is reached after about 180 min, identical to that of pure paraffin. Thus, the Zamak grid absorbs heat quantity that slows the melting during the first moments. After that, it helps to accelerate the melting process by improving the effective thermal conductivity of the paraffin. Thus, the total melting is achieved in both cases at the same time.

The time evolution of the liquid fraction of paraffin with Zamak can be approximated mathematically by a second-degree polynomial (Figure 4.5):

$$f_l(t) = -0.0021t^2 + 0.964t - 2.571 \quad (4.2)$$

4.3.2 Evolution of the temperature of the paraffin

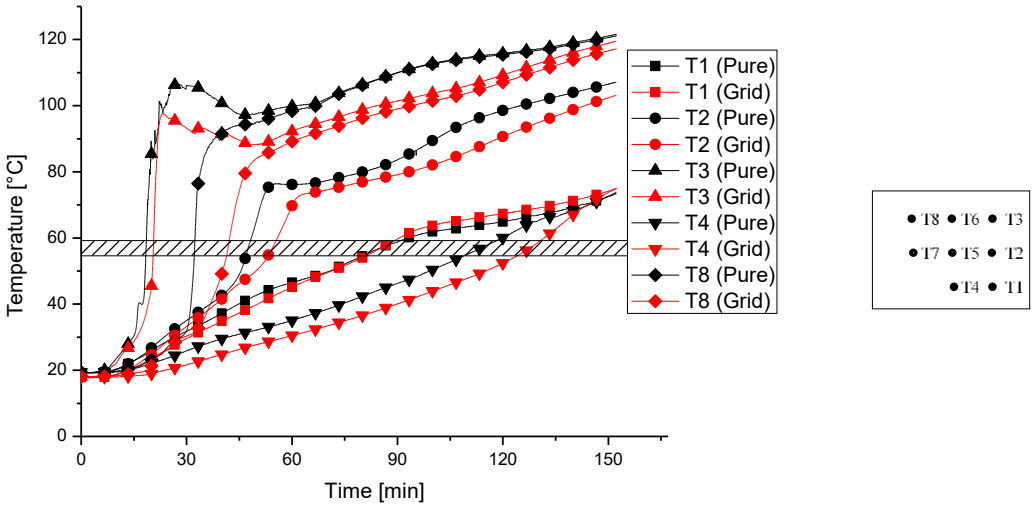

Fig. 4.8. Time evolution of paraffin temperature with and without Zamak grid.

Fig. 4.8 shows the time evolution of the paraffin temperature with and without a Zamak grid. It is observed that the temperature of the pure paraffin is higher than without Zamak. This shows clearly that the Zamak absorbs a part of the heat supplied by the heat source and the temperature of paraffin with Zamak grid becomes lower. A maximum difference of 20°C, 10°C and 42°C is recorded at T2, T3 and T8, respectively. This difference decreases during melting to an average of 7°C at the end of the melting process for the three temperatures. The temperature T1 remains almost the same in both cases with and without a Zamak grid. On the other hand, it is noted that the temperature difference in paraffin decreases by adding the Zamak grid. Indeed, the maximum temperature difference is recorded at 27 min, which reaches 83°C and 74°C for the case without and with the Zamak grid, respectively. At the end of the melting process, the temperature difference reaches 50°C and 45°C for the case without and with the Zamak grid. Thus, the Zamak grid helps to homogenize the temperature of the paraffin by reducing the average temperature difference by about 5.5°C (8%).

It is concluded that the integration of Zamak grids does not properly improve the thermo-physical properties of the paraffin to accelerate its melting process. Therefore,

it is advisable to find other materials with a better thermal conductivity - heat capacity ratio, such as aluminum and copper.

Table 4.1. Concentration of metallic additives

Denomination	Heat conductivity W/m°C	Specific heat capacity J/kg.°C	Report (λ /C_p) kg/m.s
C24H50 Tetracosane	0.2	2	0.1
Zamak	108	419	0.258
Aluminum	237	896	0.265
Copper	386	380	1.016

4.4 Perforated metals plates

Due to the unavailability of aluminum grids on the market, two perforated plates of aluminum (or copper) (Fig. 4.9) were chosen and added to the thermal cavity. The paraffin-plate volume ratio is always equal to pure paraffin.

(a) **(b)**

Fig.4.9. Perforated plates (a) copper and (b) aluminum.

4.4.1 Evolution of the melting front

Fig. 4.10 shows the comparison between the time evolution of the melting front of paraffin with and without a perforated metal plate. At 30 min, the evolution of the melting front shows that the velocity of pure paraffin melting is slightly higher than

that with an aluminum plate. Indeed, the aluminum plate absorbs part of the heat supplied by the heat source. However, the velocity of copper-paraffin fusion is higher than that of the other cases. Since the heat capacity of copper is lower than that of aluminum, the good thermal conductivity of copper can directly accelerate the melting process of paraffin.

At 60 min, the results show that the addition of the aluminum plate causes an acceleration of the melting of the paraffin; this is explained by the good thermal conductivity of the aluminum. At 120 min, the rate of paraffin melting reached 88%, 92% and 93% without , and with the aluminum and copper plates, respectively.

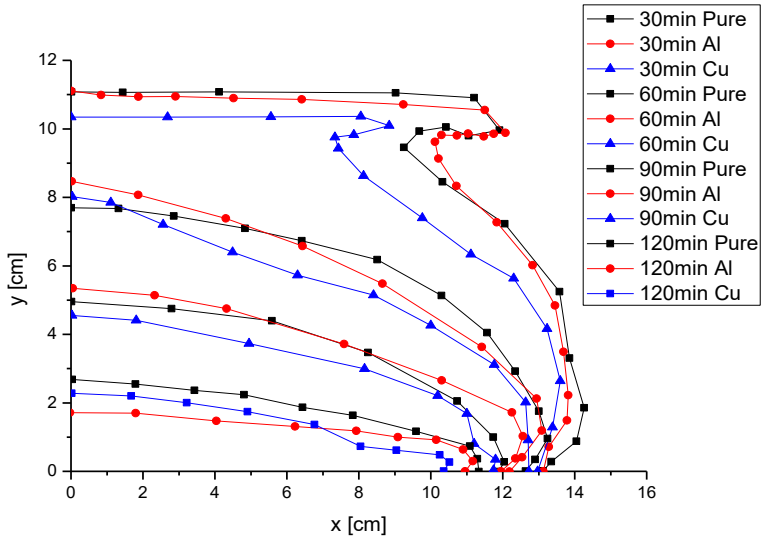

Fig. 4. 10. Time evolution of the paraffin melting front with and without metals plates.

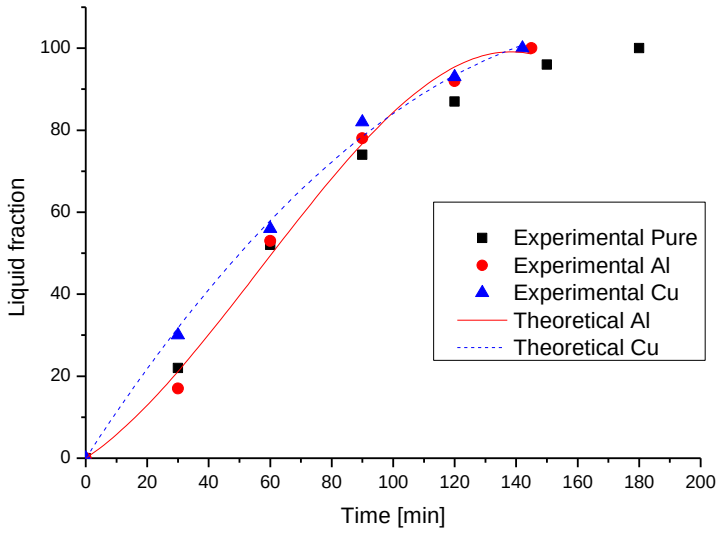

Fig. 4.11. Evolution of the liquid fraction of paraffin alone and with metal plates.

Fig. 4.11 shows the comparison between the time evolution of the liquid fraction of paraffin alone and with metal plates. Until about 30 min, the liquid fraction of paraffin alone is more important than that with aluminum plates by about 22%. However, the liquid fraction of copper paraffin is more important than the paraffin alone by about 36%. After that, the process of melting is accelerated by adding the aluminum plate and becomes the same of that of pure paraffin at about 60 min. The liquid fraction of copper paraffin is always more important than the paraffin alone by about 7%. At this time, the melting process of the paraffin with the aluminum plates accelerates and becomes more important than that of the pure paraffin until the end of the melting process. It should be noted that the total melting time of paraffin with the metal plates (aluminum 145 min and copper 142 min) is shorter than that of paraffin alone (180 min). Then, the metal plate accelerates the melting process by about 21% and 19% with copper and aluminum plate additives.

The evolution of the liquid fraction of paraffin with aluminum and copper plates can be approximated mathematically by a second or third-degree polynomial:

$$f_{l,Al}(t) = -4.63 \times 10^{-5}\, t^3 + 0.00765t^2 + 0.554t - 1.249 \quad (4.3)$$

$$f_{l,Cu}(t) = -0.00327t^2 + 1.18t - 1.084 \quad (4.4)$$

4.4.2 Evolution of the temperature of the paraffin

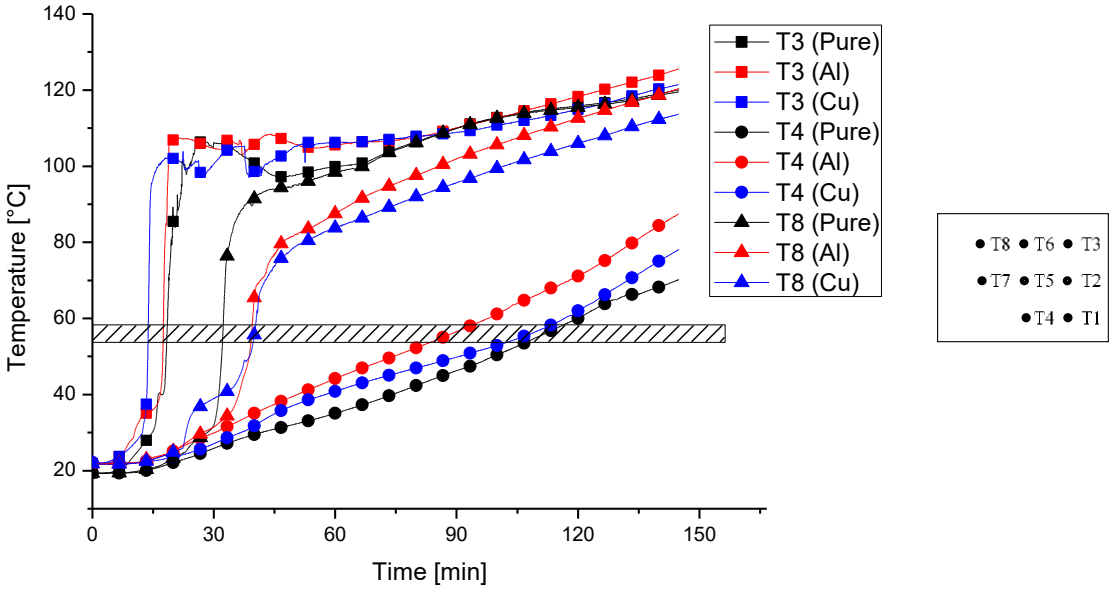

Fig. 4.12. Paraffin temperature evolution with and without metals additives.

Fig. 4.12 shows the time evolution of the temperature of pure paraffin, with aluminum plates and with copper plates. Generally, it is observed that the temperature of paraffin with aluminum is higher than that with copper, which is higher than that of paraffin alone. However, at 40 min, a value of about 91.5, 65.5, and 56 °C is recorded at T8 in the case of pure-, aluminum- and copper-paraffin, respectively. This shows that aluminum and copper absorb part of the heat supplied by the heat source and the temperature of paraffin is lower initially. Afterward, the temperature of the paraffin with metal plates rises and can exceed than that of the paraffin alone. At 80 min, the minimum temperature of paraffin (T4) reaches about 52°C and 47°C with aluminum and copper plates compared to 42°C with paraffin alone.

On the other hand, it is noted that the temperature difference in paraffin decreases by adding metal plates. Indeed, the maximum temperature difference is recorded at 27 min, which reaches 83, 79 and 71°C for the case of without, with aluminum, and with copper additives plates, respectively. At the end of the melting process, the temperature difference reaches 50, 39, and 43°C for the three cases.

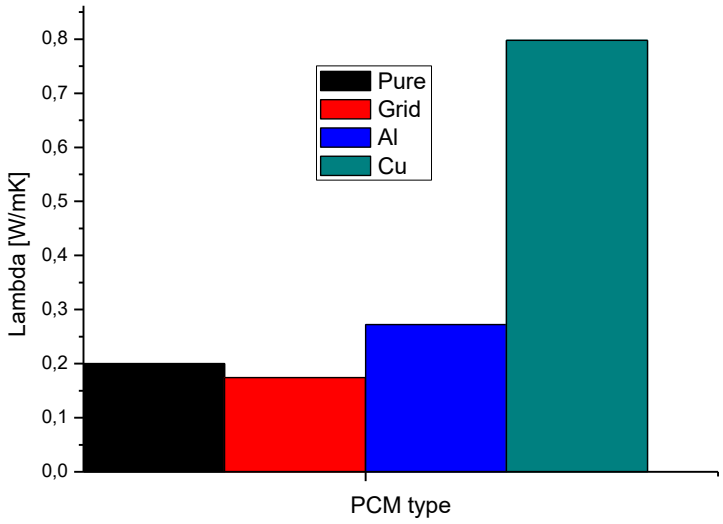

Fig. 4.13. Effective thermal conductivity of pure paraffin and metals additives.

It is concluded that metals perforated plates contribute significantly to improving the effective thermal conductivity of paraffin and accelerates the melting process. On the other hand, it helps to homogenize the temperature of the paraffin by reducing the average temperature difference by about 6°C (9%), and 8°C (12%) with aluminum and copper plates. The effective thermal conductivity becomes 0.174, 0.272, and 0.798W/mK in the cases of Zamak grid, aluminum plate and copper plate additive in the pure paraffin (Figure 4.13). Thus, the Zamak grid decreases the thermal conductivity of paraffin by about 13%. However, aluminum and copper plates can increase the thermal conductivity of paraffin by about 36% and 300%.

4.5 Energy storage

The thermal energy storage rates can be quantified based on the following expression:

$$Q_{st} = \sum_{t=t_i}^{t_s}\left[M_m C_s\left(T^{t+\Delta t} - T^t\right)\right] + \sum_{t=t_s}^{t_l}\left[M_m L_f\, f_l\right] + \sum_{t=t_l}^{t}\left[M_m C_l\left(T^{t+\Delta t} - T^t\right)\right] + \sum_{t=t_l}^{t}\left[M_{plaques} C_{plaques}\left(T^{t+\Delta t} - T^t\right)\right] \quad (4.5)$$

where Q_{st} (kJ) is the sum-up of thermal energy stored by PCM from time t = 0, M_m (kg) the mass of PCM, C_s ,and C_l (kJ/kgK) the solid and liquid heat capacity of PCM, L_f (kJ/kg) latent heat of fusion of PCM, f_l liquid fraction of PCM, $T^{t+\Delta t}$(°C) actual temperature of PCM and T^t (°C) is the previous temperature of PCM.

Fig. 4.14 shows the time evolution of the energy stored by PCM with different metal additives. At 15 min, the thermal energy stored reaches a value of 17.15, 17.38, 20.07, and 34.01 by aluminum-, Zamak-, pure-, and copper-paraffin, respectively. The good thermal conductivity of cooper accelerates the heat transfer and the energy stored increases. At 35 min, the thermal energy stored reaches a value of 69.42, 74.09, 84.37 and 89.32 kJ by Zamak- (grid), aluminum-, copper-, and pure paraffin. Thus, metal additives can decrease the stored energy by 22.28, 17.05 and 5.54% in the three cases. Indeed, the weak heat capacity of metals compared to that of paraffin causes the reduction of the effective heat capacity of a system. Thus, the quantity of thermal energy stored by the system decreases. However, on the one hand, the good heat capacity of aluminum compared to other metals and, on the other hand, the good effective thermal conductivity of aluminum– paraffin compared to paraffin alone, can accelerates heat transfer and the amount of heat stored by aluminum–paraffin becomes better at the end of melting process (145 min). The thermal energy stored reaches a value of 218.8, 226.71, 226.76, and 233.74 kJ by Zamak- (grid), pure-, copper-, and aluminum paraffin. Thus, aluminum increases the energy stored by 3.1%, but Zamak decreases the energy stored by about 3.5%. For the copper-paraffin, the global energy stored is almost the same as the paraffin pure

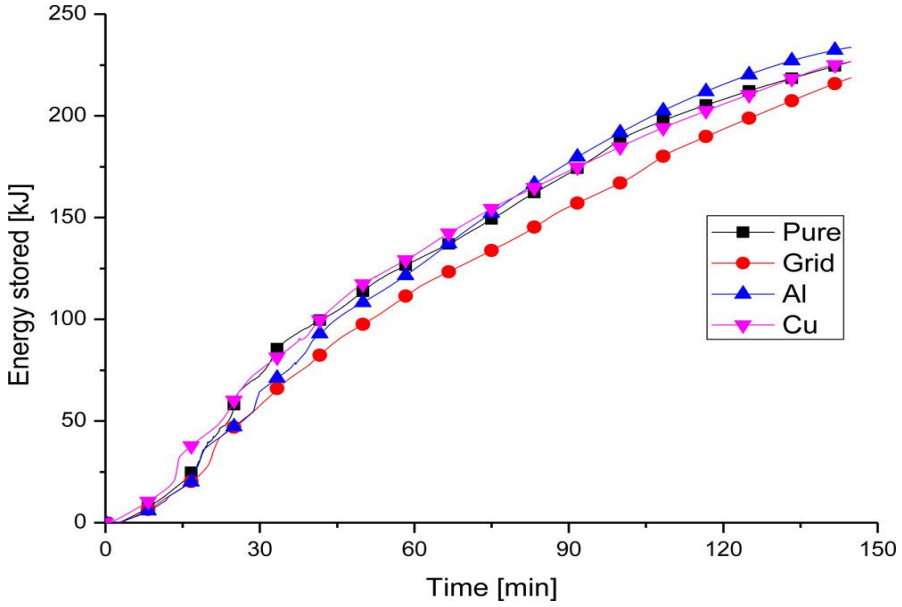

Fig. 4.14. Time evolution of the energy stored by PCM with different metal additives.

4.6 Heat flow

Fig. 4.15 shows the heat flux transferred through PCM with different metal additives. At 15 min, the heat flux transferred through the system reaches a value of 19.06, 19.31, 22.27, and 37.79 W by aluminum-, Zamak- (grid), pure-, and copper-paraffin, respectively. The best thermal conductivity of cooper accelerates the heat transfer through the PCM system to about 69.7%. At 35 min, the heat flux through the paraffin alone increases and reaches 42.54W compared to 33.06, 35.28, and 40.18W for Zamak-, aluminum-, and copper-paraffin. This phenomenon can be explained by the fact that the mass of PCM in the pure system is greater than in the metal-PCM system. The heat latent absorbed becomes more important and the heat transfer increases. However, at the end (145 min), the heat flux through the aluminum paraffin increases and reaches 26.89 W compared to 26.08 for copper– paraffin and paraffin alone and 25.17W for Zamak–paraffin.

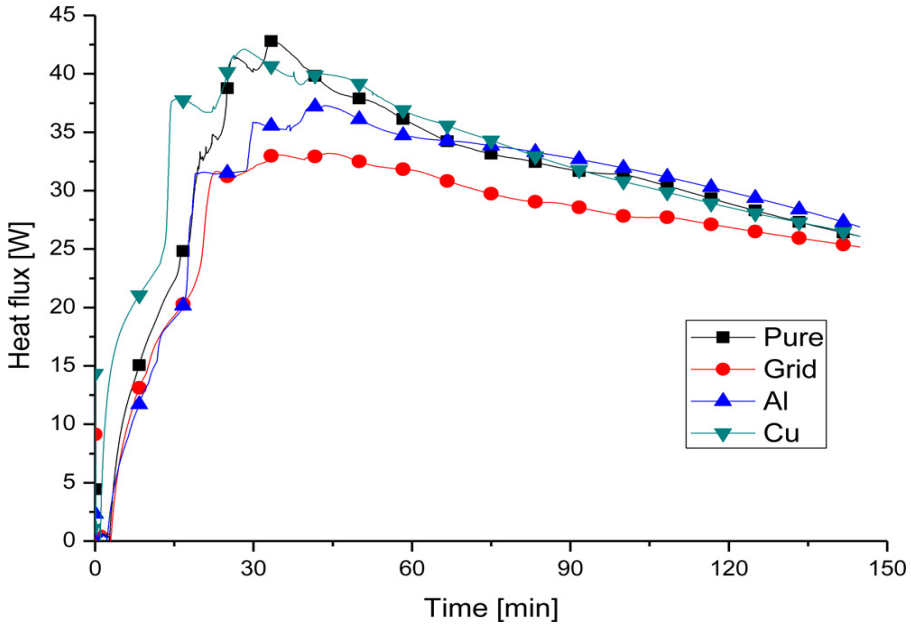

Fig.4.15. Time evolution of the heat flux transferred through PCM with different metal additives.

Experimental Study of the Concentration Effect of Aluminum

5.1 Introduction

This chapter presents an experimental study to analyze the thermal behavior of paraffin melting in a thermal cavity incorporating aluminum as an additive. The study consists to analyzing the effect of the mass concentration of aluminum added to the paraffin on the thermal behavior of the melt and the amount of the thermal energy stored.

5.2 Paraffin alone

5.2.1 Temperature and solid-liquid interface evolutions

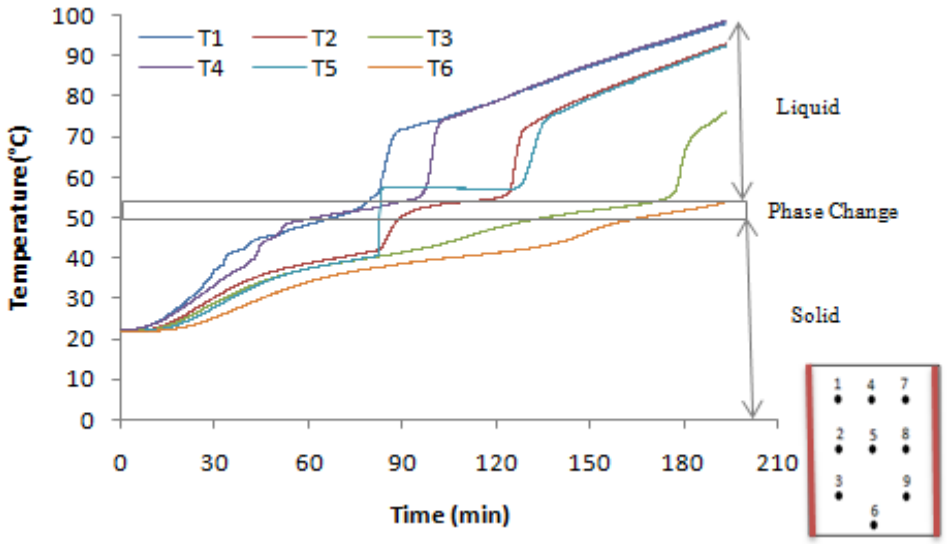

Fig.5.1.Time evolution of the temperature during the melting of the paraffin alone.

Fig. 5.1 shows the time evolution of the temperature during the melting of paraffin heated from both sides. Due to thermal symmetry, the figure shows only the temperature in the left half of the thermal cavity (T1-T6). Initially, the paraffin is still solid and heat is transferred by pure conduction, all the temperature of the thermocouples is below to the melting temperature (49-54°C). During this period, the rate of temperature increase ofT1, T2 and T3 is higher than those of T4, T5 and T6. This can be explained by the fact that the first column of thermocouples (T1, T2 and T3) are close to the heated wall and receives heat through a thin layer of liquid PCM. A quick increase (jump) of temperatures is observed when the thermal boundary layer associated to the melt front passes through each thermocouple, followed by a gradual increase of temperatures until the end of the melting process. The values for the temperatures jump decrease from the top to bottom locations of thermocouples, as shown in Fig.5.1. The decreasing trend of

temperature jump and increasing melting time between the upper and lower thermocouples affects the thermal boundary layer thickness along the solid-liquid interface

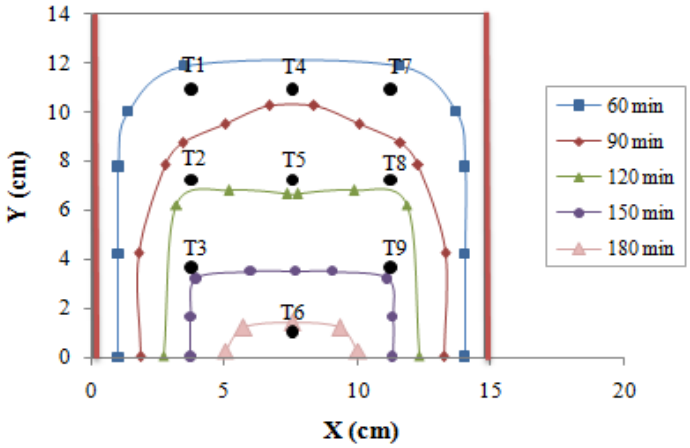

Fig. 5.2 Time evolution of the melting front of paraffin alone.

Fig. 5.2 shows the time evolution of the solid-liquid interface during melting of the paraffin alone. The position of the melting front is indicated by an average melting temperature of 51.5 °C and determined via the temperature evolution. Using linear interpolation in the vertical Y_i and horizontal X_i direction, the location of the melting temperature can be found by the temperature evolution of the two adjacent thermocouples.

$$\frac{T_i - T_f}{T_i - T_j} = \frac{X_i - X_f}{X_i - X_j} \quad (5.1)$$

$$\frac{T_i - T_f}{T_i - T_j} = \frac{Y_i - Y_f}{Y_i - Y_j} \quad (5.2)$$

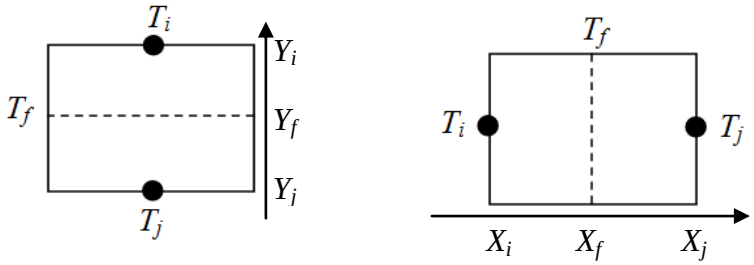

Fig. 5.3 Linear interpolation between two adjacent thermocouples

Initial measurements show that the melting process starts from the heated walls, and the solid-liquid interface is parallel to the heated walls showing that the heat transfer mechanism is predominated by pure conduction. In comparison to the bottom region of the enclosure, the liquid PCM at the top of the enclosure thickens more quickly over time. As the melting evolves, the natural convection current is strengthened and its effect on the melt front becomes more pronounced. Liquid PCM rises along each hot wall and descends along the two solid–liquid interfaces forming two symmetrical vortices in the thermal cavity as a result of buoyancy force development, and this current manifests itself by forming a curve at the melt front's top. As the solid PCM shrinks, conduction heat transfer predominates at the upper section of the cavity where the heated liquid PCM is accumulated, while convection current is confined to the lower part of the cavity. This results in diminishing convection from the hot wall to the PCM. Kamkari and Shokouhmand [215] similarly reported that during the final stage of the melting process in a rectangular enclosure, the diminishment of the convection flow at the upper part of the enclosure leads to the formation of a stratified temperature field.

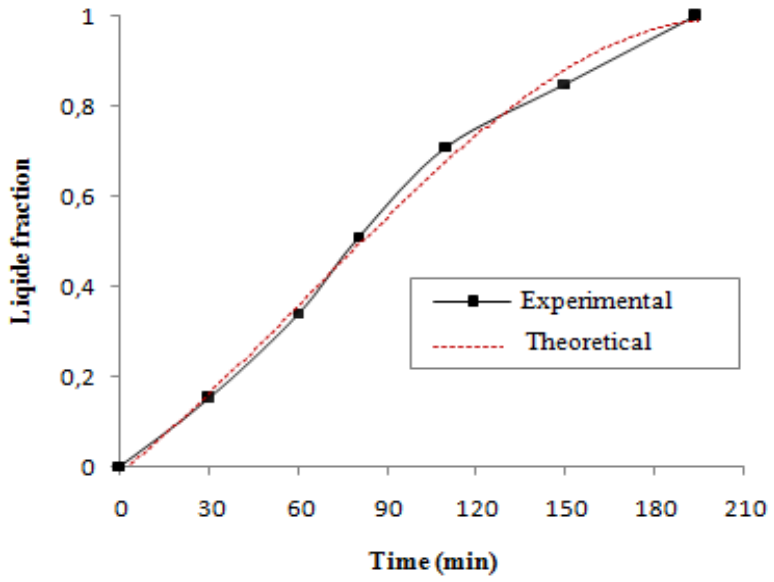

Fig.5.4. Temporal evolution of the liquid fraction

Fig. 5.4 shows the time evolution of the liquid fraction which represents the ratio of the volume of liquid paraffin to the total volume of paraffin. At the beginning of the melting process (30min),the liquid fraction reaches 15% and the conduction dominates the heat transfer with a melting rate of 3.5 g/min. Afterward, the melting rate accelerates and reaches71% after 110 min with a melting rate of 6.1 g/min due to the development of

natural convection in the liquid phase. Then, the temperature gradient in the paraffin weakens, and the convective transfer slows down the melting until the end with a rate of 2.8 g/min. The time evolution of the liquid fraction can be approximated mathematically by the following 3-degree polynomial equation:

$$f_l = -10^{-7}t^3 + 2\times10^{-5}t^2 + 0{,}005t \tag{5.3}$$

5.2.2 Energy storage

The thermal energy stored can be quantified based on the following expression:

$$Q_{st} = \sum_{t=t_i}^{t_s}\left[M_{PCM}\, C_s\left(T^{t+\Delta t}-T^t\right)\right] + \sum_{t=t_s}^{t_l}\left[M_{PCM}\, L_f\, f_l\right] + \sum_{t=t_l}^{t}\left[M_{PCM}\, C_l\left(T^{t+\Delta t}-T^t\right)\right] + \sum_{t=t_i}^{t}\left[M_{grid}\, C_{grid}\left(T^{t+\Delta t}-T^t\right)\right] + \sum_{t=t_i}^{t}\left[M_{cavity}\, C_{cavity}\left(T^{t+\Delta t}-T^t\right)\right] \tag{5.4}$$

Where $\boldsymbol{Q_{st}}$ (kJ) is the sum-up of thermal energy stored by PCM from time $\boldsymbol{t}$= 0, $\boldsymbol{M_m}$(kg) the mass of PCM, $\boldsymbol{C_s}$ and $\boldsymbol{C_l}$ (kJ/kgK) the solid and liquid heat capacity of PCM, $\boldsymbol{L_f}$ (kJ/kg) latent heat of fusion of PCM, $\boldsymbol{f_l}$ liquid fraction of PCM, $T^{t+\Delta t}$(°C) actual temperature of PCM and T^t(°C) is the previous temperature of PCM. M_{steel} is the mass of the steel plates, M_{Zamak} is the mass of the Zamak grid, Cp_{steel} and Cp_{Zamak} are the specific heat capacities of the steel and Zamak, respectively.

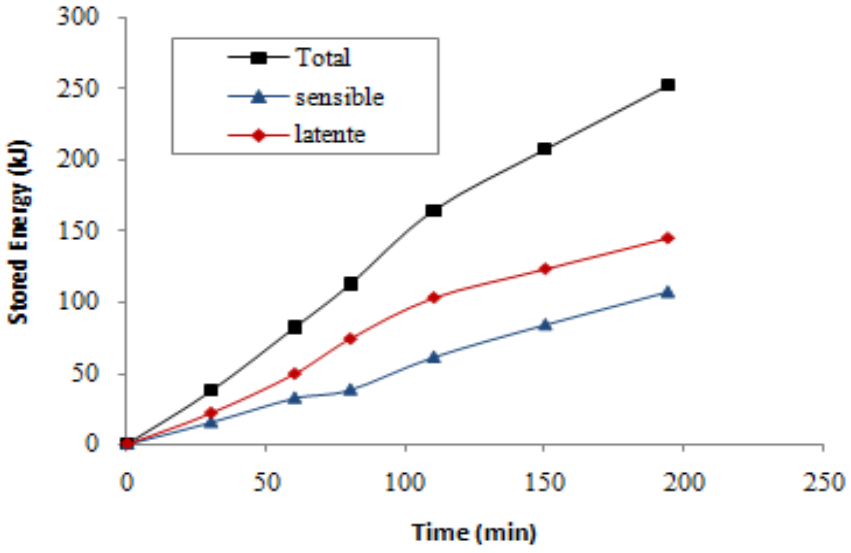

Fig.5.5. Temporal evolution of the stored energy

Fig. 5.5 Shows the time evolution of the thermal energy stored during the paraffin melting process. The total energy is composed of the sensible energy (solid or liquid states) and the latent energy (phase change) accumulated in the paraffin, Eq. (5.4). After 60min, the liquid fraction reaches 34%, and the system stores 49kJ by latent heat and 32.4 kJ by sensible heat. The latent heat represents 60 % of the thermal energy stored during the first moments of fusion. At the end of fusion, the paraffin stores 252 kJ, of which 57.5% by latent heat and 42.5% by sensible heat.

5.2.3 Heat transfer characteristics

The internal heat transfer coefficient between the cavity wall and the paraffin can be calculated as follows:

$$h = \frac{\frac{dQ_{st}}{dt}}{S(T_{hot\,wall} - T_{melting})} \tag{5.5}$$

Using the finite difference method, Eq.5.5 can be expressed:

$$h(t) = \frac{Q_{st}(t+\Delta t) - Q_{st}(t)}{S(T_{hot\,wall} - T_{melting})\Delta t} \tag{5.6}$$

Thus, the Nusselt number can be expressed as follows:

$$Nu(t) = \frac{h(t) \times height}{\lambda_{PCM}} \tag{5.7}$$

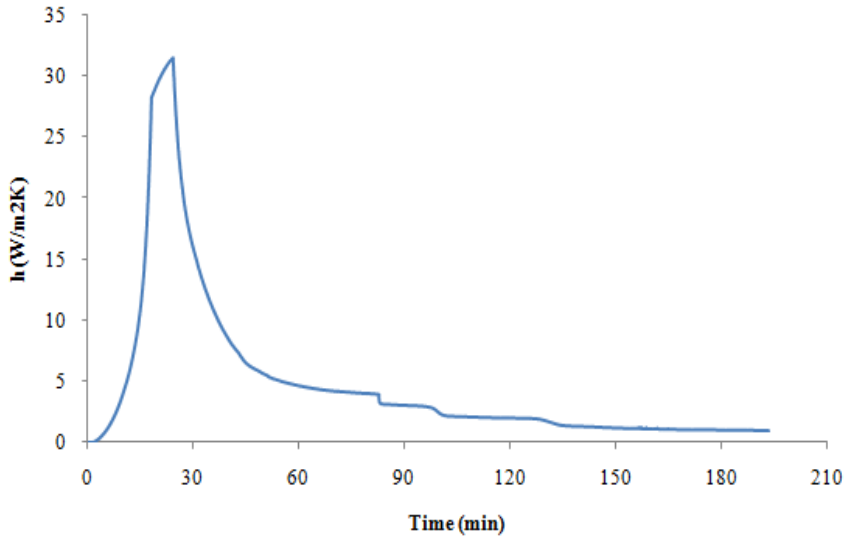

Fig.5.6. Time evolution of the heat coefficient

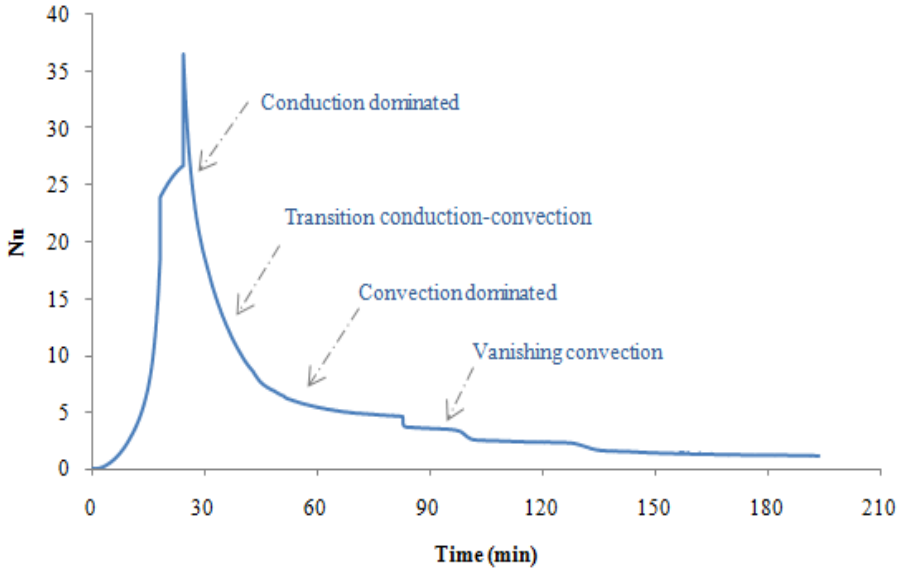

Fig.5.7. Time evolution of the average Nusselt number at the heated wall

Fig. 5.6 shows the time evolution of the internal convection coefficient between the cavity wall and the paraffin. Fig. 5.7 shows different heat transfer regimes during the melting process. Initially, conduction dominates the heat transfer and the temperature gradient is maximum between the heat source and the solid paraffin. The heat transfer rate then increases with an increase in the internal convection coefficient to reach a maximum of 31.52 W/m^2K after 24 min. A very thin layer of liquid paraffin forms near the heat source creating a very low thermal resistance, which is reflected in a significant increase in the Nusselt number at start-up (Fig.5.7) to reach a maximum of 36.6 after 24

min. With the increase in the thickness of the liquid, the Nusselt number decreases very rapidly (the end of the conduction regime) and natural convection takes place in the liquid paraffin due to the buoyancy force (transition regime).After the short period of transition from conduction to convection, Nusselt numbers display quasi-steady values corresponding to the convection-dominated stage of melting. Fig.5.6 shows that the thermal transfer by natural convection gradually decreases until it disappears at the end of melting reaching the thermal equilibrium regime and the coefficient stabilizes around 1 W/m^2K. This decreasing trend denotes the weakening of convection currents brought on by the rise in liquid PCM bulk temperature (to achieve the temperature of the hot wall) and falls in solid-liquid interface length. The interface serves as the cold source for natural convection currents in the thermal cavity.

5.3 Paraffin with aluminium plates

5.3.1 Solid-liquid interface

Fig.5.8 shows the temporal evolution of the extreme temperatures T1 and T6 during the melting of the paraffin alone, and with the 2, 4 and 8 aluminum plates. In all cases, heat is transmitted to the thermocouples by conduction through the solid PCM when the temperature is below to the melting point (49 °C).

After 80 min, T1 and T6 reach (54.6, 54.4, 53.6, and 57.4 °C), and (37.4, 38.5, 39.6, and 43.2 °C) with 0, 2, 4, and 8 aluminum plates, respectively. After 130 min, they reach (81.9, 80.5, 79.6 and 72°C), and (42.3, 45.8, 48.7, and 53.5 °C). Thus, the average temperature difference (T1 - T6) reaches 44, 43.6, 37, and 19.6°C for 0, 2, 4 ,and 8 plates, respectively. The integration of the aluminum plates leads to a decrease of the temperature gradients in the paraffin by 1, 4 and 16% in the case of 2, 4, and 8 plates, respectively. The aluminum plates promote heat penetration into the solid paraffin due to its good conductivity and slow down the thermo-convective flow in the liquid paraffin by improving the heat conduction. The addition of aluminum improves the homogenization of the paraffin temperature by 1.15 and 55% for 2, 4 and 8 plates, respectively.

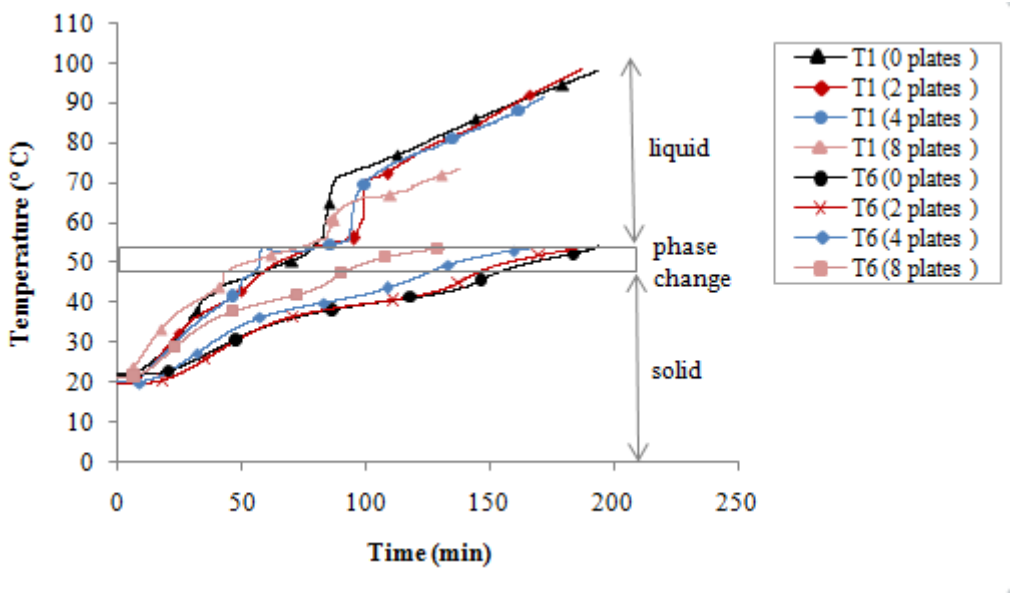

Fig. 5.8. Temporal evolution of extreme temperatures of paraffin with aluminum plates

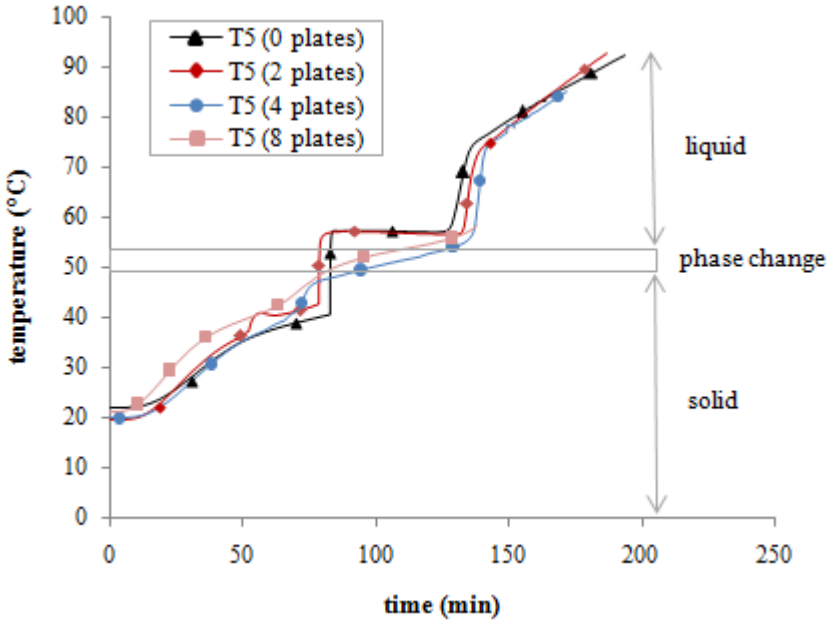

Fig. 5.9. Time evolution of the core temperature of paraffin with aluminum plates

According to Fig. 5.8, it can be observed that the increase in aluminum plates reduces the creation of air pores during solidification. Indeed, the reduction and absence of the temperature jump T5 around 80 min is an excellent indicator of this phenomenon. The greater the temperature jump, the greater the amount of air pores in the paraffin.

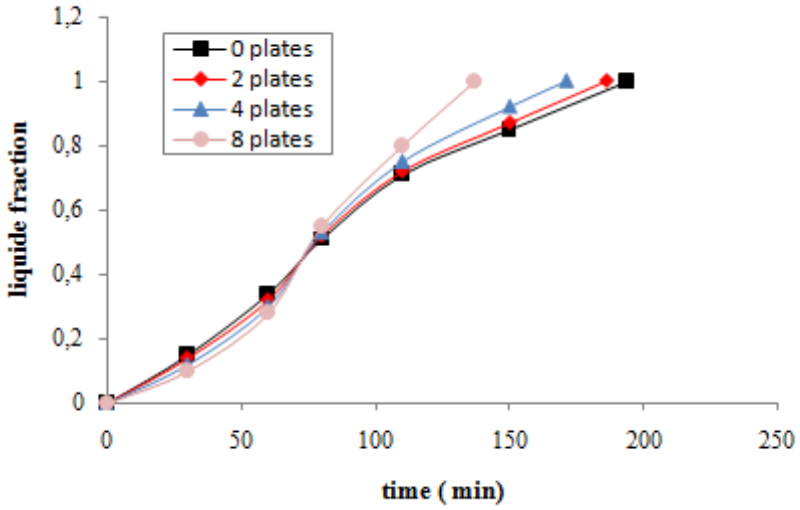

Fig. 5.10. Time evolution of the liquid fraction of paraffin with aluminum plates

Fig. 5.10 shows the comparison between the evolution of the liquid fraction of the paraffin with and without the aluminum plates. After 60min, the liquid fraction reaches around (34, 32, 30, and 28%) with a melting rate of (4.6, 4.4, 4.1, and 3.8 g/min) in the cases of (0, 2, 4, and 8 aluminum plates), respectively. It is noted that the melting of paraffin is faster with the reduction of aluminum plates in this period. Indeed, the aluminum plates absorb heat and decrease the heat absorbed by paraffin which causes a decrease in the liquid fraction rate, and a delay of the melting process by (6, 12, and 18%) for (2, 4and8 plates), respectively. At 110 min, the liquid fraction reaches 71, 72, 75, and 80%with a melting rate of (6.1, 6.6, 7.4, and 8.6 g/min) for paraffin alone and paraffin with 2, 4, and 8 aluminum plates, respectively. Aluminum contributes to accelerating the melting of paraffin by improving the effective thermal conductivity of the PCM. As evident, adding aluminum plates can accelerate the melting rate of 4, 12, and 29% for paraffin with 2, 4, and 8 plates.

5.3.2 Energy storage

By adding plates in paraffin, the thermal energy stored can be quantified based on the following expression:

$$Q_{st}=\sum_{t=t_i}^{t_s}\left[M_{PCM}\,C_s\left(T^{t+\Delta t}-T^{t}\right)\right]+\sum_{t=t_s}^{t_l}\left[M_{PCM}\,L_f\,f_l\right]+\sum_{t=t_l}^{t}\left[M_{PCM}\,C_l\left(T^{t+\Delta t}-T^{t}\right)\right]+\sum_{t=t_i}^{t}\left[M_{grid}\,C_{grid}\left(T^{t+\Delta t}-T^{t}\right)\right]$$
$$+\sum_{t=t_i}^{t}\left[M_{cavity}\,C_{cavity}\left(T^{t+\Delta t}-T^{t}\right)\right]+\sum_{t=t_i}^{t}\left[M_{plates}\,C_{plates}\left(T^{t+\Delta t}-T^{t}\right)\right] \quad (5.8)$$

Where M_{plates} is the mass of Aluminum plates and, C_{plates} are the specific heat capacities of the Aluminum.

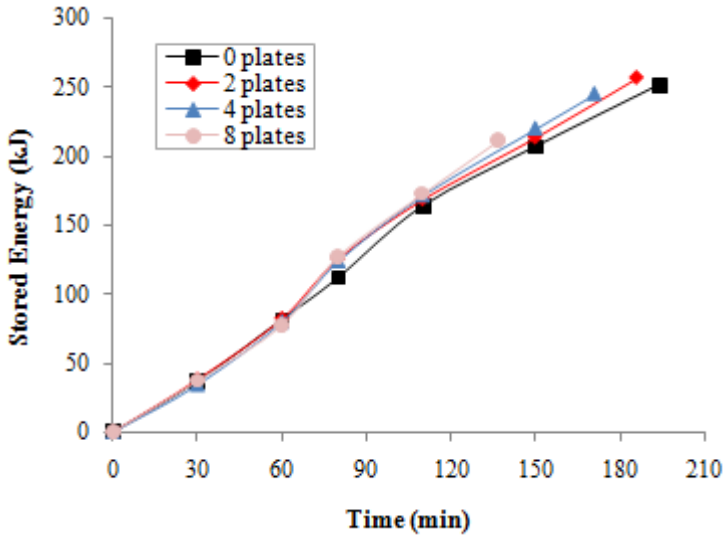

Fig.5.11. Time evolution of the energy stored in the paraffin with the aluminum plates

Fig. 5.11 shows the time evolution of the energy stored in the paraffin with the aluminum plates. The total energy stored is composed of the energy stored in the paraffin (sensible and latent), and the energy absorbed by the aluminum plates Eq. (5.8). At 60 min, the heat stored in the paraffin reaches 103.9, 82.2, 79.6, and 77.8 kJ for 0, 2, 4, and 8 aluminum plates. Over time (137 min), the energy stored in the paraffin with the plates exceeds that of the paraffin alone to reach 193.3, 199, 203.4, and 212 kJ with 0.2, and 4.8 plates, respectively. Thus, an improvement in thermal storage by 3, 5.2, and 9.6% is recorded.

5.3.3 Heat transfer characteristics

Fig. 5.12 and 5.13 show the time evolution of the convection coefficient and the mean internal Nusselt number with aluminum plates. At start-up, the aluminum mass contributes to reducing the temperature of the solid paraffin thanks to its specific heat. It thus prolongs the duration of the conductive heat transfer and decreases the maximum convection coefficient which reaches 36.6, 30.4, 26.6, and 18.1 W/m^{2}K after 24, 33, 42, and 53.5 min for the paraffin with 0, 2, 4, and 8 aluminum plates, respectively. The convection coefficient shows a decrease of 17, 25 and 50% and the conduction shows a time extension of 36, 75 and 121% compared to the paraffin alone. In adding, the increase of aluminum plates accelerates the conduction-convection transition and improves significantly the heat transfer rate throughout the melting process. The effective thermal conductivity becomes 0.259, 0.295, and 0.514W/mK in the cases of 2, 4, and 8 aluminum plates, respectively (Fig. 5.14). Thus, the aluminum plates can increase the thermal conductivity of paraffin by about 30, 50, and 155%.

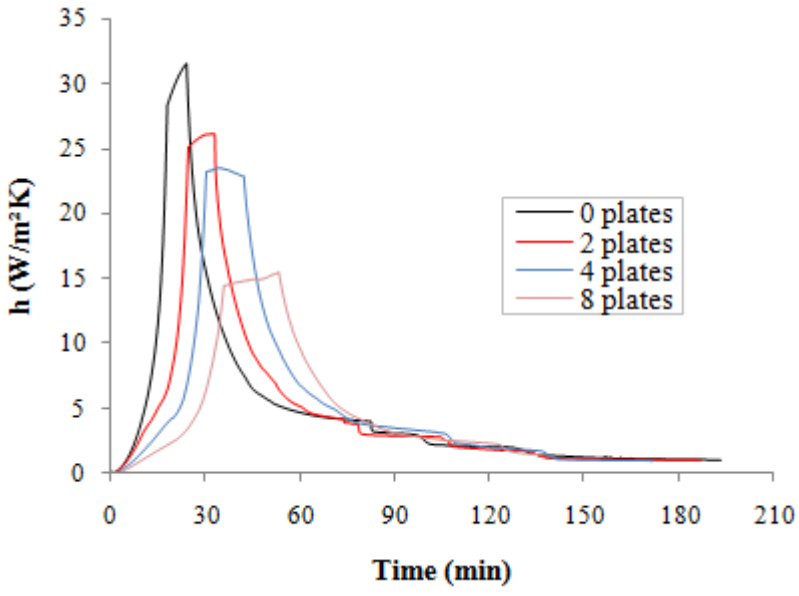

Fig. 5.12.Time evolution of the convection coefficient with aluminum plates.

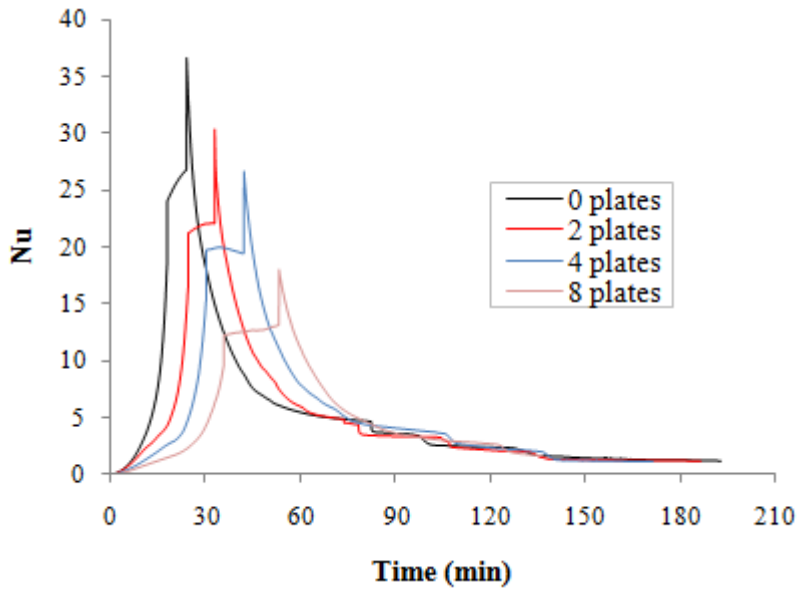

Fig. 5.13.Time evolution of the average Nusselt number with aluminum plates.

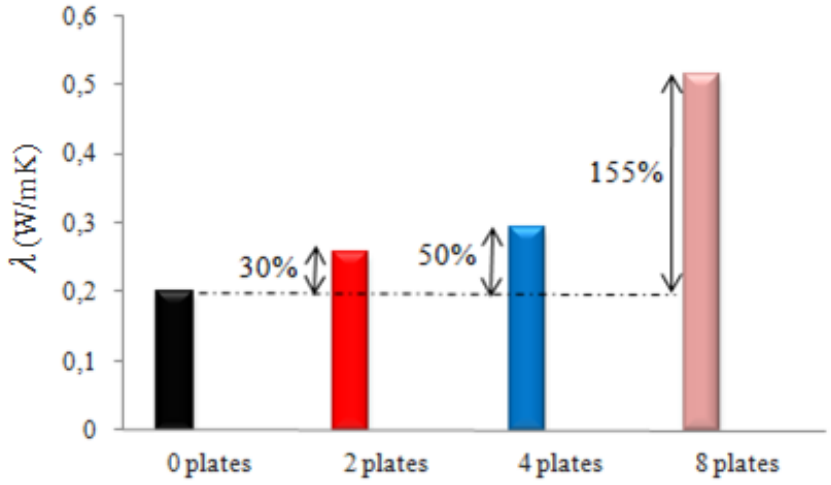

Fig. 5.14.Values of the effective thermal conductivity of paraffin with aluminum plates.

General Conclusion

General Conclusion

The present experimental work focuses on improving the effective thermal conductivity of paraffin by integrating different metallic materials with different concentrations. The first part of the experimental study concerns the thermal analysis and the acceleration of the paraffin melting process by adding various metal additives like Zamak, aluminum and copper. Through the various experiments, we have observed the following:

1. It is noted that the melting of paraffin alone is initially faster than that integrating the Zamak grid by about 8%. However, the melting process of the paraffin with the Zamak grid increases after, and the complete melting is achieved in both cases at the same time.
2. Adding the Zamak grid or aluminum perforated plates to the paraffin absorbs heat and delays the melting process during the first period. Afterward, an acceleration of the melting process is recorded. However, the liquid fraction of copper–paraffin is always more important than the paraffin alone. At the end, the copper and aluminum plate additives can accelerate the melting process of paraffin by about 21% and 19%.
3. The temperature gradient in paraffin decreases by adding metal additives plates. They can help to homogenize the temperature of the paraffin by reducing the average temperature difference by about 5.5°C (8%), 6°C (9%), and 8°C (12%) with Zamak, aluminum ,and copper plates, respectively.
4. The effective thermal conductivity becomes 0.174, 0.272 and 0.798W/mK by integrating the Zamak, aluminum and copper in the pure paraffin. Thus, the Zamak grid decreases the thermal conductivity of paraffin by about 13%. However, aluminum and copper plates can increase the thermal conductivity of paraffin to about 36% and 300%.
5. The good heat capacity of aluminum and the good effective thermal conductivity of aluminum-paraffin accelerates heat transfer and increases the amount of heat stored. Thus, aluminum increases the energy stored by 3.1%, but Zamak decreases the energy stored by about 3.5%. For copper paraffin, the global energy stored is almost the same as the pure paraffin.

In the second part of the experimental study, the influence of the number of added plates on the dynamic and thermal behavior of the paraffin melting process was investigated. The study led to the following conclusions:

1. The integration of aluminum plates leads to a decrease of the temperature gradients in the paraffin by 1.4 and 16% and improves the temperature homogenization of the paraffin by 1.15 and 55% with 2.4 and 8 plates, respectively
2. The increase in aluminum plates reduces the creation of air pores during solidification and the contraction of the paraffin during previous experiments
3. At start-up, the aluminum absorbs the heat which causes a decrease in the liquid faction, and delays the melting by 6, 12 and 18% respectively with 2,4 and 8 plates. At the end of the melting process, the addition of the aluminum plates has a significant impact on the reduction of the melting time of the paraffin with an acceleration of 4, 12,and 29% for the paraffin with 2, 4 and 8 plates.
4. Aluminum plates improve the thermal conductivity of paraffin by 30, 50 and 155% with 2, 4 ,and 8 plates
5. The good thermal capacity of aluminum increases the amount of heat stored. Thus, aluminum improves thermal storage by 3, 5.2 and 9.6% with 2,4 and 8 aluminum plates, respectively.
6. At the beginning of the melting process, the convection coefficient decreases by 17.25 and 50% and the conduction has a time extension of 36, 75 and 121%.
7. The increase in aluminum plates accelerates the conduction-convection transition and significantly improves the heat transfer rate throughout the melting process,

In perspective, it is interesting to develop a numerical simulation of the studied phenomenon in order to better exploit the obtained results and reduce the costs of the manipulations. In addition, it is interesting to optimize the size and density of the air pores created as a function of the metal plates added and their effects on the thermal and dynamic behavior of the paraffin melt.

References

References

[1] A. Sharma, V.V. Tyagi, C.R. Chen, D. Buddhi, Review on thermal energy storage with phase change materials and applications, Renew. Sust. Energy Rev. 13 (2009) 318–345.

[2] D. Zhou, C.Y. Zhao, Y. Tian, Review on thermal energy storage with phase change materials (PCMs) in building applications, Appl. Energy. 92 (2012) 593–605.

[3] M.M. Alkilani, K. Sopian, M.A. Alghoul, M. Sohif, M.H. Ruslan, Review of solar air collectors with thermal storage units, Renew. Sust. Energy Rev. 15 (2011) 1476–1490.

[4] A.J.N. Khalifa, K.H. Suffer, M.S. Mahmoud, A storage domestic solar hot water system with a back layer of phase change material, Exp. Therm. Fluid Sci. 44 (2013) 174–181.

[5] V. Pandiyarajan, M. Chinna Pandian, E. Malan, R. Velraj, R.V. Seeniraj, Experimental investigation on heat recovery from diesel engine exhaust using finned shell and tube heat exchanger and thermal storage system, Appl. Energy 88 (2011) 77–87.

[6] Z. Gu, H. Liu, Y. Li, Thermal energy recovery of air conditioning system–heat recovery system calculation and phase change materials development, Appl. Therm. Eng. 24 (2004) 2511–2526.

[7] A. Hasan, S.J. Mccormack, M.J. Huang, B. Norton, Evaluation of phase change materials for thermal regulation enhancement of building integrated photovoltaics, Sol. Energy 84 (2010) 1601–1612.

[8] H. Zhang, Q. Xu, Z. Zhao, J. Zhang, Y. Sun, L. Sun, F. Xu, Y. Sawada, Preparation and thermal performance of gypsum boards incorporated with microencapsulated phase change materials for thermal regulation, Sol. Energy Mater. Sol. Cells 102 (2012) 93–102.

[9] S.C. Fok, W. Shen, F.L. Tan, Cooling of portable hand-held electronic devices using phase change materials in finned heat sinks, Int. J. Therm. Sci. 49 (2010) 109–117.

[10] F.L. Tan, C.P. Tso, Cooling of mobile electronic devices using phase change materials, Appl. Therm. Eng. 24 (2004) 159–169.

[11] T.D. Swanson, G.C. Birur, NASA thermal control technologies for robotic spacecraft, Appl. Therm. Eng. 23 (2003) 1055–1065.

[12] N. Sarier, E. Onder, Organic phase change materials and their textile applications: an overview, Thermochim. Acta 54 (2012) 7–60.

[13] M. Murat Kenisarin, K. Mahkamov, Sol Carolina Costa, Irina Makhkamova Melting and solidification of PCMs inside a spherical capsule: A critical review, Journal of Energy Storage 27 (2020) 101082

[14] H. Shokouhmand, B. Kamkari, Experimental investigation on melting heat transfer characteristics of lauric acid in a rectangular thermal storage unit, Experimental Thermal and Fluid Science 50 (2013) 201–212

[15] S. Madrugaa, N. Harukib and A. Horibec, Experimental and numerical study of melting of the phase change material tetracosane, Int. Commun. Heat Mass Transf. 98 (2018) 163–170.

[16] Satbhai O, Roy S, Ghosh S. Role of heating location on the performance of a natural convection driven melting process inside a square-shaped thermal energy storage system. J Therm Sci Eng Appl 2018;10(6).

[17]A. N. Korti, H. Guellil, Experimental study of the effect of inclination angle on the paraffin melting process in a square cavity, Journal of Energy Storage 32 (2020) 101726

[18] M. Bechiria,b , Kacem Mansourib,, Study of heat and fluid flow during melting of PCM inside vertical cylindrical tube, International Journal of Thermal Sciences 135 (2019) 235–246

[19] Benjamin J. Jones, Dawei Sun, Shankar Krishnan, Suresh V. Garimella *, Experimental and numerical study of melting in a cylinder, International Journal of Heat and Mass Transfer 49 (2006) 2724–2738

[20] J.M. Khodadadi, Y. Zhang 1, Effects of buoyancy-driven convection on melting within spherical containers, International Journal of Heat and Mass Transfer 44 (2001) 1605±1618

[21] F.L. Tan a, S.F. Hosseinizadeh b,1, J.M. Khodadadi b,*, Liwu Fan b, Experimental and computational study of constrained melting of phase change materials (PCM) inside a spherical capsule, International Journal of Heat and Mass Transfer 52 (2009) 3464–3472

[22] Qureshi ZA, Ali HM, Khushnood S. Recent advances on thermal conductivity enhancement of phase change materials for energy storage system: A review. Int J Heat Mass Transf 2018;127:838–56. https://doi.org/10.1016/J. IJHEATMASSTRAN-SFER .2018.08.049.

[23] Gasia J, Maldonado JM, Galati F, De Simone M, Cabeza LF. Experimental evaluation of the use of fins and metal wool as heat transfer enhancement techniques in a latent heat thermal energy storage system. Energy Convers Manag 2019;184:530–8. https://doi.org/10.1016/j.enconman.2019.01.085.

[24] Wang P, Yao H, Lan Z, Peng Z, Huang Y, Ding Y. Numerical investigation of PCM melting process in sleeve tube with internal fins. Energy Convers Manag 2016;110:428–35. https://doi.org/10.1016/j.enconman.2015.12.042.

[25] Tauseef-ur-Rehman HM, Ali MM, Janjua U, Sajjad W-M. Yan, A critical review on heat transfer augmentation of phase change materials embedded with porous materials/ foams. Int J Heat Mass Transf 2019;135:649–73. https://doi.org/10.1016/J.IJHEATMASSTRANSFER.2019.02.001.

[26] Sardari PT, Grant D, Giddings D, Walker GS, Gillott M. Composite metal foam/PCM energy store design for dwelling space air heating. Energy Convers Manag 2019;201. https://doi.org/10.1016/j.enconman.2019.112151.

[27] Tiari S, Mahdavi M, Qiu S. Experimental study of a latent heat thermal energy storage system assisted by a heat pipe network. Energy Convers Manag 2017;153:362–73. https://doi.org/10.1016/j.enconman.2017.10.019.

[28] Leong KY, Abdul Rahman MR, Gurunathan BA. Nano-enhanced phase change materials: A review of thermo-physical properties, applications and challenges. J Energy Storage 2019;21:18–31. https://doi.org/10.1016/j.est.2018.11.008.

[29] B. Kamkari, H. Shokouhmand, Experimental investigation of phase change material melting in rectangular enclosures with horizontal partial fins, International Journal of Heat and Mass Transfer 78 (2014) 839–851

[30] Lin-Li Tiana,b, XunLiua,b, ShuaiChenc, Zu-GuoShena,b, Effect of fin material on MCP melting in a rectangular enclosure, Applied Thermal Engineering 167 (2020) 114764

[31] M.J. Huang a, P.C. Eames a,*, B. Norton b, Thermal regulation of building-integrated photovoltaics using phase change materials, International Journal of Heat and Mass Transfer 47 (2004) 2715–2733

[32] H. Guellil, A. N. Korti and S. Abboudi, Experimental study of the performance of a novel latentheat charging unit on charging and discharging processes, Heat Mass Transf. 55 (2018) 855–866.

[33] B. Kamkari, D. Groulx, Experimental investigation of melting ehavior of phase change material in finned rectangular enclosures under different inclination angles, https://doi.org/10.1016/j.expthermflusci.2018.04.007

[34] R. Kalbasi, M. Afrand, J. Alsarraf and M. D. Tran, Studies on optimum ¯ns number in MCP-based heat sinks, Energy 171 (2019) 1088–1099.

[35] J. Gasiaa, José Miguel Maldonadoa, Francesco Galatib, Marilena De Simoneb, Luisa F. Cabezaa,∗, Experimental evaluation of the use of fins and metal wool as heat transfer enhancement techniques in a latent heat thermal energy storage system, Energy Conversion and Management 184 (2019) 530–538

[36] Chi-ming Lai Shuichi Hokoi, Thermal performance of an aluminum honeycomb wallboard incorporating microencapsulated PCM, http://dx.doi.org/doi: 10.1016/j .enbuild. 2014.01.017

[37] R. Karami, B. Kamkari, Experimental investigation of the effect of perforated fins on thermal performance enhancement of vertical shell and tube latent heat energy storage systems, Energy Conversion and Management 210 (2020) 112679

[38] N.H.S. Tay , F. Bruno, M. Belusko, Comparison of pinned and finned tubes in a phase change thermal energy storage system using CFD, Applied Energy 104 (2013) 79–86

[39] Peilun Wang a,b, Hua Yao b, Zhipeng Lan b, Zhijian Peng a,⇑, Yun Huang b,⇑, Yulong Ding c Numerical investigation of PCM melting process in sleeve tube with internal fins, Energy Conversion and Management 110 (2016) 428–435

[40] S. Aziz, N.A.M. Amin, M.S. Abdul Majid, M. Belusko, F. Bruno CFD simulation of a TES tank comprising a PCM encapsulated in sphere with heat transfer enhancement

[41] K. Govindaraja, P. Panchabikesan, D.C. Denkenberger, V. Ramalingam, Effect of fin orientations in a spherically encapsulated phase change materials for effective heat transfer enhancement, Chem. Eng. Trans. 62 (2017) 277–282.

[42] Velraj R, Seeniraj R V., Hafner B, Faber C, Schwarzer K. Experimental analysis and numerical modelling of inward solidification on a finned vertical tube for a latent heat storage unit. Sol Energy 1997;60:281–90. doi:10.1016/S0038-092X(96)00167-3.

[43] Wickramaratne, Chatura, "Experimental Study of High-Temperature Range Latent Heat Thermal Energy Storage" (2017). University of South Florida Tampa Graduate Theses and Dissertations. https://digitalcommons.usf.edu/etd/7451

[44] Stritih U. An experimental study of enhanced heat transfer in rectangular PCM thermal storage. Int J Heat Mass Transf 2004;47:2841–7. doi:10.1016/j .ijhea tmass transfer. 2004.02.001.

[45] Hosseinizadeh SF, Tan FL, Moosania SM. Experimental and numerical studies on performance of PCM-based heat sink with different configurations of internal fins. Appl. Therm. Eng., vol. 31, Pergamon; 2011, p. 3827–38. doi:10.1016/j. applthermal eng. 2011.07.031.

[46] Zhao D, Tan G. Numerical analysis of a shell-and-tube latent heat storage unit with fins for air-conditioning application. Appl Energy 2015;138:381–92. doi:10.1016/j.apenergy.2014.10.051.

[47] Rathod MK, Banerjee J. Thermal performance enhancement of shell and tube Latent Heat Storage Unit using longitudinal fins. Appl Therm Eng 2015;75:1084–92. doi:10.1016/j.applthermaleng.2014.10.074.

[48] Rahimi M, Ranjbar AA, Ganji DD, Sedighi K, Hosseini MJ, Bahrampoury R. Analysis of geometrical and operational parameters of PCM in a fin and tube heat exchanger. Int Commun Heat Mass Transf 2014;53:109–15. doi:10.1016/j. icheatmass transfer. 2014.02.025.

[49] Al-Abidi AA, Mat S, Sopian K, Sulaiman MY, Mohammad AT. Internal and external fin heat transfer enhancement technique for latent heat thermal energy

storage in triplex tube heat exchangers. Appl Therm Eng 2013;53:147–56. doi:10.1016/j.applthermaleng.2013.01.011.

[50] Al-Abidi AA, Mat S, Sopian K, Sulaiman MY, Mohammad AT. Numerical study of PCM solidification in a triplex tube heat exchanger with internal and external fins. Int J Heat Mass Transf 2013;61:684–95. doi:10.1016/j. ijheatmasstransfer. 2013.02. 030.

[51] Mat S, Al-Abidi AA, Sopian K, Sulaiman MY, Mohammad AT. Enhance heat transfer for PCM melting in triplex tube with internal-external fins. Energy Convers Manag 2013;74:223–36. doi:10.1016/j.enconman.2013.05.003.

[52] Choi JC, Kim SD, Han GY. Heat transfer characteristics in low-temperature latent heat storage systems using salt-hydrates at heat recovery stage. Sol Energy Mater Sol Cells 1996;40:71–87. doi:10.1016/0927-0248(95)00084-4.

[53] Erek A, Ilken Z, Acar MA. Experimental and numerical investigation of thermal energy storage with a finned tube. Int J Energy Res 2005;29:283–301. doi:10. 1002/ er. 1057.

[54] Agyenim F, Eames P, Smyth M. A comparison of heat transfer enhancement in a medium temperature thermal energy storage heat exchanger using fins. Sol Energy 2009;83:1509–20. doi:10.1016/j.solener.2009.04.007.

[55] Liu Z, Sun X, Ma C. Experimental investigations on the characteristics of melting processes of stearic acid in an annulus and its thermal conductivity enhancement by fins. Energy Convers Manag 2005;46:959–69. doi:10.1016/j. enconman. 2004.05.012.

[56] Chen J, Yang D, Jiang J, Ma A, Song D. Research Progress of Phase Change Materials (PCMs) Embedded with Metal Foam (a Review). Procedia Mater Sci 2014;4:389–94. doi:10.1016/j.mspro.2014.07.579.

[57] Mills A, Farid M, Selman JR, Al-Hallaj S. Thermal conductivity enhancement of phase change materials using a graphite matrix. Appl Therm Eng 2006;26:1652–61. doi:10.1016/j.applthermaleng.2005.11.022.

[58] Fleming E, Wen S, Shi L, Da Silva AK. Experimental and theoretical analysis of an aluminum foam enhanced phase change thermal storage unit. Int J Heat Mass Transf 2015;82:273–81. doi:10.1016/j.ijheatmasstransfer.2014.11.022.

[59] Ibrahim NI, Al-Sulaiman FA, Rahman S, Yilbas BS, Sahin AZ. Heat transfer enhancement of phase change materials for thermal energy storage applications: A critical review. Renew Sustain Energy Rev 2017;74:26–50. doi:10.1016/j.rser .2017. 01 .169.

[60] G. Righetti, R. Lazzarin, M. Noro, S. Mancin,Phase change materials emb e dde d in porous matrices for hybrid thermal energy storages: Experimental results and modeling, International Journal of Refrigeration 106 (2019) 266–277

[61] V. Joshi, Manish K. Rathod, Thermal transport augmentation in latent heat thermal energy storage system by partially filled metal foam: A novel configuration, Journal of Energy Storage 22 (2019) 270–282

[62] A. Pourakabara and A. A. R. Darzib, Enhancement of phase change rate of MCP in cylindrical thermal energy storage, Applied Thermal Engineering 150 (2019) 132–142.

[63] P. Talebizadeh Sardaria, , D. Grantb, D. Giddingsa, Gavin S. Walkerb, Mark Gillottc, Composite metal foam/PCM energy store design for dwelling space air Heating, Energy Conversion and Management 201 (2019) 112151

[64] Mills A, Farid M, Selman JR, Al-Hallaj S. Thermal conductivity enhancement of phase change materials using a graphite matrix. Appl Therm Eng 2006;26:1652–61. doi:10.1016/j.applthermaleng.2005.11.022.

[65] Dukhan N, Bodke S. An improved PCM heat storage technology utilizing metal foam. 2010 12th IEEE Intersoc. Conf. Therm. Thermomechanical Phenom. Electron. Syst. ITherm 2010, IEEE; 2010, p. 1–7. doi:10.1109/ITHERM.2010.5501364.

[66] Zhong Y, Guo Q, Li S, Shi J, Liu L. Heat transfer enhancement of paraffin wax using graphite foam for thermal energy storage. Sol Energy Mater Sol Cells 2010;94:1011–4. doi:10.1016/j.solmat.2010.02.004.

[67] Zhong Y, Li S, Wei X, Liu Z, Guo Q, Shi J, et al. Heat transfer enhancement of paraffin wax using compressed expanded natural graphite for thermal energy storage. Carbon N Y 2010;48:300–4. doi:10.1016/j.carbon.2009.09.033.

[68] Siahpush A, O'Brien J, Crepeau J. Phase Change Heat Transfer Enhancement Using Copper Porous Foam. J Heat Transfer 2008;130:82301. doi:10.1115/ 1.2928010.

[69] Wu ZG, Zhao CY. Experimental investigations of porous materials in high temperature thermal energy storage systems. Sol Energy 2011;85:1371–80. doi:10. 1016/j. solener.2011.03.021.

[70] Zhao CY, Wu ZG. Heat transfer enhancement of high temperature thermal energy storage using metal foams and expanded graphite. Sol Energy Mater Sol Cells 2011;95:636–43. doi:10.1016/j.solmat.2010.09.032.

[71] Zhong L, Zhang X, Luan Y, Wang G, Feng Y, Feng D. Preparation and thermal properties of porous heterogeneous composite phase change materials based on molten salts/expanded graphite. Sol Energy 2014;107:63–73. doi:10.1016/j. solener .2014 .05.019.

[72] Zhang P, Xiao X, Meng ZN, Li M. Heat transfer characteristics of a molten-salt thermal energy storage unit with and without heat transfer enhancement. Appl Energy 2015;137:758–72. doi:10.1016/j.apenergy.2014.10.004.

[73] Sari A, Karaipekli A. Thermal conductivity and latent heat thermal energy storage characteristics of paraffin/expanded graphite composite as phase change material. Appl Therm Eng 2007;27:1271– doi:10.1016/j.applthermaleng.2006.11.004.

[74], P. Manoj Kumar a, D. Sudarvizhi a , P. Michael Joseph Stalin b , A. Aarif a , R. Abhinandhana a, A. Renuprasanth a, V. Sathya a, N. Thirukkural Ezhilan a, Thermal characteristics analysis of a phase change material under the influence of nanoparticles, https://doi.org/10.1016/j.matpr.2020.12.505

[75] M. Nitsas, I.P. Koronaki, Performance analysis of nanoparticles-enhanced PCM: An experimental approach, New Journal and we have not received input yet 25 (2021) 100963

[76] Jin Wang a, Kai Yu a, Runze Duan a, Gongnan Xie b, Bengt Sunden c, Enhanced thermal management by introducing nanoparticle composite phase change materials for cooling multiple heat sources systems, Energy 227 (2021) 120495

[77] R. Elarem a , Talal Alqahtani b , Sofiene Mellouli c , Walid Aich d,e , Nidhal Ben Khedher d , Lioua Kolsi d,f, Abdelmajid Jemni a, Numerical study of an Evacuated Tube Solar Collector incorporating a Nano-PCM as a latent heat storage system, Case Studies in Thermal Engineering 24 (2021) 100859

[78] Changda Nie a, Jiangwei Liu a, Shengxiang Deng a,b, Effect of geometric parameter and nanoparticles on PCM melting in a vertical shell-tube system, https: //doi.org/10.1016/j. applthermaleng.2020.116290

[79] Ho CJ, Gao JY. An experimental study on melting heat transfer of paraffin dispersed with Al2O3 nanoparticles in a vertical enclosure. Int J Heat Mass Transf 2013;62:2–8. doi:10.1016/j.ijheatmasstransfer.2013.02.065.

[80] Motahar S, Nikkam N, Alemrajabi AA, Khodabandeh R, Toprak MS, Muhammed M. Experimental investigation on thermal and rheological properties of n-octadecane with dispersed TiO2 nanoparticles. Int Commun Heat Mass Transf 2014;59:68–74. doi:10.1016/j.icheatmasstransfer.2014.10.016.

[81] Cui Y, Liu C, Hu S, Yu X. The experimental exploration of carbon nanofiber and carbon nanotube additives on thermal behavior of phase change materials. Sol Energy Mater Sol Cells 2011;95:1208–12. doi:10.1016/j.solmat.2011.01.021.

[82] Zhang N, Yuan Y, Yuan Y, Cao X, Yang X. Effect of carbon nanotubes on the thermal behavior of palmitic-stearic acid eutectic mixtures as phase change materials for energy storage. Sol Energy 2014;110:64–70. doi:10.1016/j.solener.2014.09.003.

[83] Shaikh S, Lafdi K, Hallinan K. Carbon nanoadditives to enhance latent energy storage of phase change materials. J Appl Phys 2008;103:94302. doi:10.1063 /1.2903 538.

[84] Wu ZG, Zhao CY. Experimental investigations of porous materials in high temperature thermal energy storage systems. Sol Energy 2011;85:1371–80. doi:10. 1016/j. solener.2011.03.021.

[85] Wang J, Xie H, Xin Z. Thermal properties of paraffin based composites containing multi-walled carbon nanotubes. Thermochim Acta 2009;488:39–42. doi:10.1016/j.tca.2009.01.022.

[86] Teng TP, Cheng CM, Cheng CP. Performance assessment of heat storage by phase change materials containing MWCNTs and graphite. Appl. Therm. Eng., vol. 50, Pergamon; 2013, p. 637–44. doi:10.1016/j.applthermaleng.2012.07.002.

[87] Fan LW, Fang X, Wang X, Zeng Y, Xiao YQ, Yu ZT, et al. Effects of various carbon nanofillers on the thermal conductivity and energy storage properties of paraffin-based nanocomposite phase change materials. Appl Energy 2013;110:163–72. doi:10.1016/j.apenergy.2013.04.043.

[88] Harish S, Orejon D, Takata Y, Kohno M. Thermal conductivity enhancement of lauric acid phase change nanocomposite with graphene nanoplatelets. Appl Therm Eng 2015;80:205–11. doi:10.1016/j.applthermaleng.2015.01.056.

[89] Zeng J-L, Zhu F-R, Yu S-B, Zhu L, Cao Z, Sun L-X, et al. Effects of copper nanowires on the properties of an organic phase change material. Sol Energy Mater Sol Cells 2012;105:174–8. doi:10.1016/j.solmat.2012.06.013.

[90] Myers PD, Alam TE, Kamal R, Goswami DY, Stefanakos E. Nitrate salts doped with CuO nanoparticles for thermal energy storage with improved heat transfer. Appl Energy 2016;165:225–33. doi:10.1016/j.apenergy.2015.11.045.

[91] Stekli, J.; Irwin, L.; Pitchumani, R. Technical Challenges And Opportunities For Concentrating Solar Power With Thermal Energy Storage. ASME Journal of Thermal Science and Engineering Applications 2013, 5, 021011.

[92] IEA-ETSAP and IRENA (2013) “Thermal Energy Storage. Technology Brief” .179

[93] Alva G, Liu L, Huang X ,Fang G. (2017) “ Thermal energy storage materials and systems for solar energy applications” Renewable and Sustainable Energy Reviews vol,68,part1,pp 693-706.

[94] Alam, Tanvir E., "Experimental Investigation of Encapsulated Phase Change Materials for Thermal Energy Storage" (2015). USF (University of South Florida) Tampa Graduate Theses and Dissertations.,

[95] Lane, G. Solar Heat Storage; CRC Press: Boca Baton, Fla., 1983.

[96] Kuravi, S.; Trahan, J.; Goswami, D.; Rahman, M.; Stefanakos, E. Thermal Energy Storage Technologies And Systems For Concentrating Solar Power Plants. Progress in Energy and Combustion Science 2013, 39, 285-319.

[97] Liu, M.; Saman, W.; Bruno, F. Review On Storage Materials And Thermal Performance Enhancement Techniques For High Temperature Phase Change Thermal Storage Systems. Renewable and Sustainable Energy Reviews 2012, 16, 2118-2132.

[98] Herrmann U, Kearney DW. Survey of thermal energy storage for parabolic trough power plants. J Sol Energy Eng Trans ASME 2002;124:145–52.

[99] Gautam A, Saini RP. A review on technical, applications and economic aspect of packed bed solar thermal energy storage system. J Energy Storage 2020; 27: 101 046.

[100] Li C, Xie B, Chen J, He Z, Chen Z, Long Y. Emerging mineral-coupled composite phase change materials for thermal energy storage. Energy Convers Manag 2019;183:633–44.

[101] Xie B, Li C, Zhang B, Yang L, Xiao G, Chen J. Evaluation of stearic acid/coconut shell charcoal composite phase change thermal energy storage materials for tankless solar water heater. Energy Built Environ 2019:0–39.

[102] Li C, Xie B, He Z, Chen J, Long Y. 3D structure fungi-derived carbon stabilized stearic acid as a composite phase change material for thermal energy storage. Renew Energy 2019;140:862–73.

[103] Mehling H, Cabeza LF. Heat and cold storage with PCM. vol. 308. Springer; 2008.

[104] Reddy KS, Mudgal V, Mallick TK. Review of latent heat thermal energy storage for improved material stability and effective load management. J Energy Storage 2018;15:205–27.

[105] Galione P, Pérez-Segarra C, Rodríguez I, Torras S, Rigola J. Numerical evaluation of multi-layered solid-PCM thermocline-like tanks as thermal energy storage systems for CSP applications. Energy Procedia 2015;69:832–41.

[106] Felix Regin A, Solanki SC, Saini JS. An analysis of a packed bed latent heat thermal energy storage system using PCM capsules: Numerical investigation. Renew Energy 2009;34:1765–73.

[107] Elfeky KE, Ahmed N, Wang Q. Numerical comparison between single PCM and multi-stage PCM based high temperature thermal energy storage for CSP tower plants. Appl Therm Eng 2018;139:609–22.

[108] Yang L, Zhang X, Xu G. Thermal performance of a solar storage packed bed using spherical capsules filled with PCM having different melting points. Energy Build 2014:639–46.

[109] Bruno F, Belusko M, Liu M, Tay NHS. Using solid-liquid phase change materials (PCMs) in thermal energy storage systems. Adv. Therm. energy storage Syst., Elsevier; 2015, p. 201–46.

[110] Li Y, Li C, Lin N, Xie B, Zhang D, Chen J. Review on tailored phase change behavior of hydrated salt as phase change materials for energy storage. Mater Today Energy 2021;22:100866.

[111] Yan t, Wang R, Z, Li T X, Wang L, W, Fred I, T (2015) « A Review of promising condidate reactions for chemical heat storage », Renewable and Sustainable Snergy Reviews, Rol,43,pp,13-31.

[112] L. Roccamena, Optimization of an innovative thermal energy storage technology at low temperatures when coupled to multi-source energy architectures (2017), THESE de DOCTORAT DE L'UNIVERSITE DE LYON

[113] H. Mehling and L. F. Cabeza, *Heat and cold storage with PCM*. 2008.

[114] G. A. Lane, *Solar Heat Storage: Latent Heat Material*. Boca Raton: CRC Press, 2017.

[115] L. Marcela Quant Colón. Study of a urea-based phase change material for thermal energy storage. Thermics [physics.class-ph]. Université de Pau et des Pays de l'Adour; Universidad del País Vasco. Facultad de ciencias, 2020.

[116] H. Nazir *et al.*, 'Recent developments in phase change materials for energy storage applications: A review', *Int. J. Heat Mass Transf.*, vol. 129, pp. 491–523, 2019.

[117] A. Hauer *et al.*, 'IEA SHC Task 42 / ECES Annex 29 – A Simple Tool for the Economic Evaluation of Thermal Energy Storages', *Energy Procedia*, vol. 91, pp. 197–206, 2016.

[118] D. Aydin, S. P. Casey, and S. Riffat, 'The latest advancements on thermochemical heat storage systems', *Renew. Sustain. Energy Rev.*, vol. 41, pp. 356–367, 2015.

[119] R. J. Clark, A. Mehrabadi, and M. Farid, 'State of the art on salt hydrate thermochemical energy storage systems for use in building applications', *J. Energy Storage*, vol. 27, no. November 2019, p. 101145, 2020.

[120] Abedin A, Rosen M, (2011) ' A Critical Review of Thermochemical Energy Storage Systems', The Open Renewable Energy Journal, Vol.4,pp 42-46.

[121] Maria de Los Angeles Ortega del Rosario. Customizable latent heat thermal energy storage and transfer system for air-cooling in buildings : design and thermal analysis. Mechanics [physics]. Université de Bordeaux, 2018.

[122] Amy S. Fleischer. *Thermal Energy Storage Using Phase Change Materials*. Springer International Publishing, 2015, pp. X, 94. isbn: 978-3-319-20922-7. doi: 10.1007/978-3 319- 20922-7.

[123] Pramod B. Salunkhe and Prashant S. Shembekar. "A review on effect of phase change material encapsulation on the thermal performance of a system". In: *Renewable and Sustainable Energy Reviews* 16.8 (2012), pp. 5603–5616. doi: 10.1016/j.rser.2012.06. 02. url: https://ideas.repec.org/a/eee/rensus/v16y2012i8p5603-5616.html.

[124] A. Abhat. "Low temperature latent heat thermal energy storage: Heat storage materials". In: *Solar Energy* 30.4 (1983), pp. 313–332. issn: 0038-092X. doi: https://doi.org/ 10.1016/0038-092X(83)90186-X. url: http://www. sciencedirect. com/science/ article/pii/0038092X8390186X.

[125] Atul Sharma et al. “Review on thermal energy storage with phase change materials and applications”. In: *Renewable and Sustainable Energy Reviews* 13.2 (2009), pp. 318– 345. issn: 1364-0321. doi: https://doi.org/10. 1016/j. rser.2007. 10. 005. url: http://www.sciencedirect.com/science/article/pii/S1364032107001402.

[126] Weiguang Su, Jo Darkwa, and Georgios Kokogiannakis. “Review of solid–liquid phase change materials and their encapsulation technologies”. In: *Renewable and Sustainable Energy Reviews* 48 (2015), pp. 373–391. issn: 1364-0321. doi: https://doi.org/10. 1016/j.rser.2015.04.044. url: http://www. sciencedirect. com/ science/article/pii/S1364032115003147.

[127] S. Kalnæs and B. Petter Jelle. “Phase change materials and products for building applications: A state-of-the-art review and future research opportunities”. In: *Energy and Buildings* 94 (2015), pp. 150–176. issn: 0378-7788. doi: https://doi.org/ 10.1016/j.enbuild.2015.02.023. url: http://www. sciencedirect. com/science/ article/pii/S0378778815001188.

[128] M. Farid, A review on phase change energy storage: materials and applications, Energy Convers. Manag. 45 (2004) 1597–1615. doi:10.1016/ j.enconman .2003. 09. 015.

[129] P. Tatsidjodoung, N. Le Pierrès, L. Luo, A review of potential materials for thermal energy storage in building applications, Renew. Sustain. Energy Rev. 18 (2013) 327–349. doi:http://dx.doi.org/10.1016/j.rser.2012.10.025.

[130] M.A KEILANY, Experimental and modeling study of a thermocline latent/sensible heat storage system integrated with a cylindrical-parabolic concentrated solar power plant (2020),DOCTORAT DE L’UNIVERSITÉ DE TOULOUSE

[131] A. Sharma, V. V. Tyagi, C. R. Chen, and D. Buddhi, “Review on thermal energy storage with phase change materials and applications,” *Renew. Sustain. Energy Rev.*, vol. 13, no. 2, pp. 318–345, 2009.

[132] Kenisarin M, Mahkamov K. Solar energy storage using phase change materials. Renew Sustain Energy Rev 2007;11:1913–65. doi:10.1016/j. rser.2006. 05. 005.

[133] Pielichowska K, Pielichowski K. Phase change materials for thermal energy storage. Prog Mater Sci 2014;65:67–123. doi:10.1016/j.pmatsci.2014.03.005.

[134] M. Necati Ozisik. *Heat Conduction*. John Wiley and Sons, Inc, 1993, pp. isbn: 0-471- 53256-8.

[135] V. S. Dušan Medveď, Milan Kvakovský, “Latent Heat Storage Systems,” *Intensive Program. “Renewable Energy Sources,”* vol. i, no. May, 2010.

[136] S. Jegadheeswaran and S. D. Pohekar, “Performance enhancement in latent heat thermal storage system : A review,” vol. 13, pp. 2225–2244, 2009.

[137] Y. Lin, Y. Jia, G. Alva, and G. Fang, “Review on thermal conductivity enhancement, thermal properties and applications of phase change materials in

thermal energy storage," *Renew. Sustain. Energy Rev.*, vol. 82, no. May 2017, pp. 2730–2742, 2018.

[138] A. Hoshi, D. R. Mills, A. Bittar, and T. S. Saitoh, "Screening of high melting point phase change materials (PCM) in solar thermal concentrating technology based on CLFR," *Sol. Energy*, vol. 79, no. 3, pp. 332–339, 2005.

[139] K. D'Avignon and M. Kummert, "Experimental assessment of a phase change material storage tank," *Appl. Therm. Eng.*, vol. 99, pp. 880–891, 2016.

[140] H. O. Paksoy, *Thermal Energy Storage for Sustainable Energy Consumption*. Springer, 2005.

[141] L. Huang, E. Günther, C. Doetsch, and H. Mehling, "Subcooling in PCM emulsions-Part 1: Experimental," *Thermochim. Acta*, vol. 509, no. 1–2, pp. 93–99, 2010.

[142] I. Dincer and R. M. A, *THERMAL ENERGY STORAGE SYSTEMS AND APPLICATIONS*, Second. WILEY, 2011.

[143] A. Safari, R. Saidur, F. A. Sulaiman, Y. Xu, and J. Dong, "A review on supercooling of Phase Change Materials in thermal energy storage systems," *Renew. Sustain. Energy Rev.*, vol. 70, no. July 2016, pp. 905–919, 2017.

[144] M. Faucheux, G. Muller, M. Havet, and A. LeBail, "Influence of surface roughness on the supercooling degree: Case of selected water/ethanol solutions frozen on aluminium surfaces," *Int. J. Refrig.*, vol. 29, no. 7, pp. 1218–1224, 2006.

[145] Agyenim F, Hewitt N, Eames P, Smyth M. A review of materials, heat transfer and phase change problem formulation for latent heat thermal energy storage systems (LHTESS). Renew Sustain Energy Rev 2010;14:615–28. doi:10.1016/j. rser.2009. 10. 015.

[146] Goswami DY, Jotshi CK, Olszewski M. Analysis Of Thermal Energy Storage In Cylindrical PCM Capsules Exbedded In A Metal Matrix. Proc. 25th Intersoc. Energy Convers. Eng. Conf., vol. 4, IEEE; n.d., p. 257–62. doi:10.1109/IECEC.1990. 71 498.

[147] Wickramaratne C, Moloney F, Pirasaci T, Kamal R, Goswami DY, Stefanakos E, et al. Experimental Study on Thermal Storage Performance of Cylindrically Encapsulated PCM in a Cylindrical Storage Tank With Axial Flow. ASME 2016 Power Conf., ASME; 2016, p. V001T08A014. doi:10.1115/POWER2016-59427.

[148] Silva PD, Gonçalves LC, Pires L. Transient behaviour of a latent-heat thermal-energy store: Numerical and experimental studies. Appl Energy 2002;73:83–98. doi:10.1016/S0306-2619(02)00060-0.

[149] Adine HA, El Qarnia H. Numerical analysis of the thermal behaviour of a shell-and-tube heat storage unit using phase change materials. Appl Math Model 2009;33:2132–44. doi:10.1016/j.apm.2008.05.016.

[150] Gong Z, Majumdar A. Finite-element analysis of cyclic heat transfer in a shell-and-tube latent heat energy storage exchanger. Appl Therm Eng 1997;17:583–91. doi:10.1016/S1359-4311(96)00054-3.

[151] Tian Y, Zhao CY. A review of solar collectors and thermal energy storage in solar thermal applications. Appl Energy 2013;104:538–53. doi:10.1016/j. apenergy. 2012.11.051.

[152] Zalba B, Marín JM, Cabeza LF, Mehling H. Review on thermal energy storage with phase change: materials, heat transfer analysis and applications. Appl Therm Eng 2003;23:251–83. doi:10.1016/S1359-4311(02)00192-8.

[153] Jegadheeswaran S, Pohekar SD. Performance enhancement in latent heat thermal storage system: A review. Renew Sustain Energy Rev 2009;13:2225–44. doi:10.1016/j.rser.2009.06.024.

[154] Agyenim F, Hewitt N, Eames P, Smyth M. A review of materials, heat transfer and phase change problem formulation for latent heat thermal energy storage systems (LHTESS). Renew Sustain Energy Rev 2010;14:615–28. doi:10.1016/j. rser.2009. 10. 015.

[155] Laing D, Bahl C, Bauer T, Lehmann D, Steinmann WD. Thermal energy storage for direct steam generation. Sol Energy 2011;85:627–33. doi:10.1016/j. solener.2010.08.015.

[156] Ibrahim NI, Al-Sulaiman FA, Rahman S, Yilbas BS, Sahin AZ. Heat transfer enhancement of phase change materials for thermal energy storage applications: A critical review. Renew Sustain Energy Rev 2017;74:26–50. doi:10.1016 /j.rser.2017 .01. 169.

[157] Liu M, Saman W, Bruno F. Review on storage materials and thermal performance enhancement techniques for high temperature phase change thermal storage systems. Renew Sustain Energy Rev 2012;16:2118–32. doi:10.1016/j. rser. 2012.01.020.

[158] Incropera FP, DeWitt DP, Bergman TL, Lavine AS. Introduction to Conduction. Fundam Heat Mass Transf 2007:997. doi:10.1016/j. applthermaleng. 2011.03.022.

[159] Jegadheeswaran, S.; Pohekar, S. Performance Enhancement In Latent Heat Thermal Storage System: A Review. Renewable and Sustainable Energy Reviews 2009, 13, 2225-2244.

[160] Lacroix, M.; Benmadda, M. Numerical Simulation Of Natural Convection-Dominated Melting And Solidification From A Finned Vertical Wall. Numerical Heat Transfer Part A 1997, 31, 71–86.

[161] Shatikian, V.; Ziskind, G.; Letan, R. Numerical Investigation Of A PCM-Based Heat Sink With Internal Fins. International Journal of Heat and Mass Transfer 2005, 48, 3689-3706.

[162] Steinmann, W.; Laing, D.; Tamme, R. Development Of PCM Storage For Process Heat And Power Generation. J. Sol. Energy Eng. 2009, 131, 041009.

[163] Shabgard H, Bergman TL, Sharifi N, Faghri A. High temperature latent heat thermal energy storage using heat pipes. Int J Heat Mass Transf 2010;53:2979–88. doi:10.1016/j.ijheatmasstransfer.2010.03.035.

[164] Sharifi N, Wang S, Bergman TL, Faghri A. Heat pipe-assisted melting of a phase change material. Int J Heat Mass Transf 2012;55:3458–69. doi:10.1016/ j.ijheatmasstransfer .2012.03.023.

[165] Shabgard H, Robak CW, Bergman TL, Faghri A. Heat transfer and exergy analysis of cascaded latent heat storage with gravity-assisted heat pipes for concentrating solar power applications. Sol Energy 2012;86:816–30. doi:10.1016/j. solener.2011.12.008.

[166] Robak CW, Bergman TL, Faghri A. Enhancement of latent heat energy storage using embedded heat pipes. Int J Heat Mass Transf 2011;54:3476–84. doi:10. 1016/j. ijheatmasstransfer.2011.03.038.

[167] Shabgard H, Allen MJ, Sharifi N, Benn SP, Faghri A, Bergman TL. Heat pipe heat exchangers and heat sinks: Opportunities, challenges, applications, analysis, and state of the art. Int J Heat Mass Transf 2015;89:138–58. doi:10.1016/j .ijheatmasstransfer.2015.05.020.

[168] Zheng Y. Thermal energy storage with encapsulated phase change materials for high temperature applications 2015:189.

[169] Jegadheeswaran, S.; Pohekar, S. Performance Enhancement In Latent Heat Thermal Storage System: A Review. Renewable and Sustainable Energy Reviews 2009, 13, 2225-2244.

[170] Wang, J.; Chen, G.; Jiang, H. Theoretical Study On A Novel Phase Change Process. International Journal of Energy Research 1999, 23, 287-294.

[171] Michels, H.; Pitz-Paal, R. Cascaded Latent Heat Storage for Parabolic Trough Solar Power Plants. Solar Energy 2007, 81, 829–837.

[172] Farid, M.; Kanzawa, A. Thermal Performance Of A Heat Storage Module sing PCM'S With Different Melting Temperatures: Mathematical Modeling. ASME Journal of Solar Energy Engineering 1989, 111, 152–157.

[173] Cárdenas, B.; León, N. High Temperature Latent Heat Thermal Energy Storage: Phase Change Materials, Design Considerations And Performance Enhancement Techniques. Renewable and Sustainable Energy Reviews 2013, 27, 724-737.

[174] Hoover, M.; Grodzka, P.; O'Neill, M. Space Thermal Control Development. Lockheed Huntsville Research and Engineering Center Final Report, LMSC-HREC D225500, vol. 81; 1971.

[175] Khodadadi, J.; Fan, L.; Babaei, H. Thermal Conductivity Enhancement Of Nanostructure-Based Colloidal Suspensions Utilized As Phase Change Materials For

Thermal Energy Storage: A Review. Renewable and Sustainable Energy Reviews 2013, 24, 418-444.

[176] Mettawee, E.; Assassa, G. Thermal Conductivity Enhancement In A Latent Heat Storage System. Solar Energy 2007, 81, 839-845.

[177] Zeng, J.; Sun, L.; Xu, F.; Tan, Z.; Zhang, Z.; Zhang, J.; Zhang, T. Study Of A PCM Based Energy Storage System Containing Ag Nanoparticles. Journal of Thermal Analysis and Calorimetry 2006, 87, 371-375.

[178] Xie, H.; Wan, J.; Chen, L. Effects On The Thase Transformation Temperature Of Nanofluids By The Nanoparticles. Journal of Materials Sciences & Technology 2008), 25, 742–744.

[179] Hong, H.; Zheng, Y.; Roy, W. Nanomaterials For Efficiently Lowering The Freezing Point Of Anti-Freeze Coolants. Journal for Nanoscience and Nanotechnology 2007, 7, 1–5.

[180] Weinstein, R.; Kopec, T.; Fleischer, A.; D'Addio, E.; Bessel, C. The Experimental Exploration Of Embedding Phase Change Materials With Graphite Nanofibers For The Thermal Management Of Electronics. Journal of Heat Transfer 2008, 130, 042405.

[181] Zeng, J.; Liu, Y.; Cao, Z.; Zhang, J.; Zhang, Z.; Sun, L.; Xu, F. Thermal Conductivity Enhancement Of Mwnts On The PANI/Tetradecanol Form-Stable PCM. Journal of Thermal Analysis and Calorimetry 2007, 91, 443-446.

[182] Kim, S.; Drzal, L. High Latent Heat Storage And High Thermal Conductive Phase Change Materials Using Exfoliated Graphite Nanoplatelets. Solar Energy Materials and Solar Cells 2009, 93, 136-142.

[183] Fang, X.; Fan, L.; Ding, Q.; Wang, X.; Yao, X.; Hou, J.; Yu, Z.; Cheng, G.; Hu, Y.; Cen, K. Increased Thermal Conductivity Of Eicosane-Based Composite Phase Change Materials In The Presence Of Graphene Nanoplatelets. Energy Fuels 2013, 27, 4041-4047.

[184] Li, J.; Lu, W.; Zeng, Y.; Luo, Z. Simultaneous Enhancement Of Latent Heat And Thermal Conductivity Of Docosane-Based Phase Change Material In The Presence Of Spongy Graphene. Solar Energy Materials and Solar Cells 2014, 128, 48-51.

[185] Khodadadi, J.; Hosseinizadeh, S. Nanoparticle-Enhanced Phase Change Materials (NEPCM) With Great Potential For Improved Thermal Energy Storage. International Communications in Heat and Mass Transfer 2007, 34, 534-543.

[186] Mesalhy, O.; Lafdi, K.; Elgafy, A.; Bowman, K. Numerical Study For Enhancing The Thermal Conductivity Of Phase Change Material (PCM) Storage Using High Thermal Conductivity Porous Matrix. Energy Conversion and Management 2005, 46, 847-867.

[187] Fiedler, T.; Öchsner, A.; Belova, I.; Murch, G. Thermal Conductivity Enhancement Of Compact Heat Sinks Using Cellular Metals. DDF 2008, 273-276, 222-226.

[188] Jegadheeswaran S, Pohekar SD. Performance enhancement in latent heat thermal storage system: A review. Renew Sustain Energy Rev 2009;13:2225–44. doi:10.1016/j.rser.2009.06.024.

[189] Fukai J, Kanou M, Kodama Y, Miyatake O. Thermal conductivity enhancement of energy storage media using carbon fibers. Energy Convers Manag 2000;41:1543–56. doi:10.1016/S0196-8904(99)00166-1.

[190] Hamada Y, Ohtsu W, Fukai J. Thermal response in thermal energy storage material around heat transfer tubes: Effect of additives on heat transfer rates. Sol Energy 2003;75:317–28. doi:10.1016/j.solener.2003.07.028.

[191] Myers PD, Yogi Goswami D, Stefanakos E. Molten Salt Spectroscopy for Quantification of Radiative Absorption in Novel Metal Chloride-Enhanced Thermal Storage Media. J Sol Energy Eng 2015;137:41002. doi:10.1115/1.4029934.

[192] Khalifa A, Tan L, Date A, Akbarzadeh A. A numerical and experimental study of solidification around axially finned heat pipes for high temperature latent heat thermal energy storage units. Appl Therm Eng 2014;70:609–19. doi:10.1016/j.applthermaleng2014.05.080.

[193] Khalifa A, Tan L, Date A, Akbarzadeh A. Performance of suspended finned heat pipes in high-temperature latent heat thermal energy storage. Appl Therm Eng 2015;81:242–52. doi:10.1016/j.applthermaleng.2015.02.030.

[194] Sharifi N, Bergman TL, Allen MJ, Faghri A. Melting and solidification enhancement using a combined heat pipe, foil approach. Int J Heat Mass Transf 2014;78:930–41. doi:10.1016/j.ijheatmasstransfer.2014.07.054.

[195] Xie YQ, Song J, Chi PT, Yu JZ. Performance Enhancement of Phase Change Thermal Energy Storage Unit Using Fin and Copper Foam. Appl Mech Mater 2012;260–261:137–41. doi:10.4028/www.scientific.net/AMM.260-261.137.

[196] Allen MJ, Sharifi N, Faghri A, Bergman TL. Effect of inclination angle during melting and solidification of a phase change material using a combined heat pipe-metal foam or foil configuration. Int J Heat Mass Transf 2015;80:767–80. doi:10.1016/j.ijheatmasstransfer.2014.09.071.

[197] Zhang HL, Baeyens J, Degrève J, Cáceres G, Segal R, Pitié F. Latent heat storage with tubular-encapsulated phase change materials (PCMs). Energy 2014; 76:66–72. doi:10.1016/j.energy.2014.03.067.

[198] Hawlader MN a, Uddin MS, Khin MM. Microencapsulated PCM thermal-energy storage system. Appl Energy 2003;74:195–202. doi:10.1016/S0306-2619(02)00146-0.

[199] Salunkhe PB, Shembekar PS. A review on effect of phase change material encapsulation on the thermal performance of a system. Renew Sustain Energy Rev 2012;16:5603–16. doi:10.1016/j.rser.2012.05.037.

[200] Liu C, Rao Z, Zhao J, Huo Y, Li Y. Review on nanoencapsulated phase change materials: Preparation, characterization and heat transfer enhancement. Nano Energy 2015;13:814–26. doi:10.1016/j.nanoen.2015.02.016.

[201] Sarı, A.; Alkan, C.; Karaipekli, A.; uzun, O. Microencapsulated N-Octacosane As Phase Change Material For Thermal Energy Storage. Solar Energy 2009, 83, 1757-1763.

[202] Qiu, X.; Lu, L.; Wang, J.; Tang, G.; Song, G. Preparation And Characterization Of Microencapsulated N-Octadecane As Phase Change Material With Different N-Butyl Methacrylate-Based Copolymer Shells. Solar Energy Materials and Solar Cells 2014, 128, 102-111.

[203] Lane, G. Solar Heat Storage; CRC Press: Boca Baton, Fla., 1983.

[204] Zhang, H.; Baeyens, J.; Degrève, J.; Cáceres, G.; Segal, R.; Pitié, F. Latent Heat Storage With Tubular-Encapsulated Phase Change Materials (Pcms). Energy 2014, 76, 66-72.

[205] Zhang, G.; Li, J.; Chen, Y.; Xiang, H.; Ma, B.; Xu, Z.; Ma, X. Encapsulation Of Copper-Based Phase Change Materials For High Temperature Thermal Energy Storage. Solar Energy Materials and Solar Cells 2014, 128, 131-137.

[206] Vicente, R.; Silva, T. Brick Masonry Walls With PCM Macrocapsules: An Experimental Approach. Applied Thermal Engineering 2014, 67, 24-34.

[207] Zhao, W. Characterization of Encapsulated Phase Change Materials For Thermal Energy Storage", Theses and Dissertations, Mechanical Engineering Department, Lehigh niversity, 2013.

[208] Zheng, Y.; Zhao, W.; Sabol, J.; Tuzla, K.; Neti, S.; Oztekin, A.; Chen, J. Encapsulated Phase Change Materials For Energy Storage - Characterization By Calorimetry. Solar Energy 2013, 87, 117-126.

[209] Mathur, A.; Kasetty, R. Thermal Energy Storage System Comprising Encapsulated Phase Change Material. United States of America Application No.-2012/0018116 A1, 2012.

[210] A. Felix Regin, S.C. Solanki, and J.S. Saini. "Heat transfer characteristics of thermal energy storage system using PCM capsules: A review". In: *Renewable and Sustainable Energy Reviews* 12.9 (2008), pp. 2438–2458. issn: 1364-0321. doi: https://doi.org/10. 1016/j.rser.2007.06.009. url: http://www. Science direct. com/ science/article/ pii/S1364032107001001.

[211] G. Ziskind. "12 - Modelling of heat transfer in phase change materials (PCMs) for thermal energy storage systems". In: *Advances in Thermal Energy Storage Systems*. Ed. by Luisa F. Cabeza. Woodhead Publishing Series in Energy. Woodhead Publishing, 2015, pp. 307–324. isbn: 978-1-78242-088-0. doi: https : / / doi . org / 10 .

1533 / 9781782420965.2.307. url: http://www.sciencedirect.com/science/article/ pii/ B9781782420880500122.

[212] V. Alexiades and Alan D. Solomon. *MATHEMATICAL MODELING OF MELTINGAND FREEZING PROCESSES*.Taylor and Francis, 1993, pp. isbn: 1-56032-125-3.

[213] H. S. Carslaw and J. C. Jaeger. *Conduction of Heat in Solids*. Oxford University Press, London, 1959, pp. isbn:

[214] M. Necati Ozisik. Heat Conduction. John Wiley and Sons, Inc, 1993, pp. isbn: 0-471-,53256-8.

[215] Shokouhmand H, Kamkari B. Experimental investigation on melting heat transfer characteristics of lauric acid in a rectangular thermal storage unit. ExpTherm Fluid Sci 2013;50:201–12. https://doi.org/10.1016/j.expthermflusci.2013.06.010.